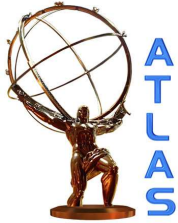


EUROPEAN ORGANISATION FOR NUCLEAR RESEARCH (CERN)



Submitted to: JHEP



CERN-PH-EP-2015-090
10th November 2015

A search for $t\bar{t}$ resonances using lepton-plus-jets events in proton-proton collisions at $\sqrt{s} = 8$ TeV with the ATLAS detector

The ATLAS Collaboration

Abstract

A search for new particles that decay into top quark pairs is reported. The search is performed with the ATLAS experiment at the LHC using an integrated luminosity of 20.3 fb^{-1} of proton-proton collision data collected at a centre-of-mass energy of $\sqrt{s} = 8$ TeV. The lepton-plus-jets final state is used, where the top pair decays to $W^+bW^-\bar{b}$, with one W boson decaying leptonically and the other hadronically. The invariant mass spectrum of top quark pairs is examined for local excesses or deficits that are inconsistent with the Standard Model predictions. No evidence for a top quark pair resonance is found, and 95% confidence-level limits on the production rate are determined for massive states in benchmark models. The upper limits on the cross-section times branching ratio of a narrow Z' boson decaying to top pairs range from 4.2 pb to 0.03 pb for resonance masses from 0.4 TeV to 3.0 TeV. A narrow leptophobic topcolour Z' boson with mass below 1.8 TeV is excluded. Upper limits are set on the cross-section times branching ratio for a broad colour-octet resonance with $\Gamma/m = 15\%$ decaying to $t\bar{t}$. These range from 4.8 pb to 0.09 pb for masses from 0.4 TeV to 3.0 TeV. A Kaluza-Klein excitation of the gluon in a Randall-Sundrum model is excluded for masses below 2.2 TeV.

© 2015 CERN for the benefit of the ATLAS Collaboration.

Reproduction of this article or parts of it is allowed as specified in the CC-BY-3.0 license.

1 Introduction

Many models of physics beyond the Standard Model (SM) predict production at the LHC of additional particles with masses near the TeV scale. This paper presents a search for such heavy particles decaying to top quark pairs ($t\bar{t}$) using data from proton–proton collisions collected at a centre-of-mass energy $\sqrt{s} = 8$ TeV with the ATLAS detector, corresponding to an integrated luminosity of 20.3 fb^{-1} .

Searches for production of heavy particles that decay to $t\bar{t}$ are of high interest at the LHC due to the role that the top quark plays in many models of physics beyond the SM (BSM). The top quark is the most massive of the fundamental particles in the SM, and it can have a large coupling to heavy Higgs bosons. Thus, heavy Higgs bosons in two-Higgs-doublet models [1, 2] can have a large branching ratio to $t\bar{t}$ final states. Furthermore, many models that propose alternative mechanisms for electroweak symmetry breaking (EWSB) incorporate new heavy particles with a larger coupling to $t\bar{t}$ than to lighter quarks. Examples include strong EWSB models such as topcolour-assisted technicolour [3] (TC2) and Composite Higgs [4–11] scenarios. Models with warped extra dimensions [12–15] form an additional class of models that predict heavy particles that decay to $t\bar{t}$ pairs. In such models, the heavy particles are the counterparts of the gluon and graviton.

The search starts by selecting events with one isolated charged lepton (electron or muon), missing transverse momentum (whose magnitude is denoted by $E_{\text{T}}^{\text{miss}}$) and hadronic jets, which are compatible with $t\bar{t} \rightarrow W^+bW^-\bar{b}$, with one W boson decaying leptonically and the other hadronically. At least one of the hadronic jets is required to be consistent with having originated from a b -quark. An estimator of the $t\bar{t}$ invariant mass ($m_{t\bar{t}}^{\text{reco}}$) is constructed with the events divided into two orthogonal classes by topology: the *boosted* topology, where the decay products of the hadronically decaying top quark are expected to be fully enclosed within one large-radius jet, and the *resolved* topology where four small-radius jets are reconstructed and attributed to the $b\bar{b}q\bar{q}'$ quarks. The $m_{t\bar{t}}^{\text{reco}}$ spectrum is scanned for localised deviations relative to the expectations from the background processes. The compatibility of the data and expectations is assessed, and limits on the production cross-section for new particles are set.

This search is designed to be sensitive to the production of any new particle that decays to $t\bar{t}$. Nonetheless the selection efficiency and acceptance can differ between particular model choices. Hence the sensitivity to a variety of different new particles was evaluated to quantify the performance of the search. The benchmark models adopted in this search include colour-singlet and colour-octet bosons with spin 0, 1 and 2 and masses from 0.4 to 3 TeV. The resonance width for the specific models varies from very narrow (1%) to a size similar to that of the experimental resolution (15%). Furthermore, the dependence of the limits on the resonance width is explored for heavy gluons up to a width of 40%. With these results, it is possible to interpret the cross-section limits in the context of a search for other new particles with the same production modes.

In addition to making use of 8 TeV data, this search incorporates several improvements with respect to the previous most sensitive ATLAS collaboration search for the same signature [16], which used a similar strategy. Trimming [17] is now used to mitigate pile-up effects on large-radius jets, a new procedure is applied to recover efficiency loss from removal of overlap between electron and jet objects in the detector, and a χ^2 variable is exploited to remove events from non- $t\bar{t}$ background processes. Furthermore, the limits on production of spin 2 bosons and on heavy gluons of varying width represent an extension compared to previous searches by the ATLAS and CMS [18] Collaborations.

2 Models tested

The details of the benchmark models considered in this search are reviewed below. Interference between these processes and SM $t\bar{t}$ production is not considered in this search.

2.1 Spin-1 colour singlet

The first class of models explored produces spin-1 colour-singlet vector bosons, Z' . This search uses topcolour-assisted technicolour Z'_{TC2} [3, 19, 20] as a benchmark. This is a leptophobic boson, with couplings only to first- and third-generation quarks, referred to as Model IV in ref. [19]. The properties of the boson are controlled by three parameters: $\cot\theta_H$, which controls the width and the production cross-section, and f_1 and f_2 , which are related to the coupling to up-type and down-type quarks respectively. Here $f_1 = 1$ and $f_2 = 0$, which maximises the fraction of Z'_{TC2} that decay to $t\bar{t}$. The parameter $\cot\theta_H$ is tuned for each mass point such that the resonance has a width of 1.2% of its mass. To account for higher-order contributions to the cross-section, the leading-order calculation is multiplied by a factor of 1.3 based on calculations performed at next-to-leading order (NLO) in QCD [21, 22].

Constraints on Z'_{TC2} have been set by the CDF [23, 24] and D0 [25] collaborations using data from proton–antiproton collisions at the Tevatron. Previous constraints at the LHC were set using proton–proton collisions at $\sqrt{s} = 7$ TeV with an integrated luminosity of 5 fb^{-1} by the ATLAS [16, 26] and CMS [27–29] collaborations, and using 20 fb^{-1} of $\sqrt{s} = 8$ TeV data by the CMS Collaboration [18]. For narrow (wide) Z'_{TC2} of width 1.2% (10%) the strongest lower bound on the allowed mass is 2.1 TeV (2.7 TeV) from the search performed by CMS at $\sqrt{s} = 8$ TeV.

2.2 Spin-1 colour octet

The second class of models considered produces spin-1 colour-octet vector bosons. Specifically, heavy Kaluza–Klein gluons, g_{KK} , as produced in Randall–Sundrum (RS) models with a single warped extra dimension [30], are used as a benchmark in this search. In this model, the g_{KK} has a nominal width of 15.3% of its mass. Previous searches using $\sqrt{s} = 7$ TeV ATLAS data [16] exclude a g_{KK} with a mass less than 2.1 TeV. The CMS Collaboration searched for similar resonances [18], using a slightly different benchmark model [31]. The CMS choice leads to a larger natural width of 20% and a larger production cross-section, and, for such a scenario, CMS excludes the existence of a g_{KK} with mass less than 2.5 TeV. In the analysis presented here, the sensitivity to the width of the colour octet is also tested for widths from 10% to 40% of the resonance mass.

2.3 Spin-2 colour singlet

The third class of models explored in this search produces spin-2 colour singlets, such as Kaluza–Klein excitations of the graviton, G_{KK} . The search uses a Randall–Sundrum model with extra dimensions where the SM fields are in the warped bulk and the fermions are localised appropriately to explain the flavour structure of the SM [12, 32, 33]. This kind of graviton is commonly referred to as a “Bulk” RS graviton and is characterised by a dimensionless coupling constant $k/\bar{M}_{\text{Pl}} \sim 1$, where k is the curvature of the warped extra dimension and $\bar{M}_{\text{Pl}} = M_{\text{Pl}}/\sqrt{8\pi}$ is the reduced Planck mass. For such gravitons, decays

to light fermions are suppressed, and the branching ratio to photons is negligible. The branching ratios to $t\bar{t}$, WW , ZZ and HH are significant. In the model used, k/\bar{M}_{Pl} is chosen to be 1, and the G_{KK} width varies from 3% to 6% in the mass range 400–2000 GeV. The branching ratio of G_{KK} decay into a $t\bar{t}$ pair rapidly increases from 18% to 50% between 400 and 600 GeV, plateauing at 68% for masses larger than 1 TeV. There have been no previous direct searches for such gravitons in the $t\bar{t}$ decay channel. The ATLAS Collaboration used the same model to explore the $G_{\text{KK}} \rightarrow ZZ$ channel [34] and excluded Bulk RS G_{KK} with mass less than 740 GeV. The CMS Collaboration performed searches in the $G_{\text{KK}} \rightarrow ZZ$ and $G_{\text{KK}} \rightarrow WW$ decay channels [35] but did not consider the case of Bulk RS gravitons with $k/\bar{M}_{\text{Pl}} > 0.5$.

2.4 Spin-0 colour singlet

The last class of models examined here produces colour-singlet scalar particles via gluon fusion which decay to $t\bar{t}$. The approach previously adopted by the CMS Collaboration [18] is followed, in which narrow scalar resonance benchmarks are generated while the interference with SM $t\bar{t}$ production is neglected. Even though such signals with negligible interference are not predicted by any particular BSM model, they can be used to evaluate the experimental sensitivities and set upper limits on the production cross-sections. The CMS Collaboration excluded such resonances with production cross-sections greater than 0.8 pb and 0.3 pb for masses of 500 and 750 GeV, respectively.

3 The ATLAS detector

The ATLAS experiment [36] is a multipurpose particle physics detector with forward-backward symmetric cylindrical geometry.¹ The inner detector (ID) consists of multiple layers of silicon pixel and microstrip detectors and a straw-tube transition radiation tracker and covers a pseudorapidity range of $|\eta| < 2.5$. The ID is surrounded by a superconducting solenoid that provides a 2 T axial magnetic field. The calorimeter system, surrounding the ID and the solenoid, covers the pseudorapidity range $|\eta| < 4.9$. It consists of high-granularity lead and liquid-argon (LAr) electromagnetic calorimeters, a steel and scintillator-tile hadronic calorimeter covering $|\eta| < 1.7$ and two copper/LAr hadronic endcap calorimeters covering $1.5 < |\eta| < 3.2$. Forward copper/LAr and tungsten/LAr calorimeter modules complete the solid-angle coverage out to $|\eta| = 4.9$. The muon spectrometer resides outside the calorimeters. It consists of multiple layers of trigger and tracking chambers within a system of air-core toroids, which enables an independent, precise measurement of muon track momenta for $|\eta| < 2.7$. The muon trigger chambers cover $|\eta| < 2.4$.

4 Data and Monte Carlo samples

This search is performed in proton–proton collision data at $\sqrt{s} = 8$ TeV collected with the ATLAS detector in 2012. The data are only used if they were recorded during stable beam conditions and with

¹ ATLAS uses a right-handed coordinate system with its origin at the nominal interaction point (IP) in the centre of the detector and the z -axis along the beam pipe. The x -axis points from the IP to the centre of the LHC ring, and the y -axis points upward. Cylindrical coordinates (r, ϕ) are used in the transverse plane, ϕ being the azimuthal angle around the beam pipe. The pseudorapidity is defined in terms of the polar angle θ as $\eta = -\ln \tan(\theta/2)$. The distance in η – ϕ space is commonly referred to as $\Delta R = \sqrt{(\Delta\phi)^2 + (\Delta\eta)^2}$.

all relevant subdetector systems operational. Lepton-plus-jets events were collected using single-electron and single-muon triggers with thresholds chosen in each case such that the efficiency is uniform for leptons satisfying offline selections including transverse momentum $p_T > 25$ GeV. The ATLAS muon trigger system suffers from a 20% inefficiency, relative to the offline event selection used in this analysis, largely due to a lack of geometrical coverage by muon chambers owing to support structures in those regions [37]. To mitigate this loss of efficiency, a large-radius-jet trigger, which triggers on anti- k_t jets (see section 5) with radius parameter $R = 1.0$, was used to collect muon-plus-jets events which failed the muon trigger. This large-radius-jet trigger recorded 17.4 fb^{-1} data. The chosen trigger threshold yields a uniform efficiency exceeding 99% for events containing a large-radius jet with reconstructed $p_T > 380$ GeV. For $t\bar{t}$ events with invariant masses above 1.5 TeV, this addition increased the overall trigger efficiency in the muon channel to 96%².

Simulated Monte Carlo (MC) samples were used for signal processes, as well as background processes producing jets and prompt leptons. The MC samples are employed to develop the event selection, provide SM background estimates, and evaluate signal efficiencies. Background contributions from processes in which there are no genuine prompt isolated leptons were estimated directly from the data as described in section 7. The MC samples were processed through the full ATLAS detector simulation [38] based on GEANT4 [39] or through a faster simulation making use of parameterised showers in the calorimeters [40]. Additional simulated proton–proton collisions generated using PYTHIA v8.1 [41] were overlaid to simulate the effects of additional collisions from the same and nearby bunch crossings (pile-up). All simulated events were then processed using the same reconstruction algorithms and analysis chain as the data. The simulated trigger and selection efficiencies were corrected to agree with the performance observed in data.

Production of Bulk RS gluon and graviton signals was modelled using MADGRAPH5 [42] interfaced with PYTHIA v8.1. For the gluon, the MSTW2008LO parton distribution function (PDF) set [43] was used, while for the graviton, the CTEQ6L1 [44] PDF set was used. The Z' signal was modelled using PYTHIA v8.1 with the MSTW2008LO PDF set. Heavy scalar signal samples were generated using MADGRAPH_AMC@NLO [45] with LO matrix elements and the CTEQ6L1 PDF set.

Pair production of top quarks is the dominant background in this search. It was simulated using the POWHEG-Box [46–49] generator r2330.3 interfaced with PYTHIA v6.427 [50] with the Perugia 2011C [51] tune and the CT10 [52] next-to-leading-order PDF set. In the MC generation of POWHEG-Box events, the parameter $hdamp$ was set to the top quark mass, corresponding to a damping of high- p_T radiation, in order to achieve good agreement with the differential cross-section measurements [53]. Alternative samples of $t\bar{t}$ events, used to evaluate uncertainties on $t\bar{t}$ modelling, were generated using the POWHEG-Box and MC@NLO v4.1 [54–56] generators interfaced with HERWIG v6.5 [57, 58] with JIMMY [59] for the modelling of the underlying event. For these samples the CT10 PDF set and the ATLAS-AUET2 [60] tune were used. In all cases, the top quark mass used was 172.5 GeV. The cross-sections for these samples were normalised to the calculation from TOP++ v2.0 [61] at next-to-next-to-leading-order (NNLO) accuracy in the strong coupling constant α_s , including resummation of next-to-next-to-leading-logarithmic (NNLL) soft gluon terms [62–67]. The top quark kinematics in all SM $t\bar{t}$ samples were corrected to account for electroweak higher-order effects [68]. This correction is applied after generating the samples, by applying a weight that depends on the flavour of the initial-partons, the centre-of-mass energy of the initial partons, and the decay angle of the tops in the centre-of-mass frame of the initial partons.

² The 4% loss here is relative to the full 20.3 fb^{-1} data set.

Production of W bosons in association with jets (W +jets) is also a significant background process. Samples of W +jets events were generated using the ALPGEN v2.13 generator [69] interfaced with PYTHIA v6.426, including up to five extra partons in the matrix element. Configurations with additional heavy quarks (a single c -quark, a $c\bar{c}$ pair or a $b\bar{b}$ pair in the hard process) were included, with the masses of heavy quarks taken into account. The CTEQ6L1 PDF set and the Perugia 2011C tune were used. The samples were normalised using data as described in section 7. Additional samples were generated with different choices of ALPGEN matrix element/parton shower matching parameters in order to estimate modelling uncertainties in the production of W +jets events.

Production of single top quarks can yield events that satisfy the analysis event selection. The POWHEG-Box generator interfaced with PYTHIA v6.246 was used to estimate the s - and Wt -channels [70–72] with the same configuration as for the $t\bar{t}$ samples. The t -channel was also generated with POWHEG-Box but in a four-flavour scheme, hence the CT10 NLO four-flavour PDF set was used. Overlap between the Wt sample and $t\bar{t}$ samples was handled using the diagram removal scheme [73]. These samples were normalised to approximate NNLO cross-sections [74–76].

Other minor background processes producing prompt isolated leptons include heavy diboson production, production of Z bosons in association with jets (Z +jets) and production of heavy gauge bosons in association with $t\bar{t}$ ($t\bar{t}V$). Production of Z +jets was modelled using ALPGEN interfaced with PYTHIA v6.426, in the same configuration used for the W +jets samples described above. The samples were normalised to the inclusive Z boson production cross-section calculated at NNLO in QCD using FEWZ [77]. Diboson production was modelled using the SHERPA [78–81] generator, with up to three extra partons in the matrix element and taking into account the mass of the b - and c -quarks. The diboson samples were normalised to calculations at NLO in QCD performed using MCFM [82] v5.8. The $t\bar{t}V$ production was modelled using MADGRAPH5 interfaced with PYTHIA v6.426 and normalised to NLO cross-section predictions [83].

5 Event selection

Events consistent with $t\bar{t}$ decaying to a single charged lepton together with hadronic jets and missing transverse momentum are selected. Electron candidates are required to have a transverse energy $E_T > 25$ GeV and $|\eta_{\text{cluster}}| < 2.47$, where η_{cluster} is the pseudorapidity of the cluster of energy deposited in the electromagnetic calorimeter, computed with respect to the centre of ATLAS detector and matched to the candidate [84]. Electron candidates in the transition region $1.37 < |\eta_{\text{cluster}}| < 1.52$ between calorimeter barrel and endcap are excluded.

In order to reduce backgrounds from non-prompt sources and hadronic showers with a high electromagnetic energy fraction in the calorimeter, electron isolation is imposed using a *mini-isolation* variable MI_{10} defined as the $\sum_{\text{tracks}} p_T^{\text{track}}$ for all tracks (except the matched lepton track) with $p_T > 1$ GeV satisfying quality selection criteria, and within a cone of size $\Delta R < 10 \text{ GeV}/E_T$ [16, 85] centred on the barycentre of the cluster. Electrons are defined to be isolated if $MI_{10}/E_T < 0.05$. The E_T here is the transverse energy of the reconstructed electron. The isolation variable MI_{10} is particularly useful in the case of boosted top quark decays since the p_T -dependent cone size reflects the p_T dependence of the separation between objects with a common boosted parent. The matching of the electron to the collision vertex [86] is imposed by requiring that the longitudinal impact parameter relative to it be less than 2 mm.

Muon candidates are required to have $p_T > 25$ GeV and $|\eta| < 2.5$. The matching of the muon to the collision vertex is imposed by the requirements that the longitudinal impact parameter relative to the

collision vertex be less than 2 mm and that the transverse impact parameter relative to the collision vertex divided by its uncertainty, $|d_0/\sigma_{d_0}|$, be less than 3.0. Muons are also required to satisfy the same MI_{10} requirement as electrons, with the cone centred on the inner-detector track associated with the muon.

Jets are reconstructed using the anti- k_t algorithm [87] applied to clusters of calorimeter cells that are topologically connected and calibrated to the hadronic energy scale [88] using a local calibration scheme [89]. Small-radius jets (radius parameter $R = 0.4$) as well as large-radius jets ($R = 1.0$) are used. The energies of all jets and the masses of the large-radius jets have been calibrated to their values at particle level [90–92]. Small-radius jets are required to satisfy $p_T > 25$ GeV and $|\eta| < 2.5$, while large-radius jets are required to satisfy $p_T > 300$ GeV and $|\eta| < 2.0$. Low- p_T central small-radius jets ($p_T < 50$ GeV, $|\eta| < 2.4$) are required to have a jet vertex fraction [93] greater than 0.5. The jet vertex fraction is defined as the total transverse momentum (using a scalar sum) of tracks in the jet that are associated with the primary vertex divided by the scalar sum of the transverse momentum of all tracks in the jet. This variable suppresses jets arising from pile-up effects. Large-radius jets have jet trimming [17] applied. In trimming, subjects are formed by applying a jet algorithm with smaller radius parameter, R_{sub} , and then soft subjects with less than a certain fraction, f_{cut} , of the original jet p_T are removed. The properties of the trimmed jet are then calculated using the surviving subjects. This procedure mitigates the effect of pile-up [94]. The trimming parameters used in this search are $f_{\text{cut}} = 0.05$ and $R_{\text{sub}} = 0.3$, and the inclusive k_t [95] algorithm is used to form the subjects.

Only small-radius jets are considered for b -jet identification (b -tagging). The b -tagging algorithm uses a multivariate approach with inputs taken from the results of separate impact parameter, secondary vertex and decay topology algorithms [96]. The operating point of the algorithm is chosen such that the b -tagging efficiency for simulated $t\bar{t}$ events is 70%. In MC simulation, factors are applied to correct for the differences between the b -tagging efficiency in simulated events and that measured in data. The factors are adapted to be appropriate for b -jets from high- p_T top quarks, for which the b -tagging efficiencies are lower.

The E_T^{miss} is calculated from the vector sum of the transverse energy of topological clusters in the calorimeter [97]. The clusters associated with the reconstructed electrons and small-radius jets are replaced by the calibrated energies of these objects. Muon transverse momenta determined from the ID and the muon spectrometer are also included in the calculation.

Overlap in identification of the relevant physics objects is possible and a procedure is implemented to remove duplication. Electrons and small-radius jets are considered for overlap removal if the cluster associated with the electron is within $\Delta R = 0.4$ of the nearest jet. In such cases, the jets have their four-momentum and jet vertex fraction recalculated after subtracting the electron four-momentum and then are removed if the recalculated values do not satisfy the original jet selection criteria. If the distance ΔR between the electron and the recalculated jet is < 0.2 , the electron candidate is likely to be from the hadronic jet. Therefore the electron is removed from the electron candidate list and its four-momentum is added to that of the recalculated jet. Muons are removed from the muon candidate list if the distance ΔR between the muon and small-radius jet is less than $0.04 + 10 \text{ GeV}/p_T$. This criterion exploits the anti-correlation between the muon p_T and its angular distance from the b -quark, in an approach similar to the isolation variable. The parameters are tuned based on signal MC simulations in order to provide a constant high efficiency as a function of resonance mass.

A set of common preselection criteria is used for events to be considered for the boosted and resolved topologies. Events are required to have exactly one lepton (electron or muon) plus multiple jets. Events recorded by the lepton triggers are required to have lepton-trigger objects that match the selected lepton.

Additionally, events must have $E_T^{\text{miss}} > 20$ GeV and $E_T^{\text{miss}} + m_T > 60$ GeV, where m_T is the transverse mass calculated as $m_T = \sqrt{2p_T E_T^{\text{miss}}(1 - \cos \phi_{\ell\nu})}$ where p_T is the transverse momentum of the lepton and $\phi_{\ell\nu}$ is the angle between the p_T and E_T^{miss} vectors.

Events are next checked against the *boosted-topology selection*. The selected lepton is required to have at least one small-radius jet within a distance of $\Delta R(\ell, j) = 1.5$ and, of these, the jet with highest p_T is termed j_{sel} . Boosted-topology events must have at least one large-radius jet with $p_T > 300$ GeV (380 GeV for the muon-plus-jets events selected by the large-radius-jet trigger), $|\eta| < 2.0$, mass $m_{\text{jet}} > 100$ GeV, first k_t splitting scale [95] $\sqrt{d_{12}} > 40$ GeV, $\Delta R > 1.5$ between the large-radius jet and j_{sel} , and $\Delta\phi > 2.3$ between the large-radius jet and lepton. The jet mass is calculated using the four-momenta of its constituent clusters, which are taken as massless. If multiple large-radius jets satisfy these criteria, the highest- p_T jet is chosen as the hadronically decaying top quark candidate. Finally, at least one of the small-radius jets in the event must be b -tagged and matched to either of the top quark candidates, as described in section 6.

Events that do not satisfy the boosted-topology selection are then tested against the criteria for the *resolved-topology selection*. These events are required to have at least four small-radius jets, with at least one of them b -tagged. A χ^2 algorithm is used to reconstruct the $t\bar{t}$ system, as described in section 6. The lowest χ^2 value is required to satisfy $\log_{10}(\chi^2) < 0.9$.

The selection efficiencies for MC simulated signal events are given in figure 1, for different models of interest. For reference, the branching ratio for $t\bar{t}$ to electron- or muon-plus-jets is about 17% for each lepton flavour taking into account leptonic tau decays [98]. There are efficiency losses from both the large-radius jet requirements and b -tagging requirement for the boosted-topology selection. For resonance masses above 1.5 TeV, the efficiencies of the resolved selections are relatively insignificant due to the χ^2 requirements and the veto of boosted selections. It can also be seen that efficiency times acceptance is smaller for isolated electrons than isolated muons above the same resonance mass point, due to the inefficiency of electron identification and overlap removal in the boosted environment.

6 Event reconstruction

Signal $t\bar{t}$ resonances should appear in the $m_{t\bar{t}}^{\text{reco}}$ spectrum as an excess of events over the SM expectation clustered around the resonance mass. Events are reconstructed assuming the final state originated from a $t\bar{t}$ decay. To calculate $m_{t\bar{t}}^{\text{reco}}$, the neutrino four-momentum must be determined. The neutrino transverse momentum is taken to be the E_T^{miss} vector. The longitudinal component of the neutrino momentum, p_z , is calculated by constraining the lepton plus missing momentum system to have the W boson mass and solving the resulting quadratic equation in the neutrino's longitudinal momentum p_z [99, 100]. If no real solution exists, the E_T^{miss} vector is varied by the minimal amount required to produce exactly one real solution. If two real solutions are found, the one with the smallest $|p_z|$ is used for the boosted-topology reconstruction, while the choice is made by the χ^2 algorithm described below for the resolved topology.

For the boosted topology, $m_{t\bar{t}}^{\text{reco}}$ is computed from the four-momenta of the neutrino, lepton, the previously selected small-radius jet, j_{sel} , and the highest- p_T large-radius jet. In this case the assignment of jets to the semileptonically decaying top quark and hadronically decaying top quark is unambiguous.

In calculating $m_{t\bar{t}}^{\text{reco}}$ for the resolved topology, a χ^2 algorithm is employed to find the best assignment of jets to the semileptonically and hadronically decaying top quarks. Using the four-momenta of the

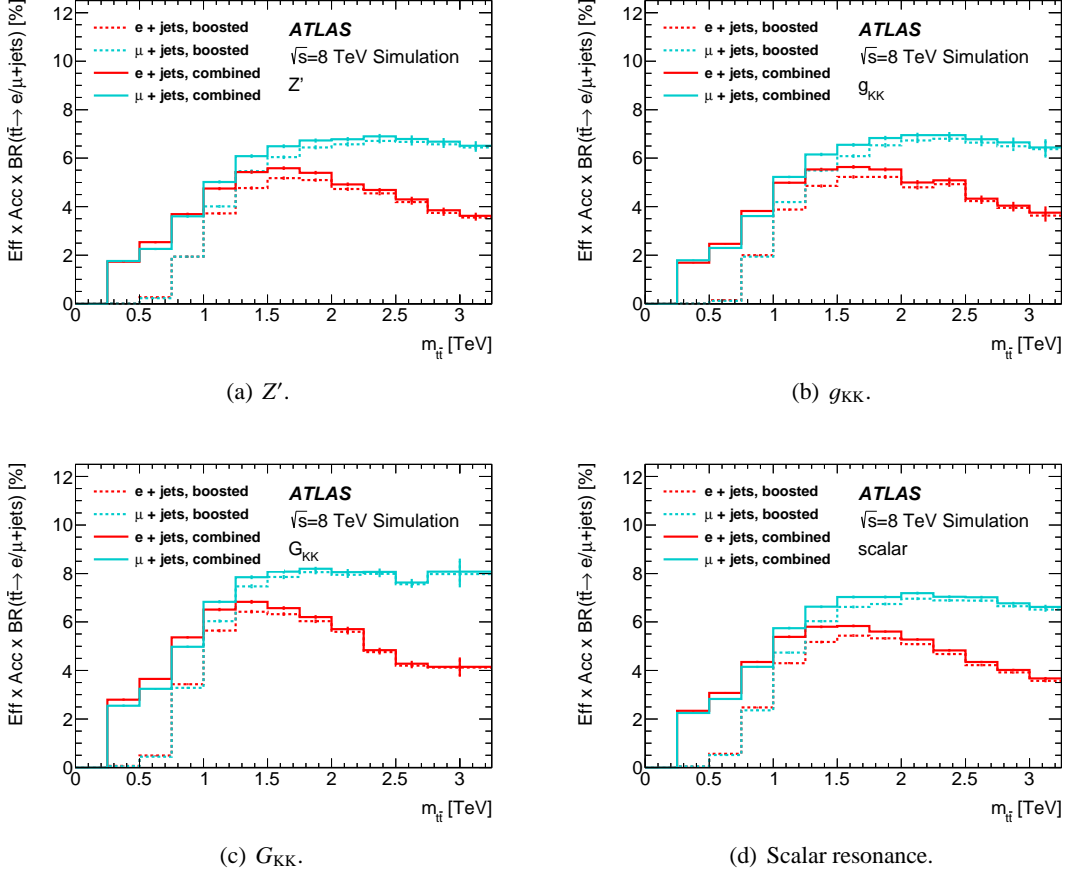


Figure 1: Selection efficiency times acceptance times branching ratio as a function of the top-antitop quark invariant mass $m_{t\bar{t}}$ at Monte Carlo generator level for the different signals in the models considered: (a) Z' , (b) g_{KK} , (c) G_{KK} , (d) scalar resonance. The dashed lines show the boosted-topology selection and the unbroken lines show the combined selection.

neutrino, lepton and all small-radius jets in the event, a χ^2 is defined using the expected top quark and W boson masses:

$$\chi^2 = \left[\frac{m_{jj} - m_W}{\sigma_W} \right]^2 + \left[\frac{m_{jjb} - m_{jj} - m_{h-W}}{\sigma_{h-W}} \right]^2 + \left[\frac{m_{j\ell\nu} - m_{t_\ell}}{\sigma_{t_\ell}} \right]^2 + \left[\frac{(p_{T,jjb} - p_{T,j\ell\nu}) - (p_{T,h} - p_{T,t_\ell})}{\sigma_{\text{diff } p_T}} \right]^2. \quad (1)$$

The first term is a constraint using the mass of the hadronically decaying W boson. The second term is a constraint using the mass difference between the hadronically decaying top quark and the hadronically decaying W boson. Since the mass of the hadronically decaying W boson, m_{jj} , and the mass of the hadronically decaying top quark, m_{jjb} , are highly correlated, the mass of the hadronically decaying W boson is subtracted from the second term so as to decouple it from the first term. The third term is a constraint using the mass of the semileptonically decaying top quark. The last term arises as a constraint on the expected transverse momentum balance between the two decaying top quarks. In the χ^2 definition above, t_h and t_ℓ refer to the hadronically and semileptonically decaying top quarks. The values of the

χ^2 central-value parameters m_W , m_{h-W} , m_{t_ℓ} and $p_{T,h} - p_{T,t_\ell}$, and the values of the width parameters σ_W , σ_{h-W} , σ_{t_ℓ} and $\sigma_{\text{diff}p_T}$ are found through Gaussian fits to the distributions of relevant reconstructed variables, using reconstructible³ MC events with Z' masses from 0.5 to 2.0 TeV. All possible neutrino p_z solutions and jet permutations with at least one b -quark candidate satisfying the b -tagging requirement are tested, and the one with the lowest χ^2 value is adopted. About 80% of these reconstructible events have the correct assignment of reconstructed objects to the hadronically and semileptonically decaying top quarks.

The resulting $m_{t\bar{t}}^{\text{reco}}$ distributions for several signal masses from the resolved- and boosted-topology reconstruction are shown in figures 2 and 3. For these figures, all events satisfying the resolved- or boosted-topology selection criteria are used. The low-mass tails arise from two effects: firstly, extra radiation from the $t\bar{t}$ system that is not included in the reconstruction can shift the reconstructed mass to lower values; secondly, before reconstruction the Breit–Wigner signal shape in $m_{t\bar{t}}$ has a tail at lower values due to the steep fall in parton luminosity with increasing partonic centre-of-mass energy. The former is particularly true for high-mass resonances, while the latter has a larger effect on broad resonances. The experimental resolution for the invariant mass of the $t\bar{t}$ system⁴ is 8% for the resolved-topology selection at a resonance mass of 400 GeV improving to 6% for 1 TeV. It is 6% in the boosted-topology selection, independent of resonance mass.

With hadronically and semileptonically decaying top quarks identified for both the boosted- and resolved-topology selections, three categories of b -tagged events are defined: those in which both decaying top quark candidates have a matching b -jet, those in which only the hadronically decaying top quark candidate has a matching b -jet and those in which only the semileptonically decaying top quark candidate has a matching b -jet. In the boosted-topology selection, the match is defined as either the selected jet, j_{sel} , or a small-radius jet within $\Delta R = 1.0$ of the large-radius jet as being a b -tagged jet. In the resolved-topology selection, the matching is determined by the χ^2 algorithm.

7 Background contributions estimated from data

Data are used to estimate the magnitudes and uncertainties of two important background contributions: W +jets and multi-jet production.

7.1 W +jets scale factors

For the W +jets background, data are used to derive scale factors that are applied to correct the normalisation and flavour fractions given by ALPGEN MC simulations of this background.

For both the resolved- and boosted-topology event selection criteria, the normalisation scale factors are determined by comparing the measured W boson charge asymmetry in data [101, 102] with that predicted by ALPGEN MC simulation. For the resolved topology, all selection criteria are applied to the data except

³ Reconstructible events are those where there is a reconstructed object within $\Delta R = 0.4$ of each visible parton from top decays, and the $\Delta\phi$ between the neutrino and the E_T^{miss} is smaller than 1. Among the events satisfying the final selection criteria, 70% (55%) are reconstructible for Z' mass of 750 GeV (400 GeV).

⁴ The experimental resolution is extracted from a Gaussian fit of the relative difference $\frac{m_{t\bar{t}}^{\text{reco,true-matched}} - m_{t\bar{t}}}{m_{t\bar{t}}}$ from reconstructible events; $m_{t\bar{t}}^{\text{reco,true-matched}}$ is the reconstructed $m_{t\bar{t}}^{\text{reco}}$ computed with the correct combination of jets identified with the parton-level information and $m_{t\bar{t}}$ is the true mass of the $t\bar{t}$ system in the MC simulation.

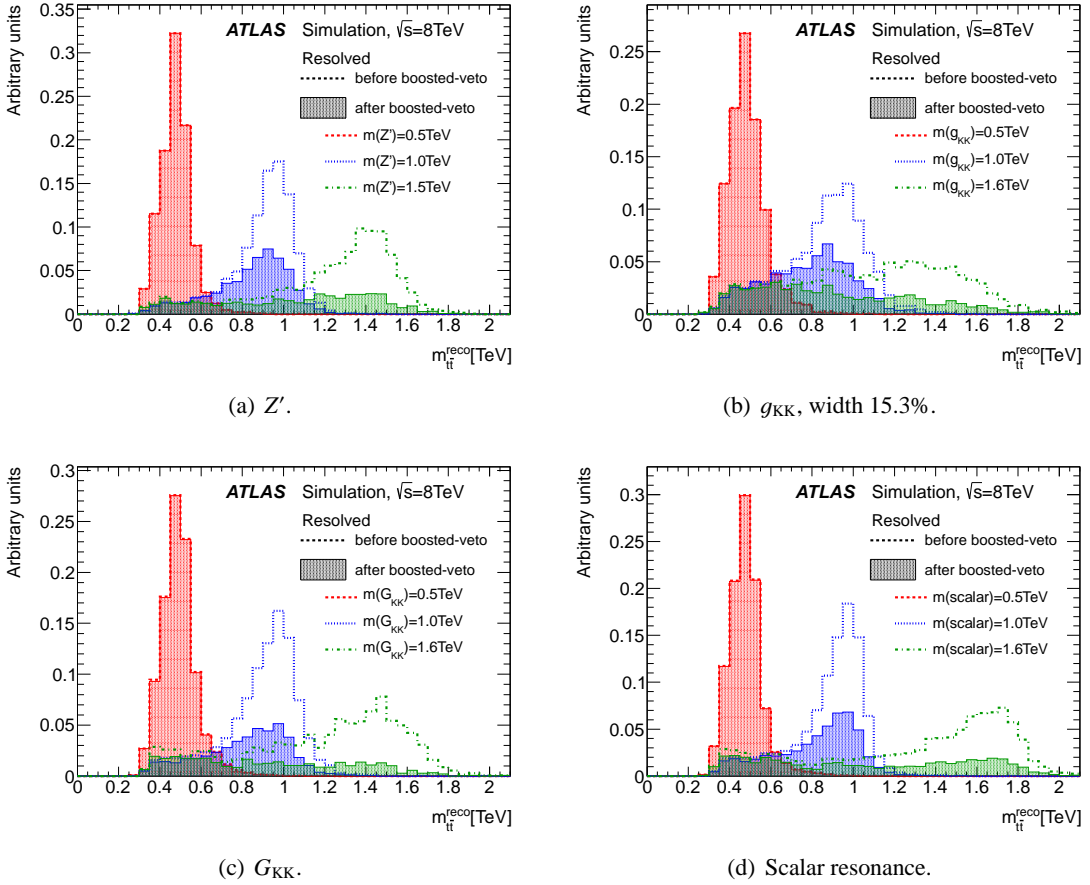


Figure 2: Reconstructed top quark pair invariant mass, $m_{t\bar{t}}^{\text{reco}}$ for the different signal models for events satisfying the resolved-topology selection and using the resolved-topology reconstruction: (a) Z' , (b) g_{KK} , (c) G_{KK} , (d) scalar resonance, before and after the veto on the boosted selection. For each signal, the two histograms are normalised to the same arbitrary luminosity.

for the b -tagging requirement. For the boosted topology, in order to decrease the statistical uncertainty on the scale factors, a relaxed set of selection criteria that does not include the b -tagging, $\Delta\phi(\text{jet}, \ell) > 2.3$, jet mass and $\sqrt{d_{12}}$ requirements is used. Any bias induced by relaxing the criteria for the boosted selection is found to be negligible compared to the statistical uncertainty in the scale factor determination. The total number of W +jets events in data, $N_{W^+} + N_{W^-}$, is given by:

$$N_{W^+} + N_{W^-} = \left(\frac{r_{\text{MC}} + 1}{r_{\text{MC}} - 1} \right) (D_{\text{corr}^+} - D_{\text{corr}^-}), \quad (2)$$

where r_{MC} is the ratio given by MC simulation of the number of W +jets events with a positively charged lepton to that with a negatively charged lepton and $D_{\text{corr}^+(-)}$ is the number of observed events with a positively (negatively) charged lepton. Contributions to $D_{\text{corr}^+(-)}$ from charge-asymmetric processes such as single top, WZ and $t\bar{t}+W$ boson production are estimated from MC simulation and are subtracted. Contributions from charge-symmetric processes such as $t\bar{t}$ production cancel in the difference on the right-hand side of eq. (2). A scale factor, C_A , applied to the MC simulated samples of W + jets events is then calculated as the ratio of $N_{W^+} + N_{W^-}$ evaluated from data to that predicted from MC simulation.

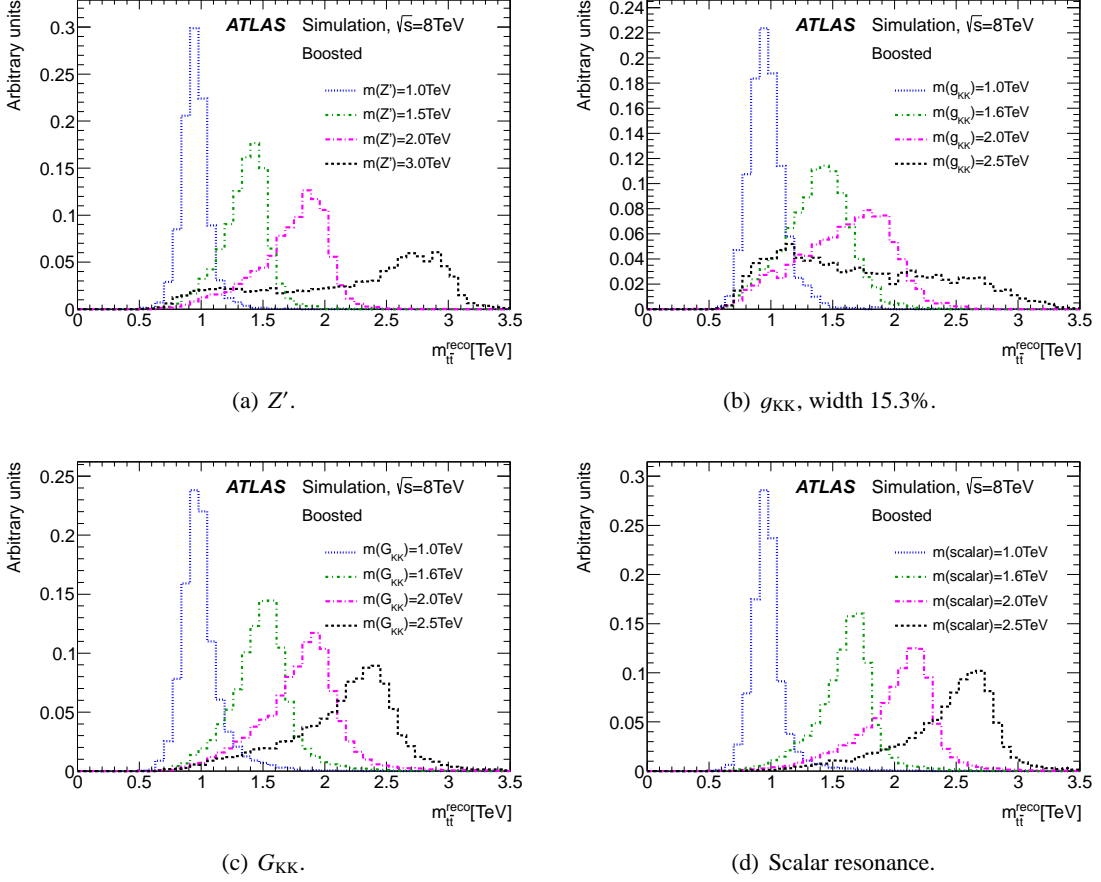


Figure 3: Reconstructed $t\bar{t}$ invariant mass for the different signal models for events satisfying the boosted-topology selection and using the boosted-topology reconstruction: (a) Z' , (b) g_{KK} , (c) G_{KK} , (d) scalar resonance.

The value and statistical uncertainty obtained for C_A in the electron (muon) channel are 1.026 ± 0.011 (0.978 ± 0.010) with the resolved selection, and 0.89 ± 0.06 (0.81 ± 0.05) with the boosted selection.

Scale factors for the relative fraction of heavy-flavour contributions from $W + b\bar{b}$, $W + c\bar{c}$, $W + c$ are also determined from data [102–104]. In determining these scale factors, events are required to satisfy all selection criteria common to the boosted- and resolved- topology selections. Exactly two small-radius jets are required without any b -tagging requirement.

The flavour fractions for $W + b\bar{b}$, $W + c\bar{c}$, $W + c$ and W +light-quark flavours are first determined from MC simulation for this sample. The ratio of the $W + b\bar{b}$ to $W + c\bar{c}$ contribution is taken from MC simulation and fixed at that value. A system of three equations is used to fit to the two-jet data sample with at least one b -tagged jet in order to determine correction factors for each of the flavour fractions determined from MC simulation:

$$\begin{pmatrix} C_A \cdot (N_{MC,W^-}^{b\bar{b}} + N_{MC,W^-}^{c\bar{c}}) & C_A \cdot N_{MC,W^-}^c & C_A \cdot N_{MC,W^-}^{\text{light}} \\ (f_{b\bar{b}} + f_{c\bar{c}}) & f_c & f_{\text{light}} \\ C_A \cdot (N_{MC,W^+}^{b\bar{b}} + N_{MC,W^+}^{c\bar{c}}) & C_A \cdot N_{MC,W^+}^c & C_A \cdot N_{MC,W^+}^{\text{light}} \end{pmatrix} \cdot \begin{pmatrix} K_{b\bar{b},c\bar{c}} \\ K_c \\ K_{\text{light}} \end{pmatrix} = \begin{pmatrix} D_{W^-} \\ 1.0 \\ D_{W^+} \end{pmatrix} \quad (3)$$

where D_{W^\pm} is the expected number of W +jets events with a positively charged or negatively charged lepton in the data. The flavour fraction is f_{flavour} , and the correction factor for a given flavour component is K_{flavour} . The different flavour labels are $b\bar{b}$, $c\bar{c}$, c , and light corresponding to $W + b\bar{b}$, $W + c\bar{c}$, $W + c$, and W +light-jets respectively. The numbers of positively charged and negatively charged leptons in the data are found by subtracting all non- W +jets contributions, which are determined from MC simulations as 35% (15%) of the selected events for the electron (muon) channel. An iterative process is used to find the K_{flavour} factors, which are then used to correct the corresponding flavour fractions f_{flavour} that are applied during the C_A factor calculation. In this iterative process, only the K_{flavour} and C_A factors are allowed to vary. The K_{flavour} factors are initially set to unity, thus altering the C_A factor calculation. New correction factors K_{flavour} are calculated by inverting eq. (3), and then the process is repeated ten times, with each repetition using the correction factors determined from the previous one. It was checked that using more than ten iterations produces only negligible changes in the extracted correction factors.

The correction factors found for the two-jet sample are extrapolated to higher jet multiplicities by keeping the same ratios between them while conserving the normalisation in each jet multiplicity bin. The K_{flavour} factors thus obtained are different from unity. For events containing electrons (muons), the extracted values and statistical uncertainties of $K_{b\bar{b}}$ and $K_{c\bar{c}}$ are 1.36 ± 0.07 (1.51 ± 0.08), K_c is 0.71 ± 0.03 (0.66 ± 0.03), and K_{light} is 0.934 ± 0.005 (0.873 ± 0.004).

This method reduces the systematic uncertainties (from the jet energy scale, b -tagging and other uncertainties) compared to using W +jets MC simulation alone. Systematic uncertainties in the W +jets normalisation and flavour-fraction corrections are determined by rederiving these scale factors when a given systematic effect is applied. The new scale factors are then used in producing the $m_{\ell\bar{\ell}}^{\text{reco}}$ mass spectrum for that particular systematic uncertainty.

7.2 Multijet estimate

The multi-jet background in events satisfying the resolved or boosted selection criteria consists of events with a jet that is misreconstructed as a lepton or with a non-prompt lepton that satisfies the identification criteria. The normalisation, $m_{\ell\bar{\ell}}^{\text{reco}}$ shape, and statistical and systematic uncertainties associated with the multi-jet background are estimated from data using a *matrix method* [103, 105].

The matrix method utilises efficiencies for leptons produced by prompt and non-prompt sources. The efficiency f is defined as the probability that a non-prompt lepton from multi-jet production that satisfies the loose identification criteria [105] also satisfies the tight identification criteria. It is derived from data in control regions dominated by multi-jet events, with prompt-lepton contributions subtracted based on MC simulations. The efficiency ϵ is defined as the probability that a lepton from prompt sources (W or Z bosons) that satisfies the loose identification criteria also satisfies the tight identification criteria. It is determined using SM MC samples with a mixture of processes similar to that in the signal region, corrected using data versus MC correction factors derived from $Z \rightarrow \ell\bar{\ell}$ events.

The number of multi-jet background events satisfying the resolved or boosted selection criteria is estimated using data events that satisfy all selection criteria, except that the loose lepton identification criteria are used. This sample contains prompt as well as non-prompt leptons.

The number of events with leptons satisfying the loose identification criteria, N_L is defined as

$$N_L = N_{\text{prompt}} + N_{\text{multi-jet}} \quad (4)$$

where N_{prompt} is the number of events with prompt leptons satisfying the loose identification criteria and $N_{\text{multi-jet}}$ is the number of events satisfying the loose identification criteria with leptons from other sources. The number of events satisfying the tight identification criteria, N_{T} is then

$$N_{\text{T}} = \epsilon \times N_{\text{prompt}} + f \times N_{\text{multi-jet}}. \quad (5)$$

Solving these two equations for N_{prompt} and $N_{\text{multi-jet}}$ gives the multi-jet contribution from events satisfying all the selection criteria.

Good shape modelling of the $m_{\ell\bar{\ell}}^{\text{reco}}$ distributions is achieved by parameterising the efficiencies as functions of relevant kinematic variables, and validated in the multi-jet control regions. Systematic uncertainties are evaluated using several different definitions of multi-jet control regions that result in slightly different f estimations. Systematic uncertainties associated with object reconstruction and MC simulation are also considered, resulting in a total normalisation uncertainty of 20%.

8 Systematic uncertainties

The systematic uncertainties can be broadly divided into two categories: uncertainties that affect reconstructed objects (such as jets) and uncertainties that affect the modelling of certain background or signal processes. Some of the uncertainties affect both the shape and the normalisation of the $m_{\ell\bar{\ell}}^{\text{reco}}$ spectra, while others affect the normalisation only. In table 1, an overview of the effects of the dominant systematic uncertainties on the background and signal yields is given. Only the impact on the overall normalisation is shown in the table, but some of the systematic uncertainties have a significant dependence on the reconstructed $t\bar{t}$ mass, which is fully taken into account in the analysis for all of these uncertainties. The systematic uncertainties with the strongest dependence are those from the jet energy scale, parton distribution functions and b -jet identification.

The dominant uncertainty on the normalisation of the total background estimate is the NNLO+NNLL $t\bar{t}$ cross-section uncertainty of 6.5%. This uncertainty includes renormalisation and factorisation scale uncertainties, combined PDF and strong-coupling uncertainties evaluated following the PDF4LHC [106] recommendations, and uncertainties associated with the value of the top quark mass. The combined PDF and strong-coupling uncertainties are extracted for each of the three PDF sets: MSTW2008 68% confidence level (CL) NNLO [43, 107], CT10 NNLO [52, 108] and NNPDF2.3 NNLO [109]; the total uncertainty associated with the PDF and strong-coupling uncertainties is one half of the size of the envelope of the three resultant error bands, with the central prediction being the midpoint of the envelope. Variations from changing the top quark mass by ± 1.0 GeV are added in quadrature to the scale uncertainties, and combined PDF and strong-coupling uncertainties.

The W +jets normalisation, determined using data, is separately evaluated for each experimental source of systematic uncertainty. An additional systematic uncertainty on the prediction is evaluated by using the simulated samples generated with varied ALPGEN matching parameters. The normalisation uncertainty on the multi-jet background is 20%, as described in section 7.

The single-top-quark background normalisation uncertainty is 7.7% [74–76]. The normalisation uncertainty on the Z +jets sample is 48%, estimated using Berends–Giele scaling [110]. The diboson normalisation uncertainty is 34%, which is a combination of the NLO PDF and scale uncertainties, and additional uncertainties from the requirements on the jet multiplicity.

Table 1: Average impact of the dominant systematic uncertainties on the total background yield and on the estimated yield for a Z' sample with $m = 1.75$ TeV. The electron and muon channel spectra are added. Any shift in yield is given in percent of the nominal value. Certain systematic uncertainties are not applicable to the Z' samples, which is indicated with a bar (–) in the table.

Systematic Uncertainties	Resolved selection yield impact [%]		Boosted selection yield impact [%]	
	total bkg.	Z'	total bkg.	Z'
Luminosity	2.5	2.8	2.6	2.8
PDF	2.4	3.6	4.7	2.3
ISR/FSR	3.7	–	1.2	–
Parton shower and fragmentation	4.8	–	1.5	–
$t\bar{t}$ normalisation	5.3	–	5.5	–
$t\bar{t}$ EW virtual correction	0.2	–	0.5	–
$t\bar{t}$ generator	0.3	–	2.6	–
$t\bar{t}$ top quark mass	0.6	–	1.4	–
W +jets generator	0.3	–	0.1	–
Multi-jet normalisation, e +jets	0.5	–	0.2	–
Multi-jet normalisation, μ +jets	0.1	–	< 0.1	–
JES+JMS, large-radius jets	0.1	2.1	9.7	2.8
JER+JMR, large-radius jets	< 0.1	0.3	1.0	0.2
JES, small-radius jets	5.6	2.6	0.4	1.4
JER, small-radius jets	1.8	1.4	< 0.1	0.2
Jet vertex fraction	0.8	0.8	0.2	< 0.1
b -tagging b -jet efficiency	1.1	2.0	2.9	17.1
b -tagging c -jet efficiency	0.1	0.7	0.1	2.1
b -tagging light-jet efficiency	< 0.1	< 0.1	0.5	0.2
Electron efficiency	0.3	0.6	0.6	1.3
Muon efficiency	0.9	1.0	1.0	1.1
MC statistical uncertainty	0.4	6.0	1.3	1.8
All systematic uncertainties	10.8	8.8	13.4	18.0

The uncertainty on the integrated luminosity is 2.8%. It is derived, following the same methodology as that detailed in Ref. [111], from a preliminary calibration of the luminosity scale derived from beam-separation scans performed in November 2012. This uncertainty is applied to all signal and background samples except multi-jet and W +jets, which are estimated from data.

The effect of the PDF uncertainty on all MC samples is estimated by taking the envelope of the NNPDF2.3, MSTW2008NLO and CT10 PDF set uncertainties at 68% CL⁵ following the PDF4LHC recommendation and normalising to the nominal cross-section. The PDF uncertainty on the $t\bar{t}$ mass spectrum has a much larger effect on the boosted sample than on the resolved sample. The effect on the total background yield is 2.1% (4.2%) after the resolved (boosted) selection. The size of the uncertainty grows with reconstructed mass, attaining values of 50% above 2 TeV in the boosted selection.

One of the dominant uncertainties affecting reconstructed objects is the jet energy scale (JES) uncertainty, especially for large-radius jets [91, 92]. Uncertainties on the jet mass scale (JMS) and the k_t splitting scales [92] are also important for this analysis. These uncertainties have an impact of 10% on the overall background yield in the boosted selection. The impact on the background estimates falls with increasing $m_{t\bar{t}}^{\text{reco}}$, varying from 22% at lowest masses to about 7% above 1.5 TeV. The impact is smaller for the

⁵ The CT10 PDF uncertainties are scaled down by a factor 1.645 to reach an approximate 68% CL.

resolved selection, since the large-radius jets are only used indirectly there via the vetoing of events that satisfy the boosted selection. For large-radius jets, uncertainties on the jet energy resolution (JER) and jet mass resolution (JMR) are also considered. These are less significant than the JES. For small-radius jets, the uncertainties on the JES, the jet reconstruction efficiency and the jet energy resolution are considered [88, 90]. The small-radius JES uncertainty is one of the most significant systematic uncertainties in the resolved selection, affecting the overall expected yield by 6%. The effect of uncertainties associated with the jet vertex fraction is also considered. The b -tagging uncertainty is modelled through simultaneous variations of the uncertainties on the efficiency and rejection [112, 113]. An additional b -tagging uncertainty⁶ is applied for high-momentum jets ($p_T > 300$ GeV) to account for uncertainties on the modelling of the track reconstruction in high- p_T environments, which is one of the dominant uncertainties for high-mass signals.

For the leptons, the uncertainties on the isolation efficiency, the single-lepton trigger and the reconstruction efficiency are estimated using $Z \rightarrow ee$ and $Z \rightarrow \mu\mu$ events. In addition, high-jet-multiplicity $Z \rightarrow \ell\ell$ events are studied, from which extra uncertainties on the isolation efficiency are assigned to account for the difference between Z and $t\bar{t}$ events. Uncertainties on the E_T^{miss} reconstruction, as well as on the energy scale and resolution of the leptons, are also considered, and generally have a smaller impact on the yield and the search sensitivity than the uncertainties mentioned above.

The uncertainty on the $t\bar{t}$ background due to uncertainties on the modelling of QCD initial- and final-state radiation (ISR/FSR) is estimated using ACERMC v3.8 [114] plus PYTHIA v6.426 MC samples by varying the PYTHIA ISR and FSR parameters within ranges allowed by a previous ATLAS measurement of $t\bar{t}$ production with a veto on additional central jet activity [115]. The QED ISR/FSR uncertainty is negligible at this level. The dependency of the $m_{t\bar{t}}^{\text{reco}}$ shape on the choice of NLO generator is accounted for by using the difference between samples generated with MC@NLO and POWHEG-Box+HERWIG as a systematic uncertainty. The parton showering and fragmentation uncertainty on the $t\bar{t}$ background is estimated by comparing the results from a sample generated with POWHEG-Box [48], interfaced with PYTHIA or HERWIG. The uncertainty on the $m_{t\bar{t}}^{\text{reco}}$ distribution arising from the uncertainty in the top quark mass is evaluated by comparing the $m_{t\bar{t}}^{\text{reco}}$ spectrum using the nominal sample to those generated with top quark masses of 170 and 175 GeV, and multiplying the difference by 0.4 (to approximate a one standard deviation uncertainty, corresponding to ± 1.0 GeV). The uncertainty on the electroweak corrections to top quark pair production is modelled by changing the difference of each correction factor from unity by $\pm 10\%$.

For the W +jets background, the uncertainty on the $m_{t\bar{t}}^{\text{reco}}$ distribution is estimated by reweighting the events to the kinematics of MC samples generated with a different matching scale or functional form of the factorisation scale [69].

9 Comparison of data with expected background contributions

After all event selection criteria are applied, 223,330 events remain for the resolved topology and 8,206 events are selected for the boosted topology. The event yields from data and from expected background processes are listed in table 2 together with the associated systematic uncertainties.

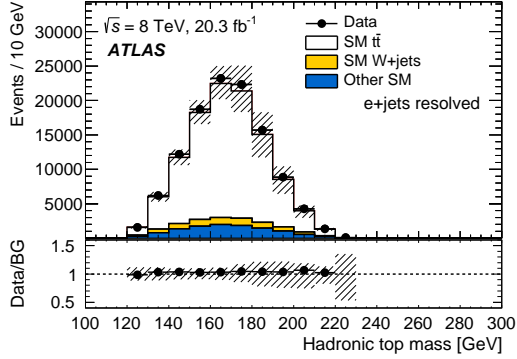
⁶ The additional b -tagging uncertainty is an extrapolation of the uncertainty from regions of lower p_T . Depending on the p_T of the jet, it is approximately 12% to 33% for b -jets and 17% to 30% for c -jets, added in quadrature to the uncertainty on the jet b -tagging efficiency correction factor for the 200–300 GeV region.

Table 2: Data and expected background event yields after the resolved and boosted selections. The sum in quadrature of all systematic uncertainties on the expected background yields is also given.

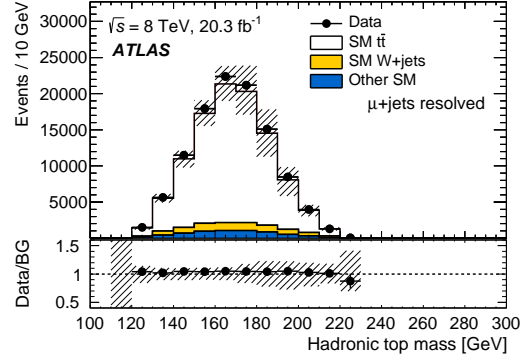
Resolved-topology selection			
Type	e +jets	μ +jets	Sum
$t\bar{t}$	$93,000 \pm 11,000$	$91,000 \pm 11,000$	$184,000 \pm 22,000$
Single top	$3,800 \pm 500$	$3,800 \pm 500$	$7,600 \pm 1,000$
$t\bar{t}V$	274 ± 40	267 ± 40	541 ± 80
Multi-jet e	$5,300 \pm 1,100$	–	$5,300 \pm 1,100$
Multi-jet μ	–	$1,050 \pm 240$	$1,050 \pm 240$
W +jets	$6,600 \pm 800$	$7,100 \pm 800$	$13,700 \pm 1,500$
Z +jets	$1,400 \pm 750$	650 ± 340	$2,000 \pm 1,080$
Dibosons	320 ± 120	310 ± 120	620 ± 240
Total	$110,000 \pm 12,000$	$105,000 \pm 12,000$	$215,000 \pm 24,000$
Data	114,377	108,953	223,330
Boosted-topology selection			
Type	e +jets	μ +jets	Sum
$t\bar{t}$	$4,100 \pm 600$	$4,000 \pm 600$	$8,100 \pm 1,200$
Single top	138 ± 20	154 ± 20	290 ± 40
$t\bar{t}V$	37 ± 6	38 ± 7	75 ± 13
Multi-jet e	91 ± 18	–	91 ± 18
Multi-jet μ	–	8.6 ± 1.6	8.6 ± 1.6
W +jets	260 ± 50	290 ± 50	550 ± 100
Z +jets	31 ± 16	17 ± 9	48 ± 25
Dibosons	21 ± 8	20 ± 8	41 ± 16
Total	$4,700 \pm 600$	$4,500 \pm 600$	$9,200 \pm 1,200$
Data	4,148	4,058	8,206

Good agreement is observed between the data and the total expected background. Figure 4 shows the reconstructed mass of the semileptonically and hadronically decaying top quark candidates, and the mass of the hadronically decaying W boson candidate for the resolved selection. The equivalent distributions for the boosted selection are the mass of the semileptonically decaying top quark candidate and the mass of the large-radius jet; both are shown in figure 5. Figure 6 shows the distribution of the transverse momentum and first k_t splitting scale of the selected large-radius jets.

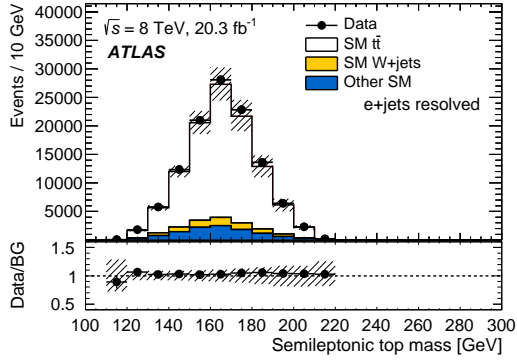
The $t\bar{t}$ invariant mass spectra for the resolved and the boosted selections in the electron and muon channels, separated by b -tagging category, are shown in figures 7 and 8. Figure 9 shows the $t\bar{t}$ invariant mass spectrum for all channels added together. The data generally agree with the expected background with slight shape differences seen especially in the high-mass regions; these deviations are consistent with the uncertainties.



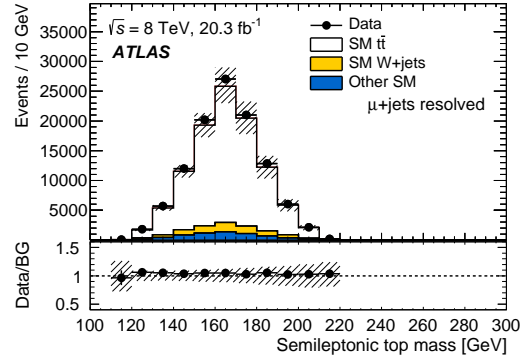
(a) e +jets channel.



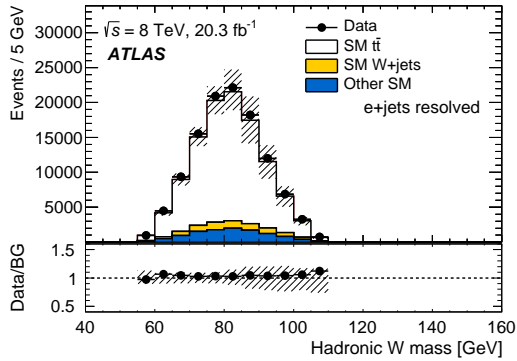
(b) μ +jets channel.



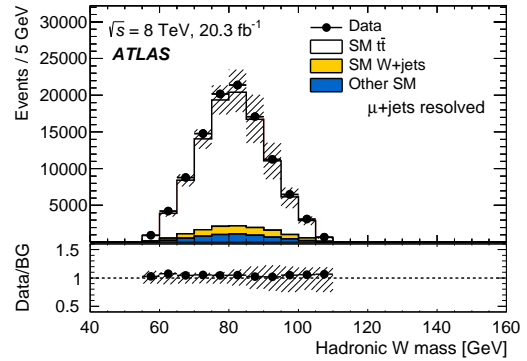
(c) e +jets channel.



(d) μ +jets channel.

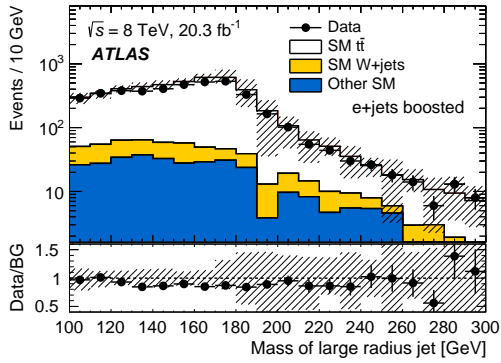


(e) e +jets channel.

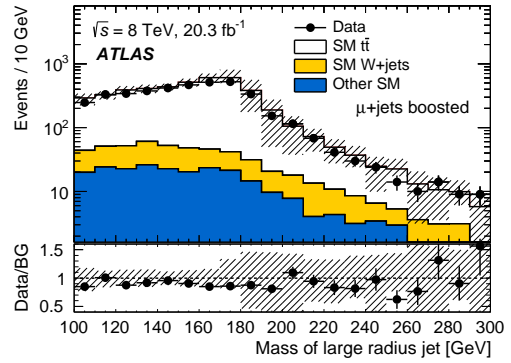


(f) μ +jets channel.

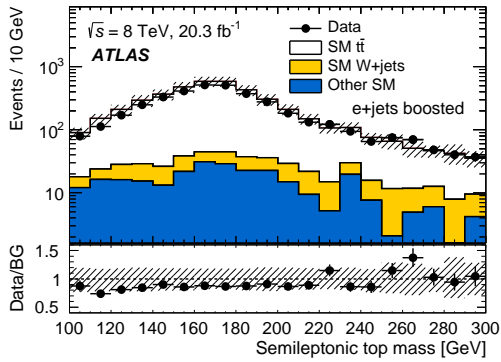
Figure 4: Reconstructed mass of the hadronically decaying top quark candidate, semileptonically decaying top quark candidate, and hadronically decaying W -boson candidate after the resolved-topology selection in the electron and muon channels. The SM background components are shown as stacked histograms. The shaded areas indicate the total systematic uncertainties.



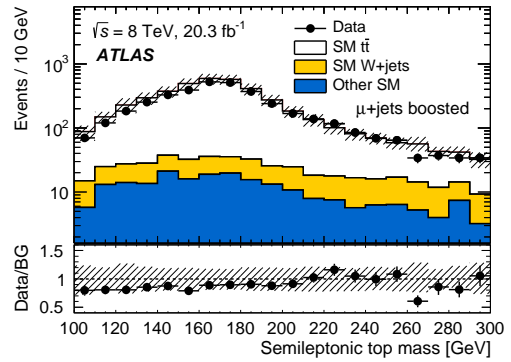
(a) e +jets channel.



(b) μ +jets channel.

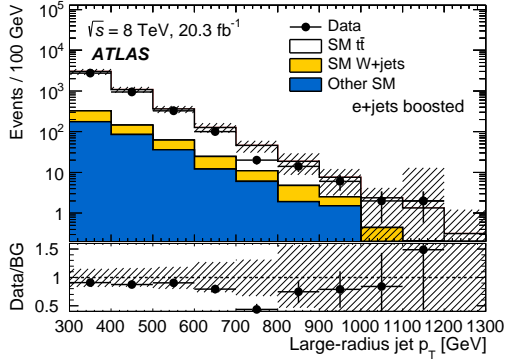


(c) e +jets channel.

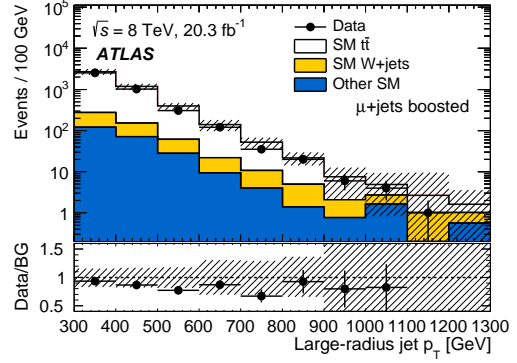


(d) μ +jets channel.

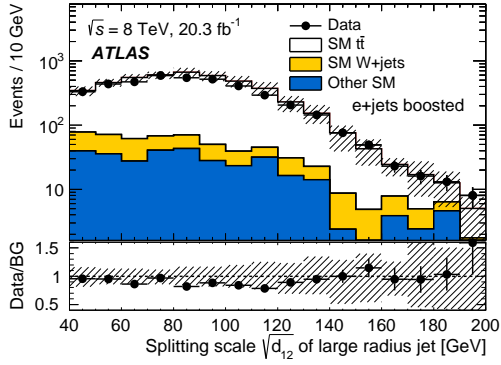
Figure 5: The invariant mass of the large-radius jets and the invariant mass of the semileptonically decaying top quark candidate, after the boosted selection. The SM background components are shown as stacked histograms. The shaded areas indicate the total systematic uncertainties.



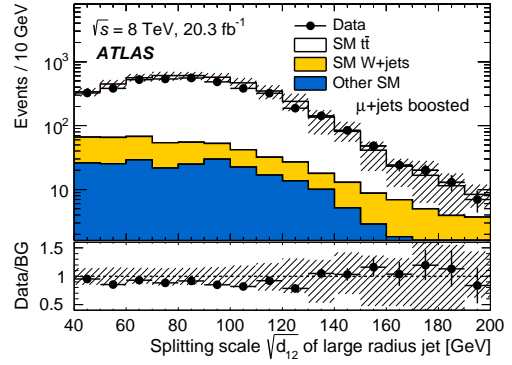
(a) e +jets channel.



(b) μ +jets channel.

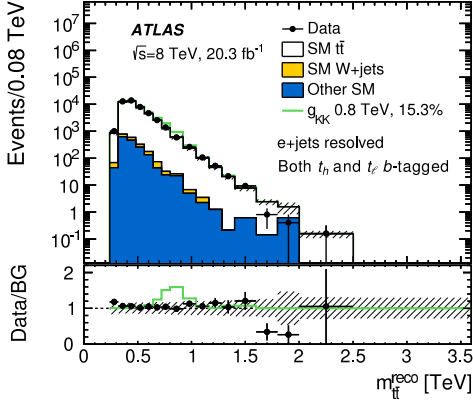


(c) e +jets channel.

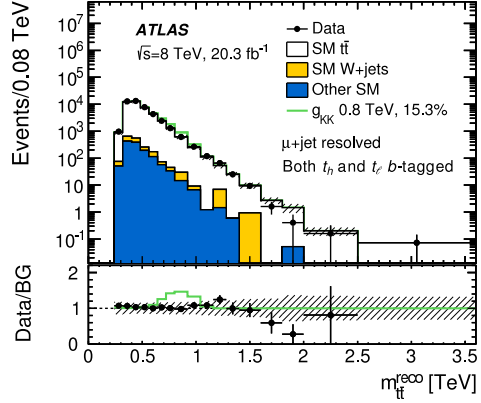


(d) μ +jets channel.

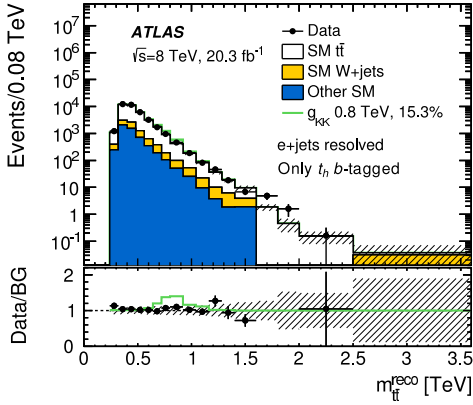
Figure 6: The transverse momentum, p_T , and first k_t splitting scale, $\sqrt{d_{12}}$, of the large-radius jet after the boosted selection. The SM background components are shown as stacked histograms. The shaded areas indicate the total systematic uncertainties.



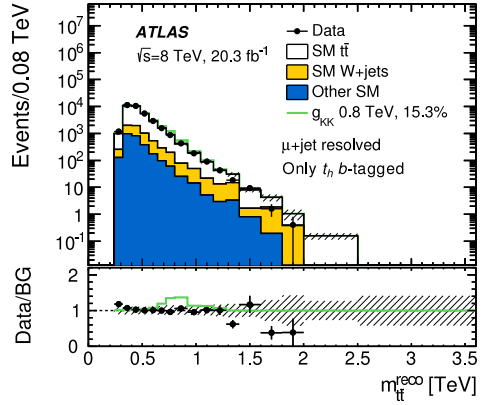
(a) Electron channel, resolved selection, both top candidates have b -tagged jets.



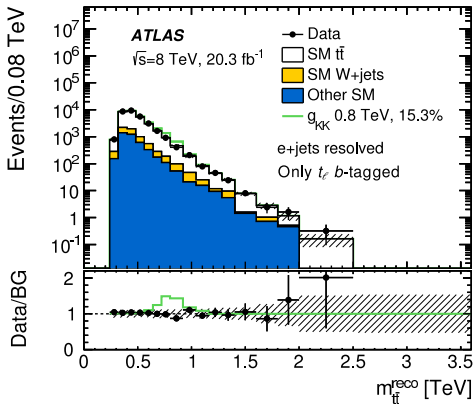
(b) Muon channel, resolved selection, both top candidates have b -tagged jets.



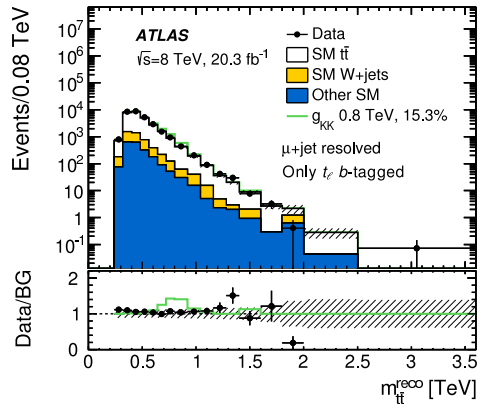
(c) Electron channel, resolved selection, only the hadronic top candidate has a b -tagged jet.



(d) Muon channel, resolved selection, only the hadronic top candidate has a b -tagged jet.

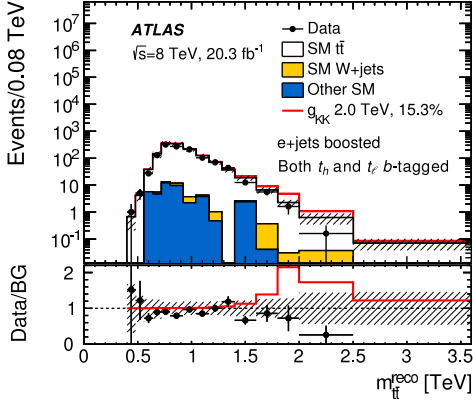


(e) Electron channel, resolved selection, only the semileptonic top candidate has a b -tagged jet.

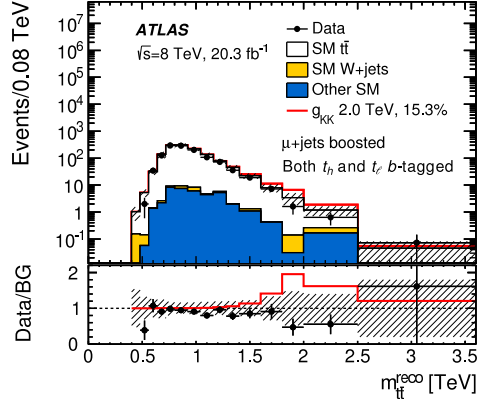


(f) Muon channel, resolved selection, only the semileptonic top candidate has a b -tagged jet.

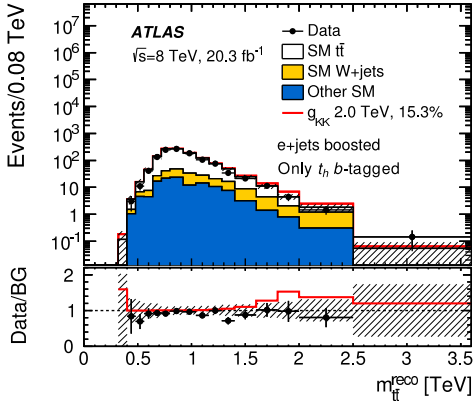
Figure 7: The spectrum of the reconstructed $t\bar{t}$ invariant mass, $m_{t\bar{t}}^{\text{reco}}$, for the different channels, before any nuisance parameter fit, after the resolved-topology selection. The SM background components are shown as stacked histograms. The shaded areas indicate the total systematic uncertainties. The green line shows the expected distribution for a hypothetical g_{KK} of mass 0.8 TeV, width 15.3%.



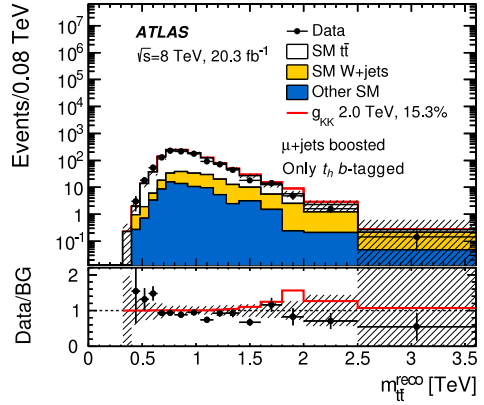
(a) Electron channel, boosted selection, both top candidates have b -tagged jets.



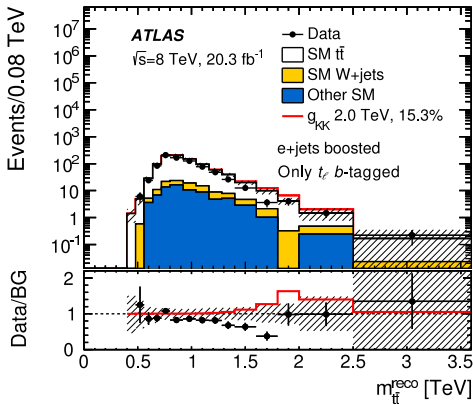
(b) Muon channel, boosted selection, both top candidates have b -tagged jets.



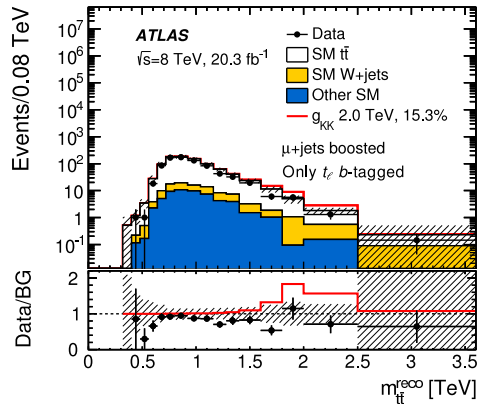
(c) Electron channel, boosted selection, only the hadronic top candidate has a b -tagged jet.



(d) Muon channel, boosted selection, only the hadronic top candidate has a b -tagged jet.

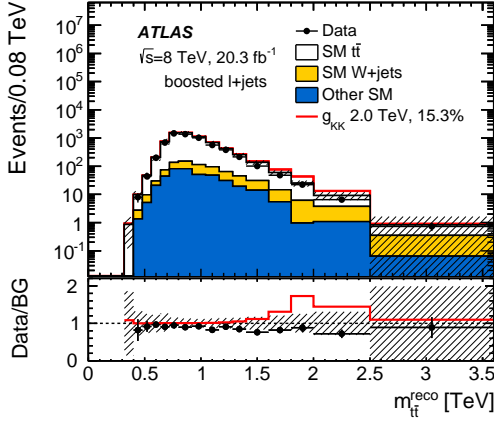


(e) Electron channel, boosted selection, only the semileptonic top candidate has a b -tagged jet.

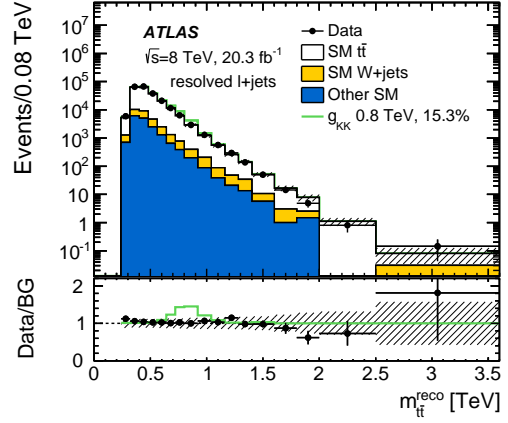


(f) Muon channel, boosted selection, only the semileptonic top candidate has a b -tagged jet.

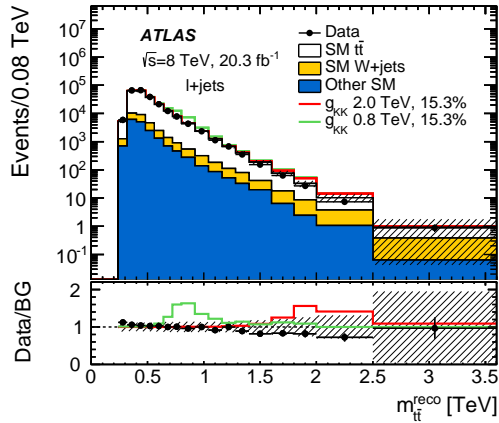
Figure 8: The $m_{\bar{t}t}^{\text{reco}}$ spectrum for the different channels, before any nuisance parameter fit, after the boosted-topology selection. The SM background components are shown as stacked histograms. The shaded areas indicate the total systematic uncertainties. The red line shows the expected distribution for a hypothetical g_{KK} of mass 2.0 TeV, width 15.3%.



(a) Boosted selections.



(b) Resolved selections.



(c) All selections.

Figure 9: The $m_{t\bar{t}}^{\text{reco}}$ distributions, before any nuisance parameter fit, summed over (a) all 6 boosted channels, (b) all 6 resolved channels, and (c) all 12 channels compared with data. The SM background components are shown as stacked histograms. The shaded areas indicate the total systematic uncertainties. The red (green) line shows the expected distribution for a hypothetical g_{KK} of mass 2.0 (0.8) TeV, width 15.3%.

10 Results

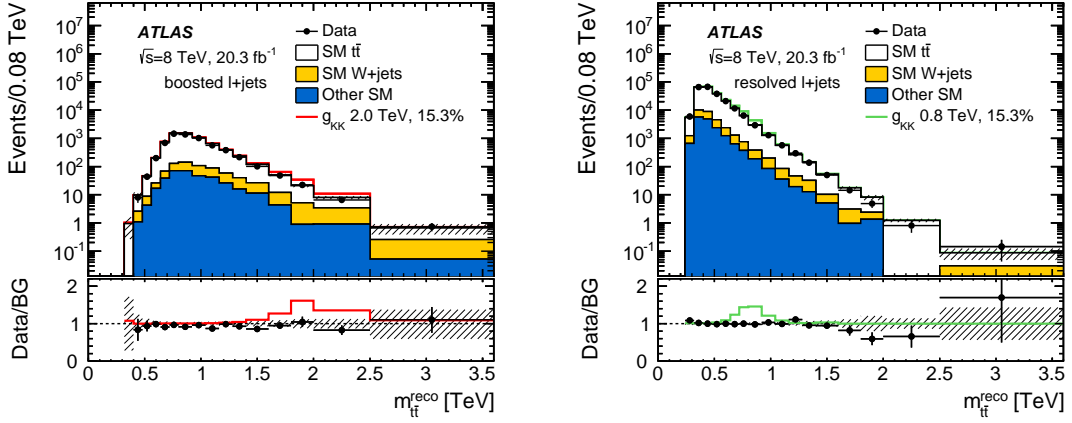
The final discriminating observables that are used to search for a massive resonance are the twelve $t\bar{t}$ invariant mass spectra: three b -tag categories for two selections and two decay channels. After the reconstruction of the $t\bar{t}$ mass spectra, the data and expected background distributions are compared using BUMP HUNTER [116], which is a hypothesis-testing tool that searches the data for local excesses or deficits compared to the expected background, taking the look-elsewhere effect [117] into account over the full mass spectrum. The search is performed on three combinations of the spectra: the six channels of the resolved selections, the six channels of the boosted selections and the twelve channels. The most significant deviation of the data from the expected background spectrum is required to appear at the same place in each of the channels of a combination. After accounting for the systematic uncertainties, no significant deviation from the total expected background is found. Upper limits are set on the cross-section times branching ratio for each of the signal models using a profile likelihood-ratio test. The CL_s prescription [118] is used to derive one-sided 95% CL limits. The results are obtained using the HIST-FITTER [119] framework with all spectra from the 12 channels, excluding bins with few events with $m_{t\bar{t}}^{\text{reco}}$ below 400 GeV in the boosted channels or above 2 TeV in the resolved channels.

The statistical and systematic uncertainties on the expected distributions are included in this CL_s procedure as nuisance parameters in the likelihood fits. The nuisance parameters for the systematic uncertainties are constrained by a Gaussian probability density function with a width corresponding to the size of the uncertainty considered. Correlations between different channels and bins are taken into account. The product of the various probability density functions forms the likelihood function that is maximised in the fit by adjusting the free parameter (the signal strength) and nuisance parameters. The expected $m_{t\bar{t}}^{\text{reco}}$ distributions are compared to data in figure 10 after a fit of nuisance parameters under the background-only hypothesis. It can be seen that the uncertainties are smaller than in figure 9 and that the procedure is able to produce a good-quality fit to the data.

The expected and observed limits using different signal models are presented in figure 11. Here the expected limits are obtained by taking the nominal background estimates as the expected data. For the Z'_{TC2} benchmark, limits on the production cross-sections vary from 4.2 pb to 0.03 pb for masses from 0.4 TeV to 3 TeV. A Z'_{TC2} of width 1.2% is excluded for masses less than 1.8 TeV, while masses below 2.0 TeV are expected to be excluded. The Z'_{TC2} mass limits are stronger for a width of 2% (3%), reaching 2.0 TeV (2.3 TeV). For the g_{KK} benchmark, limits on the production cross-sections vary from 4.8 pb for a mass of 0.4 TeV, to 0.09 pb for a mass of 3 TeV. A g_{KK} of width 15.3% is excluded for masses less than 2.2 TeV, while masses below 2.3 TeV are expected to be excluded. The cross-section limits in the G_{KK} model range from 2.5 pb for a mass of 0.4 TeV to 0.03 pb for 2.5 TeV, with no mass range excluded in the benchmark scenario. The cross-section limits on a narrow scalar resonance range from 3.0 pb for a mass of 0.4 TeV to 0.03 pb for 2.5 TeV. The cross-section limits are generally stronger for the latter two benchmark models than those for the spin-1 resonances due to higher acceptance.

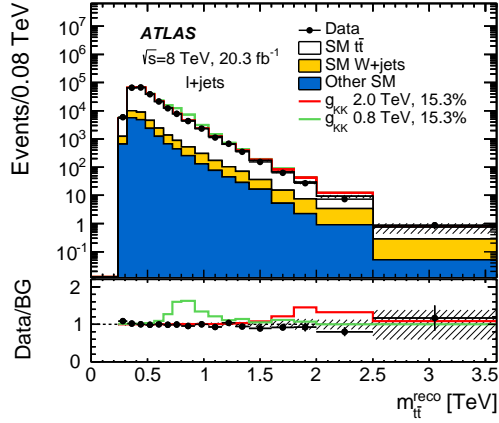
The width dependence of the cross-section limits was also evaluated for the g_{KK} models. The results are presented in figure 12. For a 1 TeV resonance, the limits weaken by approximately a factor of two as the width increases from 10% to 40%. The effect is stronger for 2 TeV and 3 TeV resonances, where the limits weaken by a factor of three over this width range.

The observed upper limits on the cross-section times $t\bar{t}$ branching ratio are larger than the expected limits, especially for $t\bar{t}$ resonance masses greater than 1.8 TeV. This arises from the use of the profile likelihood method which allows the data to constrain the systematic uncertainties using the full $m_{t\bar{t}}^{\text{reco}}$ distribution,



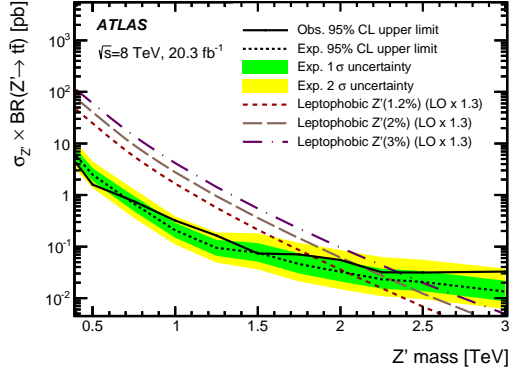
(a) Boosted selections.

(b) Resolved selections.

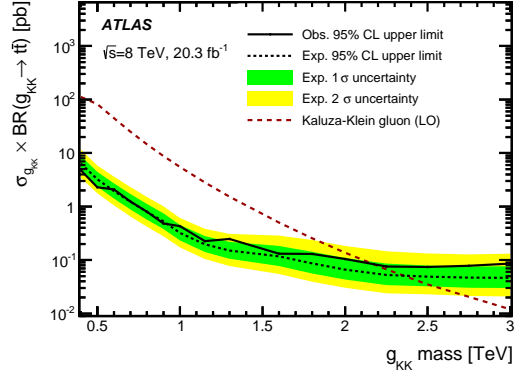


(c) All selections.

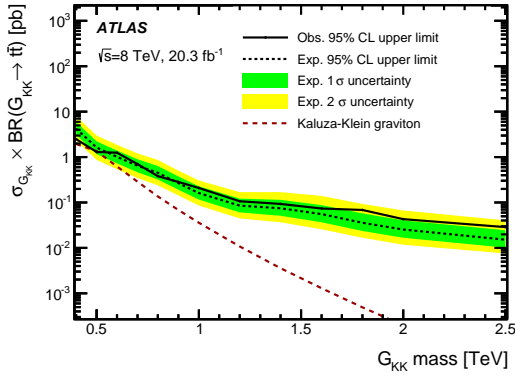
Figure 10: The $m_{t\bar{t}}^{\text{reco}}$ distributions, after the nuisance-parameter fit under the background-only hypothesis, summed over (a) all 6 boosted channels, (b) all 6 resolved channels, and (c) all 12 channels compared with data. The SM background components are shown as stacked histograms. The shaded areas indicate the total systematic uncertainties. The red (green) line shows the expected distribution for a hypothetical g_{KK} of mass 2.0 (0.8) TeV, width 15.3%.



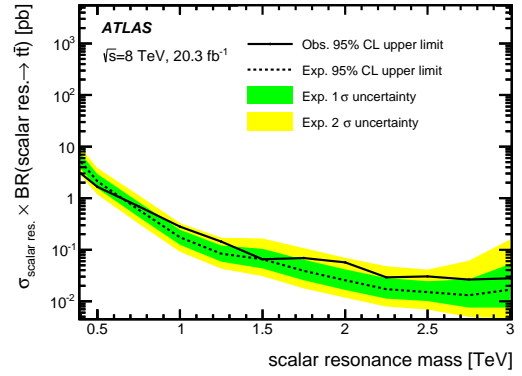
(a) Z' , resolved and boosted combination.



(b) g_{KK} , resolved and boosted combination.



(c) G_{KK} , resolved and boosted combination.



(d) Scalar resonance, resolved and boosted combination.

Figure 11: Observed and expected upper limits on the production cross-section times branching ratio to $t\bar{t}$ final states as a function of the mass of (a) Topcolour-assisted-technicolour Z'_{TC2} , (b) Bulk RS Kaluza–Klein gluon, (c) Bulk RS Kaluza–Klein graviton, (d) scalar resonance. The expected limits are derived from nominal (pre-fit) background estimates. The theoretical predictions for the production cross-section times branching ratio at the corresponding masses are also shown.

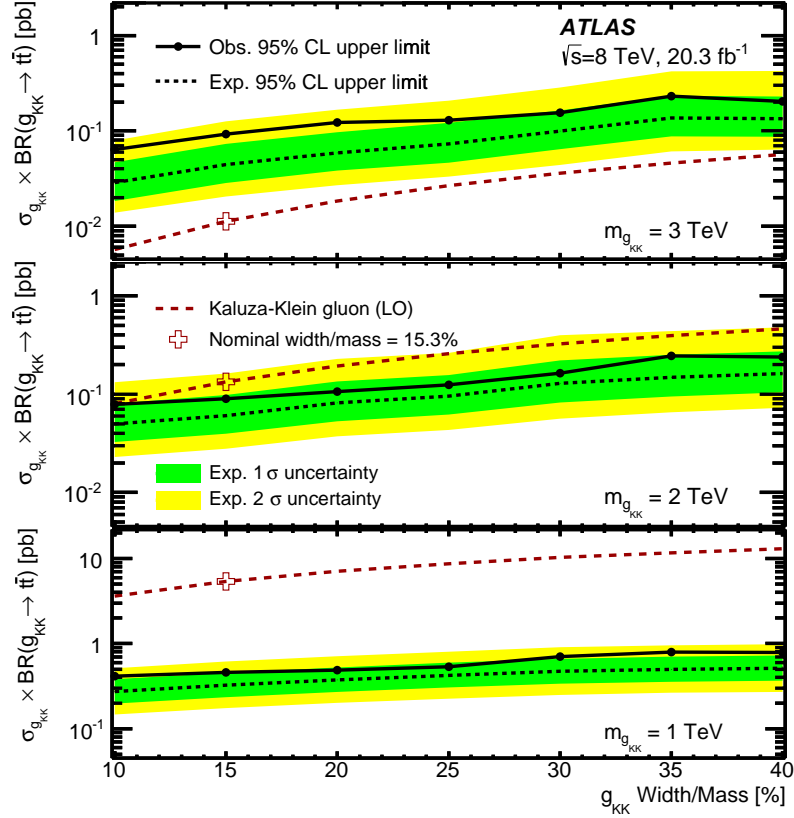


Figure 12: Observed and expected upper limits on the production cross-section for a Kaluza–Klein gluon times its branching ratio to $t\bar{t}$, as a function of its width, for three representative mass values. The expected limits are derived from nominal (pre-fit) background estimates. The theoretical predictions for the production cross-section times branching ratio at the corresponding widths are also shown.

thanks to the abundant data. The maximisation of the likelihood can change the central values of the nuisance parameters and their associated uncertainties. In the region of $m_{t\bar{t}}^{\text{reco}}$ above 1.5 TeV, the background prediction as seen in figure 9 is slightly higher than the data, which would lead to the anticipation that the observed limits should be slightly better than the expected ones. However, the central values of some nuisance parameters are significantly shifted in the fit. In the high- $m_{t\bar{t}}^{\text{reco}}$ region one of the dominant uncertainties is the high- p_T jet b -tagging extrapolation uncertainty, as detailed in section 8. This uncertainty is reduced to half of its original size by the fit, and the central value is also shifted downwards by approximately one pre-fit standard deviation. As this uncertainty is associated with reconstructed physics objects, it has correlated effects on the predictions of BSM signal and SM background. The 1σ change in the central value of this nuisance parameter reduces the acceptance of high-mass signals in the boosted selection considerably: approximately 25% for a Z' with a mass of 2 TeV. As a consequence, the observed upper limits on the cross-section obtained from the fit to the data are larger than the expected ones fitted to the nominal background estimates. Constraints from the fit are also observed in the nuisance parameters associated with other major systematic uncertainties such as the PDF, the shape of W +jets background, the energy and mass scales for both the large-radius and small-radius jets, b -tagging efficiencies, and $t\bar{t}$ MC modelling. These constraints are understood through their impact on the fitted $m_{t\bar{t}}^{\text{reco}}$ distributions. A few of the other nuisance parameters also have their central values changed slightly by the fit, but their impact on the signal acceptance and hence cross-section limits are much smaller than the one detailed

above.

Studies were done to understand the origin of the shifted nuisance parameter associated with the high- p_T jet b -tagging extrapolation uncertainty, in particular to investigate its potential origin as a mis-modelling of the $t\bar{t}$ background. Indeed an equally good fit can be obtained by introducing an additional *ad hoc* uncertainty in the modelling of the SM $t\bar{t}$ background with a similar dependency on $m_{t\bar{t}}^{\text{reco}}$. Such a mis-modelling would not reduce the signal acceptance and results in more stringent limits on the cross-section times $t\bar{t}$ branching ratio. Ultimately, no method was found to unambiguously ascertain the origin of this mis-modelling. The limits presented here are those with a 1σ change in the fitted value of the nuisance parameter associated with the high- p_T jet b -tagging extrapolation uncertainty, which correspond to more conservative results. An upper cross-section limit was generated using expected data constructed from a background-only model built from the nuisance parameters fitted to real data. It excludes a g_{KK} of width 15.3% for masses less than 2.1 TeV, compared to 2.2 TeV generated using nominal background estimates.

11 Summary

A search for heavy particles decaying to $t\bar{t}$ in the lepton-plus-jets decay channel was carried out with the ATLAS experiment at the LHC. The search uses data corresponding to an integrated luminosity of 20.3 fb^{-1} of proton–proton collisions at a centre-of-mass energy of 8 TeV. No excess of events beyond the Standard Model predictions is observed in the $t\bar{t}$ invariant mass spectra. Upper limits on the cross-section times branching ratio are set for four different signal models: a narrow ($\leq 3\%$ width) Z' boson, a broad (15.3% width) Randall–Sundrum Kaluza–Klein gluon, a Bulk Randall–Sundrum Kaluza–Klein graviton, and a narrow scalar resonance. Based on these results, the existence of a narrow leptophobic topcolour Z' in the range $0.4 \text{ TeV} < m_{Z'} < 1.8 \text{ TeV}$ is excluded at 95% CL. A broad Kaluza–Klein gluon with mass between 0.4 TeV and 2.2 TeV is also excluded at 95% CL. These results probe new physics at higher mass than previous ATLAS searches for the same signature, and the results are applicable to a broader variety of heavy resonances.

Acknowledgements

We thank CERN for the very successful operation of the LHC, as well as the support staff from our institutions without whom ATLAS could not be operated efficiently.

We acknowledge the support of ANPCyT, Argentina; YerPhI, Armenia; ARC, Australia; BMWFW and FWF, Austria; ANAS, Azerbaijan; SSTC, Belarus; CNPq and FAPESP, Brazil; NSERC, NRC and CFI, Canada; CERN; CONICYT, Chile; CAS, MOST and NSFC, China; COLCIENCIAS, Colombia; MSMT CR, MPO CR and VSC CR, Czech Republic; DNRF, DNSRC and Lundbeck Foundation, Denmark; EPLANET, ERC and NSRF, European Union; IN2P3-CNRS, CEA-DSM/IRFU, France; GNSF, Georgia; BMBF, DFG, HGF, MPG and AvH Foundation, Germany; GSRT and NSRF, Greece; RGC, Hong Kong SAR, China; ISF, MINERVA, GIF, I-CORE and Benoziyo Center, Israel; INFN, Italy; MEXT and JSPS, Japan; CNRST, Morocco; FOM and NWO, Netherlands; BRF and RCN, Norway; MNiSW and NCN, Poland; GRICES and FCT, Portugal; MNE/IFA, Romania; MES of Russia and NRC KI, Russian Federation; JINR; MSTD, Serbia; MSSR, Slovakia; ARRS and MIZŠ, Slovenia; DST/NRF, South Africa; MINECO, Spain; SRC and Wallenberg Foundation, Sweden; SER, SNSF and Cantons of Bern

and Geneva, Switzerland; NSC, Taiwan; TAEK, Turkey; STFC, the Royal Society and Leverhulme Trust, United Kingdom; DOE and NSF, United States of America.

The crucial computing support from all WLCG partners is acknowledged gratefully, in particular from CERN and the ATLAS Tier-1 facilities at TRIUMF (Canada), NDGF (Denmark, Norway, Sweden), CC-IN2P3 (France), KIT/GridKA (Germany), INFN-CNAF (Italy), NL-T1 (Netherlands), PIC (Spain), ASGC (Taiwan), RAL (UK) and BNL (USA) and in the Tier-2 facilities worldwide.

References

- [1] T.D. Lee, *A Theory of Spontaneous T Violation*, *Phys. Rev.* **D8** (1973) 1226–1239.
- [2] G. Branco et al., *Theory and phenomenology of two-Higgs-doublet models*, *Phys. Rept.* **516** (2012) 1–102, [arXiv:1106.0034 \[hep-ph\]](#).
- [3] C. T. Hill, *Topcolor assisted technicolor*, *Phys. Lett.* **B345** (1995) 483–489, [arXiv:hep-ph/9411426 \[hep-ph\]](#).
- [4] D. B. Kaplan and H. Georgi, *SU(2) x U(1) Breaking by Vacuum Misalignment*, *Phys. Lett.* **B136** (1984) 183.
- [5] D. B. Kaplan, H. Georgi, and S. Dimopoulos, *Composite Higgs Scalars*, *Phys. Lett.* **B136** (1984) 187.
- [6] H. Georgi, D. B. Kaplan, and P. Galison, *Calculation of the Composite Higgs Mass*, *Phys. Lett.* **B143** (1984) 152.
- [7] T. Banks, *Constraints on SU(2) x U(1) breaking by vacuum misalignment*, *Nucl. Phys.* **B243** (1984) 125.
- [8] H. Georgi and D. B. Kaplan, *Composite Higgs and Custodial SU(2)*, *Phys. Lett.* **B145** (1984) 216.
- [9] M. J. Dugan, H. Georgi, and D. B. Kaplan, *Anatomy of a Composite Higgs Model*, *Nucl. Phys.* **B254** (1985) 299.
- [10] H. Georgi, *A Tool Kit for Builders of Composite Models*, *Nucl. Phys.* **B266** (1986) 274.
- [11] B. Bellazzini, C. Csáki, and J. Serra, *Composite Higgses*, *Eur. Phys. J.* **C74** (2014) 2766, [arXiv:1401.2457 \[hep-ph\]](#).
- [12] L. Randall and R. Sundrum, *A Large mass hierarchy from a small extra dimension*, *Phys. Rev. Lett.* **83** (1999) 3370–3373, [arXiv:hep-ph/9905221 \[hep-ph\]](#).
- [13] K. Agashe, A. Delgado, M. J. May, and R. Sundrum, *RS1, custodial isospin and precision tests*, *JHEP* **0308** (2003) 050, [arXiv:hep-ph/0308036 \[hep-ph\]](#).
- [14] H. Davoudiasl, J. Hewett, and T. Rizzo, *Bulk gauge fields in the Randall-Sundrum model*, *Phys. Lett.* **B473** (2000) 43–49, [arXiv:hep-ph/9911262 \[hep-ph\]](#).
- [15] A. Pomarol, *Gauge bosons in a five-dimensional theory with localized gravity*, *Phys. Lett.* **B486** (2000) 153–157, [arXiv:hep-ph/9911294 \[hep-ph\]](#).
- [16] ATLAS Collaboration, *Search for $t\bar{t}$ resonances in the lepton plus jets final state with ATLAS using 4.7 fb⁻¹ of pp collisions at $\sqrt{s} = 7$ TeV*, *Phys. Rev.* **D88** (2013) 012004, [arXiv:1305.2756 \[hep-ex\]](#).
- [17] D. Krohn, J. Thaler, and L.-T. Wang, *Jet Trimming*, *JHEP* **1002** (2010) 084, [arXiv:0912.1342 \[hep-ph\]](#).
- [18] CMS Collaboration, *Searches for new physics using the $t\bar{t}$ invariant mass distribution in pp collisions at $\sqrt{s}=8$ TeV*, *Phys. Rev. Lett.* **111** (2013) 211804, [arXiv:1309.2030 \[hep-ex\]](#).

- [19] R. M. Harris, C. T. Hill, and S. J. Parke, *Cross section for topcolor $Z'(t)$ decaying to $t\bar{t}$* , [arXiv:hep-ph/9911288](#) [hep-ph].
- [20] R. M. Harris and S. Jain, *Cross Sections for Leptophobic Topcolor Z' Decaying to Top-Antitop*, *Eur. Phys. J.* **C72** (2012) 2072, [arXiv:1112.4928](#) [hep-ph].
- [21] J. Gao et al., *Next-to-leading order QCD corrections to the heavy resonance production and decay into top quark pair at the LHC*, *Phys. Rev.* **D82** (2010) 014020, [arXiv:1004.0876](#) [hep-ph].
- [22] F. Caola, K. Melnikov, and M. Schulze, *A complete next-to-leading order QCD description of resonant Z' production and decay into $t\bar{t}$ final states*, *Phys. Rev.* **D87** (2013) 034015, [arXiv:1211.6387](#) [hep-ph].
- [23] T. Aaltonen et al., CDF Collaboration, *Search for resonant production of $t\bar{t}$ decaying to jets in $p\bar{p}$ collisions at $\sqrt{s} = 1.96$ TeV*, *Phys. Rev.* **D84** (2011) 072003, [arXiv:1108.4755](#) [hep-ex].
- [24] T. Aaltonen et al., CDF Collaboration, *Search for Resonant Top-Antitop Production in the Lepton Plus Jets Decay Mode Using the Full CDF Data Set*, *Phys. Rev. Lett.* **110** (2013) 121802, [arXiv:1211.5363](#) [hep-ex].
- [25] V.M. Abazov, et al., D0 Collaboration, *Search for a Narrow $t\bar{t}$ Resonance in $p\bar{p}$ Collisions at $\sqrt{s} = 1.96$ TeV*, *Phys. Rev.* **D85** (2012) 051101, [arXiv:1111.1271](#) [hep-ex].
- [26] ATLAS Collaboration, *Search for resonances decaying into top-quark pairs using fully hadronic decays in pp collisions with ATLAS at $\sqrt{s} = 7$ TeV*, *JHEP* **1301** (2013) 116, [arXiv:1211.2202](#) [hep-ex].
- [27] CMS Collaboration, *Search for Z' resonances decaying to $t\bar{t}$ in dilepton+jets final states in pp collisions at $\sqrt{s} = 7$ TeV*, *Phys. Rev.* **D87** (2013) 072002, [arXiv:1211.3338](#) [hep-ex].
- [28] CMS Collaboration, *Search for resonant $t\bar{t}$ production in lepton+jets events in pp collisions at $\sqrt{s} = 7$ TeV*, *JHEP* **1212** (2012) 015, [arXiv:1209.4397](#) [hep-ex].
- [29] CMS Collaboration, *Search for anomalous t t -bar production in the highly-boosted all-hadronic final state*, *JHEP* **1209** (2012) 029, [arXiv:1204.2488](#) [hep-ex].
- [30] B. Lillie, L. Randall, and L.-T. Wang, *The Bulk RS KK-gluon at the LHC*, *JHEP* **0709** (2007) 074, [arXiv:hep-ph/0701166](#) [hep-ph].
- [31] K. Agashe et al., *LHC signals from warped extra dimensions*, *Phys. Rev.* **D77** (2008) 015003, [arXiv:hep-ph/0612015](#) [hep-ph].
- [32] K. Agashe, H. Davoudiasl, G. Perez, and A. Soni, *Warped Gravitons at the LHC and Beyond*, *Phys. Rev.* **D76** (2007) 036006, [arXiv:hep-ph/0701186](#) [hep-ph].
- [33] A. L. Fitzpatrick, J. Kaplan, L. Randall, and L.-T. Wang, *Searching for the Kaluza-Klein Graviton in Bulk RS Models*, *JHEP* **0709** (2007) 013, [arXiv:hep-ph/0701150](#) [hep-ph].
- [34] ATLAS Collaboration, *Search for resonant diboson production in the $llq\bar{q}$ final state in pp collisions at $\sqrt{s} = 8$ TeV with the ATLAS detector*, *Eur. Phys. J.* **C75** (2015) 69, [arXiv:1409.6190](#) [hep-ex].
- [35] CMS Collaboration, *Search for massive resonances decaying into pairs of boosted bosons in semi-leptonic final states at $\sqrt{s} = 8$ TeV*, *JHEP* **1408** (2014) 174, [arXiv:1405.3447](#) [hep-ex].

- [36] ATLAS Collaboration, *The ATLAS Experiment at the CERN Large Hadron Collider*, **JINST** **3** (2008) S08003.
- [37] ATLAS Collaboration, *Muon reconstruction efficiency and momentum resolution of the ATLAS experiment in proton-proton collisions at $\sqrt{s}=7$ TeV in 2010*, **Eur. Phys. J.** **C74** (2014) 3034, [arXiv:1404.4562 \[hep-ex\]](#).
- [38] ATLAS Collaboration, *The ATLAS Simulation Infrastructure*, **Eur. Phys. J.** **C70** (2010) 823–874, [arXiv:1005.4568 \[physics.ins-det\]](#).
- [39] S. Agostinelli et al., *GEANT4: A simulation toolkit*, **Nucl. Instrum. Meth.** **A506** (2003) 250–303.
- [40] ATLAS Collaboration, *The simulation principle and performance of the ATLAS fast calorimeter simulation FastCaloSim*, ATL-PHYS-PUB-2010-013 (2010), <http://cds.cern.ch/record/1300517>.
- [41] T. Sjöstrand, S. Mrenna, and P. Z. Skands, *A Brief Introduction to PYTHIA 8.1*, **Comput. Phys. Commun.** **178** (2008) 852–867, [arXiv:0710.3820 \[hep-ph\]](#).
- [42] J. Alwall et al., *MadGraph 5 : Going Beyond*, **JHEP** **1106** (2011) 128, [arXiv:1106.0522 \[hep-ph\]](#).
- [43] A. Martin, W. Stirling, R. Thorne, and G. Watt, *Parton distributions for the LHC*, **Eur. Phys. J.** **C63** (2009) 189–285, [arXiv:0901.0002 \[hep-ph\]](#).
- [44] J. Pumplin et al., *New generation of parton distributions with uncertainties from global QCD analysis*, **JHEP** **0207** (2002) 012, [arXiv:hep-ph/0201195 \[hep-ph\]](#).
- [45] J. Alwall et al., *The automated computation of tree-level and next-to-leading order differential cross sections, and their matching to parton shower simulations*, **JHEP** **1407** (2014) 079, [arXiv:1405.0301 \[hep-ph\]](#).
- [46] S. Frixione, P. Nason, and G. Ridolfi, *A Positive-weight next-to-leading-order Monte Carlo for heavy flavour hadroproduction*, **JHEP** **0709** (2007) 126, [arXiv:0707.3088 \[hep-ph\]](#).
- [47] P. Nason, *A New method for combining NLO QCD with shower Monte Carlo algorithms*, **JHEP** **0411** (2004) 040, [arXiv:hep-ph/0409146 \[hep-ph\]](#).
- [48] S. Frixione, P. Nason, and C. Oleari, *Matching NLO QCD computations with Parton Shower simulations: the POWHEG method*, **JHEP** **0711** (2007) 070, [arXiv:0709.2092 \[hep-ph\]](#).
- [49] S. Alioli, P. Nason, C. Oleari, and E. Re, *A general framework for implementing NLO calculations in shower Monte Carlo programs: the POWHEG BOX*, **JHEP** **1006** (2010) 043, [arXiv:1002.2581 \[hep-ph\]](#).
- [50] T. Sjöstrand, S. Mrenna, and P. Z. Skands, *PYTHIA 6.4 Physics and Manual*, **JHEP** **0605** (2006) 026, [arXiv:hep-ph/0603175 \[hep-ph\]](#).
- [51] P. Z. Skands, *Tuning Monte Carlo Generators: The Perugia Tunes*, **Phys. Rev.** **D82** (2010) 074018, [arXiv:1005.3457 \[hep-ph\]](#).
- [52] H.-L. Lai et al., *New parton distributions for collider physics*, **Phys. Rev.** **D82** (2010) 074024, [arXiv:1007.2241 \[hep-ph\]](#).

- [53] ATLAS Collaboration, *Comparison of Monte Carlo generator predictions to ATLAS measurements of top pair production at 7 TeV*, ATL-PHYS-PUB-2015-002 (2015), <http://cdsweb.cern.ch/record/1981319>.
- [54] S. Frixione and B. R. Webber, *Matching NLO QCD computations and parton shower simulations*, *JHEP* **0206** (2002) 029, [arXiv:hep-ph/0204244](https://arxiv.org/abs/hep-ph/0204244) [[hep-ph](#)].
- [55] S. Frixione, P. Nason, and B. R. Webber, *Matching NLO QCD and parton showers in heavy flavor production*, *JHEP* **0308** (2003) 007, [arXiv:hep-ph/0305252](https://arxiv.org/abs/hep-ph/0305252) [[hep-ph](#)].
- [56] S. Frixione, F. Stoeckli, P. Torrielli, B. R. Webber, and C. D. White, *The MC@NLO 4.0 Event Generator*, [arXiv:1010.0819](https://arxiv.org/abs/1010.0819) [[hep-ph](#)].
- [57] G. Corcella et al., *HERWIG 6: An Event generator for hadron emission reactions with interfering gluons (including supersymmetric processes)*, *JHEP* **0101** (2001) 010, [arXiv:hep-ph/0011363](https://arxiv.org/abs/hep-ph/0011363) [[hep-ph](#)].
- [58] G. Corcella et al., *HERWIG 6.5 release note*, [arXiv:hep-ph/0210213](https://arxiv.org/abs/hep-ph/0210213) [[hep-ph](#)].
- [59] J. M. Butterworth, J. R. Forshaw, and M. H. Seymour, *Multiparton interactions in photoproduction at HERA*, *Z. Phys.* **C72** (1996) 637–646, [arXiv:hep-ph/9601371](https://arxiv.org/abs/hep-ph/9601371) [[hep-ph](#)].
- [60] ATLAS Collaboration, *New ATLAS event generator tunes to 2010 data*, ATL-PHYS-PUB-2011-008 (2011), <http://cds.cern.ch/record/1345343>.
- [61] M. Czakon and A. Mitov, *Top++: A Program for the Calculation of the Top-Pair Cross-Section at Hadron Colliders*, *Comput. Phys. Commun.* **185** (2014) 2930, [arXiv:1112.5675](https://arxiv.org/abs/1112.5675) [[hep-ph](#)].
- [62] M. Beneke, P. Falgari, S. Klein, and C. Schwinn, *Hadronic top-quark pair production with NNLL threshold resummation*, *Nucl. Phys.* **B855** (2012) 695–741, [arXiv:1109.1536](https://arxiv.org/abs/1109.1536) [[hep-ph](#)].
- [63] M. Cacciari et al., *Top-pair production at hadron colliders with next-to-next-to-leading logarithmic soft-gluon resummation*, *Phys. Lett.* **B710** (2012) 612–622, [arXiv:1111.5869](https://arxiv.org/abs/1111.5869) [[hep-ph](#)].
- [64] P. Baernreuther, M. Czakon, and A. Mitov, *Percent Level Precision Physics at the Tevatron: First Genuine NNLO QCD Corrections to $q\bar{q} \rightarrow t\bar{t} + X$* , *Phys. Rev. Lett.* **109** (2012) 132001, [arXiv:1204.5201](https://arxiv.org/abs/1204.5201) [[hep-ph](#)].
- [65] M. Czakon and A. Mitov, *NNLO corrections to top-pair production at hadron colliders: the all-fermionic scattering channels*, *JHEP* **1212** (2012) 054, [arXiv:1207.0236](https://arxiv.org/abs/1207.0236) [[hep-ph](#)].
- [66] M. Czakon and A. Mitov, *NNLO corrections to top pair production at hadron colliders: the quark-gluon reaction*, *JHEP* **1301** (2013) 080, [arXiv:1210.6832](https://arxiv.org/abs/1210.6832) [[hep-ph](#)].
- [67] M. Czakon, P. Fiedler, and A. Mitov, *Total Top-Quark Pair-Production Cross Section at Hadron Colliders Through $O(\alpha_s^4)$* , *Phys. Rev. Lett.* **110** (2013) 252004, [arXiv:1303.6254](https://arxiv.org/abs/1303.6254) [[hep-ph](#)].
- [68] J. Kühn, A. Scharf, and P. Uwer, *Weak Interactions in Top-Quark Pair Production at Hadron Colliders: An Update*, *Phys. Rev.* **D91** (2015) 1, 014020, [arXiv:1305.5773](https://arxiv.org/abs/1305.5773) [[hep-ph](#)].
- [69] M. L. Mangano et al., *ALPGEN, a generator for hard multiparton processes in hadronic collisions*, *JHEP* **0307** (2003) 001, [arXiv:hep-ph/0206293](https://arxiv.org/abs/hep-ph/0206293) [[hep-ph](#)].

- [70] S. Alioli, P. Nason, C. Oleari, and E. Re, *NLO single-top production matched with shower in POWHEG: s- and t-channel contributions*, *JHEP* **0909** (2009) 111, [arXiv:0907.4076 \[hep-ph\]](#).
- [71] R. Frederix, E. Re, and P. Torrielli, *Single-top t-channel hadroproduction in the four-flavour scheme with POWHEG and aMC@NLO*, *JHEP* **1209** (2012) 130, [arXiv:1207.5391 \[hep-ph\]](#).
- [72] E. Re, *Single-top Wt-channel production matched with parton showers using the POWHEG method*, *Eur. Phys. J.* **C71** (2011) 1547, [arXiv:1009.2450 \[hep-ph\]](#).
- [73] S. Frixione et al., *Single-top hadroproduction in association with a W boson*, *JHEP* **0807** (2008) 029, [arXiv:0805.3067 \[hep-ph\]](#).
- [74] N. Kidonakis, *NNLL resummation for s-channel single top quark production*, *Phys. Rev.* **D81** (2010) 054028, [arXiv:1001.5034 \[hep-ph\]](#).
- [75] N. Kidonakis, *Next-to-next-to-leading-order collinear and soft gluon corrections for t-channel single top quark production*, *Phys. Rev.* **D83** (2011) 091503, [arXiv:1103.2792 \[hep-ph\]](#).
- [76] N. Kidonakis, *Two-loop soft anomalous dimensions for single top quark associated production with a W^- or H^-* , *Phys. Rev.* **D82** (2010) 054018, [arXiv:1005.4451 \[hep-ph\]](#).
- [77] R. Gavin, Y. Li, F. Petriello, and S. Quackenbush, *W Physics at the LHC with FEWZ 2.1*, *Comput. Phys. Commun.* **184** (2013) 208–214, [arXiv:1201.5896 \[hep-ph\]](#).
- [78] T. Gleisberg et al., *Event generation with SHERPA 1.1*, *JHEP* **0902** (2009) 007, [arXiv:0811.4622 \[hep-ph\]](#).
- [79] S. Höche, F. Krauss, S. Schumann, and F. Siegert, *QCD matrix elements and truncated showers*, *JHEP* **0905** (2009) 053, [arXiv:0903.1219 \[hep-ph\]](#).
- [80] T. Gleisberg and S. Höche, *Comix, a new matrix element generator*, *JHEP* **0812** (2008) 039, [arXiv:0808.3674 \[hep-ph\]](#).
- [81] S. Schumann and F. Krauss, *A Parton shower algorithm based on Catani-Seymour dipole factorisation*, *JHEP* **0803** (2008) 038, [arXiv:0709.1027 \[hep-ph\]](#).
- [82] J. M. Campbell and R. Ellis, *MCFM for the Tevatron and the LHC*, *Nucl. Phys. Proc. Suppl.* **205-206** (2010) 10–15, [arXiv:1007.3492 \[hep-ph\]](#).
- [83] M. Garzelli, A. Kardos, C. Papadopoulos, and Z. Trocsanyi, *$t\bar{t}W^\pm$ and $t\bar{t}Z$ Hadroproduction at NLO accuracy in QCD with Parton Shower and Hadronization effects*, *JHEP* **1211** (2012) 056, [arXiv:1208.2665 \[hep-ph\]](#).
- [84] ATLAS Collaboration, *Electron reconstruction and identification efficiency measurements with the ATLAS detector using the 2011 LHC proton-proton collision data*, *Eur. Phys. J.* **C74** (2014) 2941, [arXiv:1404.2240 \[hep-ex\]](#).
- [85] K. Rehermann and B. Tweedie, *Efficient Identification of Boosted Semileptonic Top Quarks at the LHC*, *JHEP* **1103** (2011) 059, [arXiv:1007.2221 \[hep-ph\]](#).
- [86] ATLAS Collaboration, *Performance of primary vertex reconstruction in proton-proton collisions at $\sqrt{s} = 7$ TeV in the ATLAS experiment*, ATLAS-CONF-2010-069 (2010), <http://cdsweb.cern.ch/record/1281344>.

- [87] M. Cacciari, G. P. Salam, and G. Soyez, *The Anti- k_t jet clustering algorithm*, **JHEP** **0804** (2008) 063, [arXiv:0802.1189 \[hep-ph\]](#).
- [88] ATLAS Collaboration, *Jet energy measurement with the ATLAS detector in proton-proton collisions at $\sqrt{s} = 7$ TeV*, **Eur. Phys. J.** **C73** (2013) 2304, [arXiv:1112.6426 \[hep-ex\]](#).
- [89] Ç. İşsever, K. Borras, and D. Wegener, *An improved weighting algorithm to achieve software compensation in a fine grained LAr calorimeter*, **Nucl. Instr. and Meth.** **A545** (2005) 803–812, [arXiv:physics/0408129 \[physics\]](#).
- [90] ATLAS Collaboration, *Jet energy measurement and its systematic uncertainty in proton-proton collisions at $\sqrt{s} = 7$ TeV with the ATLAS detector*, **Eur. Phys. J.** **C75** (2015) 17, [arXiv:1406.0076 \[hep-ex\]](#).
- [91] ATLAS Collaboration, *Jet mass and substructure of inclusive jets in $\sqrt{s} = 7$ TeV pp collisions with the ATLAS experiment*, **JHEP** **1205** (2012) 128, [arXiv:1203.4606 \[hep-ex\]](#).
- [92] ATLAS Collaboration, *Performance of large-R jets and jet substructure reconstruction with the ATLAS detector*, ATLAS-CONF-2012-065 (2012), <http://cdsweb.cern.ch/record/1459530>.
- [93] ATLAS Collaboration, *Pile-up subtraction and suppression for jets in ATLAS*, ATLAS-CONF-2013-083 (2013), <http://cdsweb.cern.ch/record/1570994>.
- [94] ATLAS Collaboration, *Performance of jet substructure techniques for large-R jets in proton-proton collisions at $\sqrt{s} = 7$ TeV using the ATLAS detector*, **JHEP** **1309** (2013) 076, [arXiv:1306.4945 \[hep-ex\]](#).
- [95] S. D. Ellis and D. E. Soper, *Successive combination jet algorithm for hadron collisions*, **Phys. Rev.** **D48** (1993) 3160–3166, [arXiv:9305266 \[hep-ph\]](#).
- [96] ATLAS Collaboration, *Calibration of the performance of b-tagging for c and light-flavour jets in the 2012 ATLAS data*, ATLAS-CONF-2014-046 (2014), <http://cds.cern.ch/record/1741020>.
- [97] ATLAS Collaboration, *Performance of Missing Transverse Momentum Reconstruction in Proton-Proton Collisions at 7 TeV with ATLAS*, **Eur. Phys. J.** **C72** (2012) 1844, [arXiv:1108.5602 \[hep-ex\]](#).
- [98] K.A. Olive et al., Particle Data Group, *Review of Particle Physics*, **Chin. Phys.** **C38** (2014) 090001.
- [99] T. Aaltonen et al., CDF Collaboration, *Observation of Single Top Quark Production and Measurement of $|V_{tb}|$ with CDF*, **Phys. Rev.** **D82** (2010) 112005, [arXiv:1004.1181 \[hep-ex\]](#).
- [100] ATLAS Collaboration, *Measurement of the t-channel single top-quark production cross section in pp collisions at $\sqrt{s} = 7$ TeV with the ATLAS detector*, **Phys. Lett.** **B717** (2012) 330–350, [arXiv:1205.3130 \[hep-ex\]](#).
- [101] ATLAS Collaboration, *Measurement of the charge asymmetry in top quark pair production in pp collisions at $\sqrt{s} = 7$ TeV using the ATLAS detector*, **Eur. Phys. J.** **C72** (2012) 2039, [arXiv:1203.4211 \[hep-ex\]](#).

- [102] ATLAS Collaboration, *Measurements of top quark pair relative differential cross-sections with ATLAS in pp collisions at $\sqrt{s} = 7$ TeV*, *Eur. Phys. J.* **C73** (2013) 2261, [arXiv:1207.5644 \[hep-ex\]](#).
- [103] ATLAS Collaboration, *Measurement of the top quark pair production cross-section with ATLAS in the single lepton channel*, *Phys. Lett.* **B711** (2012) 244–263, [arXiv:1201.1889 \[hep-ex\]](#).
- [104] ATLAS Collaboration, *Measurement of the cross section for the production of a W boson in association with b-jets in pp collisions at $\sqrt{s} = 7$ TeV with the ATLAS detector*, *Phys. Lett.* **B707** (2012) 418–437, [arXiv:1109.1470 \[hep-ex\]](#).
- [105] ATLAS Collaboration, *Estimation of non-prompt and fake lepton backgrounds in final states with top quarks produced in proton-proton collisions at $\sqrt{s} = 8$ TeV with the ATLAS detector*, ATLAS-CONF-2014-058 (2014), <http://cds.cern.ch/record/1951336>.
- [106] M. Botje et al., *The PDF4LHC Working Group Interim Recommendations*, [arXiv:1101.0538 \[hep-ph\]](#).
- [107] A. Martin, W. Stirling, R. Thorne, and G. Watt, *Uncertainties on α_s in global PDF analyses and implications for predicted hadronic cross sections*, *Eur. Phys. J.* **C64** (2009) 653–680, [arXiv:0905.3531 \[hep-ph\]](#).
- [108] J. Gao et al., *CT10 next-to-next-to-leading order global analysis of QCD*, *Phys. Rev.* **D89** (2014) 033009, [arXiv:1302.6246 \[hep-ph\]](#).
- [109] R. D. Ball et al., *Parton distributions with LHC data*, *Nucl. Phys.* **B867** (2013) 244–289, [arXiv:1207.1303 \[hep-ph\]](#).
- [110] ATLAS Collaboration, *Measurement of the top quark-pair production cross section with ATLAS in pp collisions at $\sqrt{s} = 7$ TeV*, *Eur. Phys. J.* **C71** (2011) 1577, [arXiv:1012.1792 \[hep-ex\]](#).
- [111] ATLAS Collaboration, *Improved luminosity determination in pp collisions at $\sqrt{s} = 7$ TeV using the ATLAS detector at the LHC*, *Eur. Phys. J.* **C73** (2013) 2518, [arXiv:1302.4393 \[hep-ex\]](#).
- [112] ATLAS Collaboration, *Measurement of the b-tag Efficiency in a Sample of Jets Containing Muons with 5 fb^{-1} of Data from the ATLAS Detector*, ATLAS-CONF-2012-043 (2012), <http://cdsweb.cern.ch/record/1435197>.
- [113] ATLAS Collaboration, *Measurement of the Mistag Rate with 5 fb^{-1} of Data Collected by the ATLAS Detector*, ATLAS-CONF-2012-040 (2012), <http://cdsweb.cern.ch/record/1435194>.
- [114] B. P. Kersevan and E. Richter-Was, *The Monte Carlo event generator AcerMC versions 2.0 to 3.8 with interfaces to PYTHIA 6.4, HERWIG 6.5 and ARIADNE 4.1*, *Comput. Phys. Commun.* **184** (2013) 919–985, [arXiv:hep-ph/0405247 \[hep-ph\]](#).
- [115] ATLAS Collaboration, *Measurement of $t\bar{t}$ production with a veto on additional central jet activity in pp collisions at $\sqrt{s} = 7$ TeV using the ATLAS detector*, *Eur. Phys. J.* **C72** (2012) 2043, [arXiv:1203.5015 \[hep-ex\]](#).
- [116] G. Choudalakis, *On hypothesis testing, trials factor, hypertests and the BumpHunter*, [arXiv:1101.0390 \[physics.data-an\]](#).

- [117] L. Lyons, *Open statistical issues in Particle Physics*, *Ann. Appl. Stat.* **2** (2008) 887–915, [arXiv:0811.1663](#) [Stat.AP].
- [118] A. L. Read, *Presentation of search results: The CL(s) technique*, *J. Phys. G* **28** (2002) 2693–2704.
- [119] M. Baak et al., *HistFitter software framework for statistical data analysis*, [arXiv:1410.1280](#) [hep-ex].

The ATLAS Collaboration

G. Aad⁸⁵, B. Abbott¹¹³, J. Abdallah¹⁵¹, O. Abdinov¹¹, R. Aben¹⁰⁷, M. Abolins⁹⁰, O.S. AbouZeid¹⁵⁸, H. Abramowicz¹⁵³, H. Abreu¹⁵², R. Abreu³⁰, Y. Abulaiti^{146a,146b}, B.S. Acharya^{164a,164b,a}, L. Adamczyk^{38a}, D.L. Adams²⁵, J. Adelman¹⁰⁸, S. Adomeit¹⁰⁰, T. Adye¹³¹, A.A. Affolder⁷⁴, T. Agatonovic-Jovin¹³, J.A. Aguilar-Saavedra^{126a,126f}, S.P. Ahlen²², F. Ahmadov^{65,b}, G. Aielli^{133a,133b}, H. Akerstedt^{146a,146b}, T.P.A. Åkesson⁸¹, G. Akimoto¹⁵⁵, A.V. Akimov⁹⁶, G.L. Alberghi^{20a,20b}, J. Albert¹⁶⁹, S. Albrand⁵⁵, M.J. Alconada Verzini⁷¹, M. Aleksa³⁰, I.N. Aleksandrov⁶⁵, C. Alexa^{26a}, G. Alexander¹⁵³, T. Alexopoulos¹⁰, M. Alhroob¹¹³, G. Alimonti^{91a}, L. Alio⁸⁵, J. Alison³¹, S.P. Alkire³⁵, B.M.M. Allbrooke¹⁸, P.P. Allport⁷⁴, A. Aloisio^{104a,104b}, A. Alonso³⁶, F. Alonso⁷¹, C. Alpigiani⁷⁶, A. Altheimer³⁵, B. Alvarez Gonzalez³⁰, D. Álvarez Piqueras¹⁶⁷, M.G. Alviggi^{104a,104b}, B.T. Amadio¹⁵, K. Amako⁶⁶, Y. Amaral Coutinho^{24a}, C. Amelung²³, D. Amidei⁸⁹, S.P. Amor Dos Santos^{126a,126c}, A. Amorim^{126a,126b}, S. Amoroso⁴⁸, N. Amram¹⁵³, G. Amundsen²³, C. Anastopoulos¹³⁹, L.S. Ancu⁴⁹, N. Andari³⁰, T. Andeen³⁵, C.F. Anders^{58b}, G. Anders³⁰, J.K. Anders⁷⁴, K.J. Anderson³¹, A. Andreazza^{91a,91b}, V. Andrei^{58a}, S. Angelidakis⁹, I. Angelozzi¹⁰⁷, P. Anger⁴⁴, A. Angerami³⁵, F. Anghinolfi³⁰, A.V. Anisenkov^{109,c}, N. Anjos¹², A. Annovi^{124a,124b}, M. Antonelli⁴⁷, A. Antonov⁹⁸, J. Antos^{144b}, F. Anulli^{132a}, M. Aoki⁶⁶, L. Aperio Bella¹⁸, G. Arabidze⁹⁰, Y. Arai⁶⁶, J.P. Araque^{126a}, A.T.H. Arce⁴⁵, F.A. Arduh⁷¹, J-F. Arguin⁹⁵, S. Argyropoulos⁴², M. Arik^{19a}, A.J. Armbruster³⁰, O. Arnaez³⁰, V. Arnal⁸², H. Arnold⁴⁸, M. Arratia²⁸, O. Arslan²¹, A. Artamonov⁹⁷, G. Artoni²³, S. Asai¹⁵⁵, N. Asbah⁴², A. Ashkenazi¹⁵³, B. Åsman^{146a,146b}, L. Asquith¹⁴⁹, K. Assamagan²⁵, R. Astalos^{144a}, M. Atkinson¹⁶⁵, N.B. Atlay¹⁴¹, B. Auerbach⁶, K. Augsten¹²⁸, M. Aurousseau^{145b}, G. Avolio³⁰, B. Axen¹⁵, M.K. Ayoub¹¹⁷, G. Azuelos^{95,d}, M.A. Baak³⁰, A.E. Baas^{58a}, C. Bacci^{134a,134b}, H. Bachacou¹³⁶, K. Bachas¹⁵⁴, M. Backes³⁰, M. Backhaus³⁰, P. Bagiachi^{132a,132b}, P. Bagnaia^{132a,132b}, Y. Bai^{33a}, T. Bain³⁵, J.T. Baines¹³¹, O.K. Baker¹⁷⁶, P. Balek¹²⁹, T. Balestri¹⁴⁸, F. Balli⁸⁴, E. Banas³⁹, Sw. Banerjee¹⁷³, A.A.E. Bannoura¹⁷⁵, H.S. Bansil¹⁸, L. Barak³⁰, E.L. Barberio⁸⁸, D. Barberis^{50a,50b}, M. Barbero⁸⁵, T. Barillari¹⁰¹, M. Barisonzi^{164a,164b}, T. Barklow¹⁴³, N. Barlow²⁸, S.L. Barnes⁸⁴, B.M. Barnett¹³¹, R.M. Barnett¹⁵, Z. Barnovska⁵, A. Baroncelli^{134a}, G. Barone⁴⁹, A.J. Barr¹²⁰, F. Barreiro⁸², J. Barreiro Guimarães da Costa⁵⁷, R. Bartoldus¹⁴³, A.E. Barton⁷², P. Bartos^{144a}, A. Basalae¹²³, A. Bassalat¹¹⁷, A. Basye¹⁶⁵, R.L. Bates⁵³, S.J. Batista¹⁵⁸, J.R. Batley²⁸, M. Battaglia¹³⁷, M. Bauge^{132a,132b}, F. Bauer¹³⁶, H.S. Bawa^{143,e}, J.B. Beacham¹¹¹, M.D. Beattie⁷², T. Beau⁸⁰, P.H. Beauchemin¹⁶¹, R. Beccherle^{124a,124b}, P. Bechtel²¹, H.P. Beck^{17,f}, K. Becker¹²⁰, M. Becker⁸³, S. Becker¹⁰⁰, M. Beckingham¹⁷⁰, C. Becot¹¹⁷, A.J. Beddall^{19c}, A. Beddall^{19c}, V.A. Bednyakov⁶⁵, C.P. Bee¹⁴⁸, L.J. Beamster¹⁰⁷, T.A. Beermann¹⁷⁵, M. Begel²⁵, J.K. Behr¹²⁰, C. Belanger-Champagne⁸⁷, W.H. Bell⁴⁹, G. Bella¹⁵³, L. Bellagamba^{20a}, A. Bellerive²⁹, M. Bellomo⁸⁶, K. Belotskiy⁹⁸, O. Beltramello³⁰, O. Benary¹⁵³, D. Bencheikroun^{135a}, M. Bender¹⁰⁰, K. Bendtz^{146a,146b}, N. Benekos¹⁰, Y. Benhammou¹⁵³, E. Benhar Nocchioli⁴⁹, J.A. Benitez Garcia^{159b}, D.P. Benjamin⁴⁵, J.R. Bensinger²³, S. Bentvelsen¹⁰⁷, L. Beresford¹²⁰, M. Beretta⁴⁷, D. Berge¹⁰⁷, E. Bergeaas Kuutmann¹⁶⁶, N. Berger⁵, F. Berghaus¹⁶⁹, J. Beringer¹⁵, C. Bernard²², N.R. Bernard⁸⁶, C. Bernius¹¹⁰, F.U. Bernlochner²¹, T. Berry⁷⁷, P. Berta¹²⁹, C. Bertella⁸³, G. Bertoli^{146a,146b}, F. Bertolucci^{124a,124b}, C. Bertsche¹¹³, D. Bertsche¹¹³, M.I. Besana^{91a}, G.J. Besjes¹⁰⁶, O. Bessidskaia Bylund^{146a,146b}, M. Bessner⁴², N. Besson¹³⁶, C. Betancourt⁴⁸, S. Bethke¹⁰¹, A.J. Bevan⁷⁶, W. Bhimji⁴⁶, R.M. Bianchi¹²⁵, L. Bianchini²³, M. Bianco³⁰, O. Biebel¹⁰⁰, S.P. Bieniek⁷⁸, M. Biglietti^{134a}, J. Bilbao De Mendizabal⁴⁹, H. Bilokon⁴⁷, M. Bindi⁵⁴, S. Binet¹¹⁷, A. Bingul^{19c}, C. Bini^{132a,132b}, C.W. Black¹⁵⁰, J.E. Black¹⁴³, K.M. Black²², D. Blackburn¹³⁸, R.E. Blair⁶, J.-B. Blanchard¹³⁶, J.E. Blanco⁷⁷, T. Blazek^{144a}, I. Bloch⁴², C. Blocker²³, W. Blum^{83,*}, U. Blumenschein⁵⁴, G.J. Bobbink¹⁰⁷, V.S. Bobrovnikov^{109,c}, S.S. Bocchetta⁸¹, A. Bocci⁴⁵, C. Bock¹⁰⁰, M. Boehler⁴⁸, J.A. Bogaerts³⁰, A.G. Bogdanchikov¹⁰⁹,

C. Bohm^{146a}, V. Boisvert⁷⁷, T. Bold^{38a}, V. Boldea^{26a}, A.S. Boldyrev⁹⁹, M. Bomben⁸⁰, M. Bona⁷⁶, M. Boonekamp¹³⁶, A. Borisov¹³⁰, G. Borissov⁷², S. Borroni⁴², J. Bortfeldt¹⁰⁰, V. Bortolotto^{60a,60b,60c}, K. Bos¹⁰⁷, D. Boscherini^{20a}, M. Bosman¹², J. Boudreau¹²⁵, J. Bouffard², E.V. Bouhova-Thacker⁷², D. Boumediene³⁴, C. Bourdarios¹¹⁷, N. Bousson¹¹⁴, A. Boveia³⁰, J. Boyd³⁰, I.R. Boyko⁶⁵, I. Bozic¹³, J. Bracinik¹⁸, A. Brandt⁸, G. Brandt⁵⁴, O. Brandt^{58a}, U. Bratzler¹⁵⁶, B. Brau⁸⁶, J.E. Brau¹¹⁶, H.M. Braun^{175,*}, S.F. Brazzale^{164a,164c}, K. Brendlinger¹²², A.J. Brennan⁸⁸, L. Brenner¹⁰⁷, R. Brenner¹⁶⁶, S. Bressler¹⁷², K. Bristow^{145c}, T.M. Bristow⁴⁶, D. Britton⁵³, D. Britzger⁴², F.M. Brochu²⁸, I. Brock²¹, R. Brock⁹⁰, J. Bronner¹⁰¹, G. Brooijmans³⁵, T. Brooks⁷⁷, W.K. Brooks^{32b}, J. Brosamer¹⁵, E. Brost¹¹⁶, J. Brown⁵⁵, P.A. Bruckman de Renstrom³⁹, D. Bruncko^{144b}, R. Bruneliere⁴⁸, A. Bruni^{20a}, G. Bruni^{20a}, M. Bruschi^{20a}, L. Bryngemark⁸¹, T. Buanes¹⁴, Q. Buat¹⁴², P. Buchholz¹⁴¹, A.G. Buckley⁵³, S.I. Buda^{26a}, I.A. Budagov⁶⁵, F. Buehrer⁴⁸, L. Bugge¹¹⁹, M.K. Bugge¹¹⁹, O. Bulekov⁹⁸, D. Bullock⁸, H. Burckhart³⁰, S. Burdin⁷⁴, B. Burghgrave¹⁰⁸, S. Burke¹³¹, I. Burmeister⁴³, E. Busato³⁴, D. Büscher⁴⁸, V. Büscher⁸³, P. Bussey⁵³, J.M. Butler²², A.I. Butt³, C.M. Buttar⁵³, J.M. Butterworth⁷⁸, P. Butti¹⁰⁷, W. Buttinger²⁵, A. Buzatu⁵³, R. Buzykaev^{109,c}, S. Cabrera Urbán¹⁶⁷, D. Caforio¹²⁸, V.M. Cairo^{37a,37b}, O. Cakir^{4a}, P. Calafiura¹⁵, A. Calandri¹³⁶, G. Calderini⁸⁰, P. Calfayan¹⁰⁰, L.P. Caloba^{24a}, D. Calvet³⁴, S. Calvet³⁴, R. Camacho Toro³¹, S. Camarda⁴², P. Camarri^{133a,133b}, D. Cameron¹¹⁹, L.M. Caminada¹⁵, R. Caminal Armadans¹², S. Campana³⁰, M. Campanelli⁷⁸, A. Campoverde¹⁴⁸, V. Canale^{104a,104b}, A. Canepa^{159a}, M. Cano Bret⁷⁶, J. Cantero⁸², R. Cantrill^{126a}, T. Cao⁴⁰, M.D.M. Capeans Garrido³⁰, I. Caprini^{26a}, M. Caprini^{26a}, M. Capua^{37a,37b}, R. Caputo⁸³, R. Cardarelli^{133a}, T. Carli³⁰, G. Carlino^{104a}, L. Carminati^{91a,91b}, S. Caron¹⁰⁶, E. Carquin^{32a}, G.D. Carrillo-Montoya⁸, J.R. Carter²⁸, J. Carvalho^{126a,126c}, D. Casadei⁷⁸, M.P. Casado¹², M. Casolino¹², E. Castaneda-Miranda^{145b}, A. Castelli¹⁰⁷, V. Castillo Gimenez¹⁶⁷, N.F. Castro^{126a,g}, P. Catastini⁵⁷, A. Catinaccio³⁰, J.R. Catmore¹¹⁹, A. Cattai³⁰, J. Caudron⁸³, V. Cavaliere¹⁶⁵, D. Cavalli^{91a}, M. Cavalli-Sforza¹², V. Cavasinni^{124a,124b}, F. Ceradini^{134a,134b}, B.C. Cerio⁴⁵, K. Cerny¹²⁹, A.S. Cerqueira^{24b}, A. Cerri¹⁴⁹, L. Cerrito⁷⁶, F. Cerutti¹⁵, M. Cerv³⁰, A. Cervelli¹⁷, S.A. Cetin^{19b}, A. Chafaq^{135a}, D. Chakraborty¹⁰⁸, I. Chalupkova¹²⁹, P. Chang¹⁶⁵, B. Chapleau⁸⁷, J.D. Chapman²⁸, D.G. Charlton¹⁸, C.C. Chau¹⁵⁸, C.A. Chavez Barajas¹⁴⁹, S. Cheatham¹⁵², A. Chegwidden⁹⁰, S. Chekanov⁶, S.V. Chekulaev^{159a}, G.A. Chelkov^{65,h}, M.A. Chelstowska⁸⁹, C. Chen⁶⁴, H. Chen²⁵, K. Chen¹⁴⁸, L. Chen^{33d,i}, S. Chen^{33c}, X. Chen^{33f}, Y. Chen⁶⁷, H.C. Cheng⁸⁹, Y. Cheng³¹, A. Cheplakov⁶⁵, E. Cheremushkina¹³⁰, R. Cherkaoui El Moursli^{135e}, V. Chernyatin^{25,*}, E. Cheu⁷, L. Chevalier¹³⁶, V. Chiarella⁴⁷, J.T. Childers⁶, G. Chiodini^{73a}, A.S. Chisholm¹⁸, R.T. Chislett⁷⁸, A. Chitan^{26a}, M.V. Chizhov⁶⁵, K. Choi⁶¹, S. Chouridou⁹, B.K.B. Chow¹⁰⁰, V. Christodoulou⁷⁸, D. Chromek-Burckhart³⁰, M.L. Chu¹⁵¹, J. Chudoba¹²⁷, A.J. Chuinard⁸⁷, J.J. Chwastowski³⁹, L. Chytka¹¹⁵, G. Ciapetti^{132a,132b}, A.K. Ciftci^{4a}, D. Cincă⁵³, V. Cindro⁷⁵, I.A. Cioara²¹, A. Ciocio¹⁵, Z.H. Citron¹⁷², M. Ciubancan^{26a}, A. Clark⁴⁹, B.L. Clark⁵⁷, P.J. Clark⁴⁶, R.N. Clarke¹⁵, W. Cleland¹²⁵, C. Clement^{146a,146b}, Y. Coadou⁸⁵, M. Cobal^{164a,164c}, A. Coccaro¹³⁸, J. Cochran⁶⁴, L. Coffey²³, J.G. Cogan¹⁴³, B. Cole³⁵, S. Cole¹⁰⁸, A.P. Colijn¹⁰⁷, J. Collot⁵⁵, T. Colombo^{58c}, G. Compostella¹⁰¹, P. Conde Muiño^{126a,126b}, E. Coniavitis⁴⁸, S.H. Connell^{145b}, I.A. Connelly⁷⁷, S.M. Consonni^{91a,91b}, V. Consorti⁴⁸, S. Constantinescu^{26a}, C. Conta^{121a,121b}, G. Conti³⁰, F. Conventi^{104a,j}, M. Cooke¹⁵, B.D. Cooper⁷⁸, A.M. Cooper-Sarkar¹²⁰, T. Cornelissen¹⁷⁵, M. Corradi^{20a}, F. Corriveau^{87,k}, A. Corso-Radu¹⁶³, A. Cortes-Gonzalez¹², G. Cortiana¹⁰¹, G. Costa^{91a}, M.J. Costa¹⁶⁷, D. Costanzo¹³⁹, D. Côté⁸, G. Cottin²⁸, G. Cowan⁷⁷, B.E. Cox⁸⁴, K. Cranmer¹¹⁰, G. Cree²⁹, S. Crépe-Renaudin⁵⁵, F. Crescioli⁸⁰, W.A. Cribbs^{146a,146b}, M. Crispin Ortuzar¹²⁰, M. Cristinziani²¹, V. Croft¹⁰⁶, G. Crosetti^{37a,37b}, T. Cuhadar Donszelmann¹³⁹, J. Cummings¹⁷⁶, M. Curatolo⁴⁷, C. Cuthbert¹⁵⁰, H. Czirr¹⁴¹, P. Czodrowski³, S. D'Auria⁵³, M. D'Onofrio⁷⁴, M.J. Da Cunha Sargedas De Sousa^{126a,126b}, C. Da Via⁸⁴, W. Dabrowski^{38a}, A. Dafinca¹²⁰, T. Dai⁸⁹, O. Dale¹⁴, F. Dallaire⁹⁵, C. Dallapiccola⁸⁶, M. Dam³⁶, J.R. Dandoy³¹, N.P. Dang⁴⁸, A.C. Daniells¹⁸, M. Danninger¹⁶⁸, M. Dano Hoffmann¹³⁶, V. Dao⁴⁸, G. Darbo^{50a},

S. Darmora⁸, J. Dassoulas³, A. Dattagupta⁶¹, W. Davey²¹, C. David¹⁶⁹, T. Davidek¹²⁹, E. Davies^{120,l},
 M. Davies¹⁵³, P. Davison⁷⁸, Y. Davygora^{58a}, E. Dawe⁸⁸, I. Dawson¹³⁹, R.K. Daya-Ishmukhametova⁸⁶,
 K. De⁸, R. de Asmundis^{104a}, S. De Castro^{20a,20b}, S. De Cecco⁸⁰, N. De Groot¹⁰⁶, P. de Jong¹⁰⁷,
 H. De la Torre⁸², F. De Lorenzi⁶⁴, L. De Nooij¹⁰⁷, D. De Pedis^{132a}, A. De Salvo^{132a}, U. De Sanctis¹⁴⁹,
 A. De Santo¹⁴⁹, J.B. De Vivie De Regie¹¹⁷, W.J. Dearnaley⁷², R. Debbe²⁵, C. Debenedetti¹³⁷,
 D.V. Dedovich⁶⁵, I. Deigaard¹⁰⁷, J. Del Peso⁸², T. Del Prete^{124a,124b}, D. Delgove¹¹⁷, F. Deliot¹³⁶,
 C.M. Delitzsch⁴⁹, M. Deliyergiyev⁷⁵, A. Dell'Acqua³⁰, L. Dell'Asta²², M. Dell'Orso^{124a,124b},
 M. Della Pietra^{104a,j}, D. della Volpe⁴⁹, M. Delmastro⁵, P.A. Delsart⁵⁵, C. Deluca¹⁰⁷, D.A. DeMarco¹⁵⁸,
 S. Demers¹⁷⁶, M. Demichev⁶⁵, A. Demilly⁸⁰, S.P. Denisov¹³⁰, D. Derendarz³⁹, J.E. Derkaoui^{135d},
 F. Derue⁸⁰, P. Dervan⁷⁴, K. Desch²¹, C. Deterre⁴², P.O. Deviveiros³⁰, A. Dewhurst¹³¹, S. Dhaliwal²³,
 A. Di Ciaccio^{133a,133b}, L. Di Ciaccio⁵, A. Di Domenico^{132a,132b}, C. Di Donato^{104a,104b},
 A. Di Girolamo³⁰, B. Di Girolamo³⁰, A. Di Mattia¹⁵², B. Di Micco^{134a,134b}, R. Di Nardo⁴⁷,
 A. Di Simone⁴⁸, R. Di Sipio¹⁵⁸, D. Di Valentino²⁹, C. Diaconu⁸⁵, M. Diamond¹⁵⁸, F.A. Dias⁴⁶,
 M.A. Diaz^{32a}, E.B. Diehl⁸⁹, J. Dietrich¹⁶, S. Diglio⁸⁵, A. Dimitrievska¹³, J. Dingfelder²¹, P. Dita^{26a},
 S. Dita^{26a}, F. Dittus³⁰, F. Djama⁸⁵, T. Djobava^{51b}, J.I. Djuvslund^{58a}, M.A.B. do Vale^{24c}, D. Dobos³⁰,
 M. Dobre^{26a}, C. Doglioni⁴⁹, T. Dohmae¹⁵⁵, J. Dolejsi¹²⁹, Z. Dolezal¹²⁹, B.A. Dolgoshein^{98,*},
 M. Donadelli^{24d}, S. Donati^{124a,124b}, P. Dondero^{121a,121b}, J. Donini³⁴, J. Dopke¹³¹, A. Doria^{104a},
 M.T. Dova⁷¹, A.T. Doyle⁵³, E. Drechsler⁵⁴, M. Dris¹⁰, E. Dubreuil³⁴, E. Duchovni¹⁷², G. Duckeck¹⁰⁰,
 O.A. Ducu^{26a,85}, D. Duda¹⁷⁵, A. Dudarev³⁰, L. Duflot¹¹⁷, L. Duguid⁷⁷, M. Dührssen³⁰, M. Dunford^{58a},
 H. Duran Yildiz^{4a}, M. Düren⁵², A. Durglishvili^{51b}, D. Duschinger⁴⁴, M. Dyndal^{38a}, C. Eckardt⁴²,
 K.M. Ecker¹⁰¹, R.C. Edgar⁸⁹, W. Edson², N.C. Edwards⁴⁶, W. Ehrenfeld²¹, T. Eifert³⁰, G. Eigen¹⁴,
 K. Einsweiler¹⁵, T. Ekelof¹⁶⁶, M. El Kacimi^{135c}, M. Ellert¹⁶⁶, S. Elles⁵, F. Ellinghaus⁸³, A.A. Elliot¹⁶⁹,
 N. Ellis³⁰, J. Elmsheuser¹⁰⁰, M. Elsing³⁰, D. Emeliyanov¹³¹, Y. Enari¹⁵⁵, O.C. Endner⁸³, M. Endo¹¹⁸,
 J. Erdmann⁴³, A. Ereditato¹⁷, G. Ernis¹⁷⁵, J. Ernst², M. Ernst²⁵, S. Errede¹⁶⁵, E. Ertel⁸³, M. Escalier¹¹⁷,
 H. Esch⁴³, C. Escobar¹²⁵, B. Esposito⁴⁷, A.I. Etienne¹³⁶, E. Etzion¹⁵³, H. Evans⁶¹, A. Ezhilov¹²³,
 L. Fabbri^{20a,20b}, G. Facini³¹, R.M. Fakhruddinov¹³⁰, S. Falciano^{132a}, R.J. Falla⁷⁸, J. Faltova¹²⁹,
 Y. Fang^{33a}, M. Fanti^{91a,91b}, A. Farbin⁸, A. Farilla^{134a}, T. Farooque¹², S. Farrell¹⁵, S.M. Farrington¹⁷⁰,
 P. Farthouat³⁰, F. Fassi^{135e}, P. Fassnacht³⁰, D. Fassouliotis⁹, M. Fauci Giannelli⁷⁷, A. Favareto^{50a,50b},
 L. Fayard¹¹⁷, P. Federic^{144a}, O.L. Fedin^{123,m}, W. Fedorko¹⁶⁸, S. Feigl³⁰, L. Felgioni⁸⁵, C. Feng^{33d},
 E.J. Feng⁶, H. Feng⁸⁹, A.B. Fenyuk¹³⁰, P. Fernandez Martinez¹⁶⁷, S. Fernandez Perez³⁰, J. Ferrando⁵³,
 A. Ferrari¹⁶⁶, P. Ferrari¹⁰⁷, R. Ferrari^{121a}, D.E. Ferreira de Lima⁵³, A. Ferrer¹⁶⁷, D. Ferrere⁴⁹,
 C. Ferretti⁸⁹, A. Ferretto Parodi^{50a,50b}, M. Fiascaris³¹, F. Fiedler⁸³, A. Filipčić⁷⁵, M. Filipuzzi⁴²,
 F. Filthaut¹⁰⁶, M. Fincke-Keeler¹⁶⁹, K.D. Finelli¹⁵⁰, M.C.N. Fiolhais^{126a,126c}, L. Fiorini¹⁶⁷, A. Firan⁴⁰,
 A. Fischer², C. Fischer¹², J. Fischer¹⁷⁵, W.C. Fisher⁹⁰, E.A. Fitzgerald²³, M. Flechl⁴⁸, I. Fleck¹⁴¹,
 P. Fleischmann⁸⁹, S. Fleischmann¹⁷⁵, G.T. Fletcher¹³⁹, G. Fletcher⁷⁶, T. Flick¹⁷⁵, A. Floderus⁸¹,
 L.R. Flores Castillo^{60a}, M.J. Flowerdew¹⁰¹, A. Formica¹³⁶, A. Forti⁸⁴, D. Fournier¹¹⁷, H. Fox⁷²,
 S. Fracchia¹², P. Francavilla⁸⁰, M. Franchini^{20a,20b}, D. Francis³⁰, L. Franconi¹¹⁹, M. Franklin⁵⁷,
 M. Fraternali^{121a,121b}, D. Freeborn⁷⁸, S.T. French²⁸, F. Friedrich⁴⁴, D. Froidevaux³⁰, J.A. Frost¹²⁰,
 C. Fukunaga¹⁵⁶, E. Fullana Torregrosa⁸³, B.G. Fulsom¹⁴³, J. Fuster¹⁶⁷, C. Gabaldon⁵⁵, O. Gabizon¹⁷⁵,
 A. Gabrielli^{20a,20b}, A. Gabrielli^{132a,132b}, S. Gadatsch¹⁰⁷, S. Gadomski⁴⁹, G. Gagliardi^{50a,50b}, P. Gagnon⁶¹,
 C. Galea¹⁰⁶, B. Galhardo^{126a,126c}, E.J. Gallas¹²⁰, B.J. Gallop¹³¹, P. Gallus¹²⁸, G. Galster³⁶, K.K. Gan¹¹¹,
 J. Gao^{33b,85}, Y. Gao⁴⁶, Y.S. Gao^{143,e}, F.M. Garay Walls⁴⁶, F. Garbersson¹⁷⁶, C. García¹⁶⁷,
 J.E. García Navarro¹⁶⁷, M. Garcia-Sciveres¹⁵, R.W. Gardner³¹, N. Garelli¹⁴³, V. Garonne¹¹⁹, C. Gatti⁴⁷,
 A. Gaudiello^{50a,50b}, G. Gaudio^{121a}, B. Gaur¹⁴¹, L. Gauthier⁹⁵, P. Gauzzi^{132a,132b}, I.L. Gavrilenko⁹⁶,
 C. Gay¹⁶⁸, G. Gaycken²¹, E.N. Gazis¹⁰, P. Ge^{33d}, Z. Gece¹⁶⁸, C.N.P. Gee¹³¹, D.A.A. Geerts¹⁰⁷,
 Ch. Geich-Gimbel²¹, M.P. Geisler^{58a}, C. Gemme^{50a}, M.H. Genest⁵⁵, S. Gentile^{132a,132b}, M. George⁵⁴,
 S. George⁷⁷, D. Gerbaudo¹⁶³, A. Gershon¹⁵³, H. Ghazlane^{135b}, B. Giacobbe^{20a}, S. Giagu^{132a,132b},

V. Giangiobbe¹², P. Giannetti^{124a,124b}, B. Gibbard²⁵, S.M. Gibson⁷⁷, M. Gilchriese¹⁵, T.P.S. Gillam²⁸, D. Gillberg³⁰, G. Gilles³⁴, D.M. Gingrich^{3,d}, N. Giokaris⁹, M.P. Giordani^{164a,164c}, F.M. Giorgi^{20a}, F.M. Giorgi¹⁶, P.F. Giraud¹³⁶, P. Giromini⁴⁷, D. Giugni^{91a}, C. Giuliani⁴⁸, M. Giulini^{58b}, B.K. Gjelsten¹¹⁹, S. Gkaitatzis¹⁵⁴, I. Gkialas¹⁵⁴, E.L. Gkoukousis¹¹⁷, L.K. Gladilin⁹⁹, C. Glasman⁸², J. Glatzer³⁰, P.C.F. Glaysher⁴⁶, A. Glazov⁴², M. Goblirsch-Kolb¹⁰¹, J.R. Goddard⁷⁶, J. Godlewski³⁹, S. Goldfarb⁸⁹, T. Golling⁴⁹, D. Golubkov¹³⁰, A. Gomes^{126a,126b,126d}, R. Gonçalo^{126a}, J. Goncalves Pinto Firmino Da Costa¹³⁶, L. Gonella²¹, S. González de la Hoz¹⁶⁷, G. Gonzalez Parra¹², S. Gonzalez-Sevilla⁴⁹, L. Goossens³⁰, P.A. Gorbounov⁹⁷, H.A. Gordon²⁵, I. Gorelov¹⁰⁵, B. Gorini³⁰, E. Gorini^{73a,73b}, A. Gorišek⁷⁵, E. Gornicki³⁹, A.T. Goshaw⁴⁵, C. Gössling⁴³, M.I. Gostkin⁶⁵, D. Goujdami^{135c}, A.G. Goussiou¹³⁸, N. Govender^{145b}, H.M.X. Grabas¹³⁷, L. Graber⁵⁴, I. Grabowska-Bold^{38a}, P. Grafström^{20a,20b}, K.-J. Grahn⁴², J. Gramling⁴⁹, E. Gramstad¹¹⁹, S. Grancagnolo¹⁶, V. Grassi¹⁴⁸, V. Gratchev¹²³, H.M. Gray³⁰, E. Graziani^{134a}, Z.D. Greenwood^{79,n}, K. Gregersen⁷⁸, I.M. Gregor⁴², P. Grenier¹⁴³, J. Griffiths⁸, A.A. Grillo¹³⁷, K. Grimm⁷², S. Grinstein^{12,o}, Ph. Gris³⁴, J.-F. Grivaz¹¹⁷, J.P. Grohs⁴⁴, A. Grohsjean⁴², E. Gross¹⁷², J. Grosse-Knetter⁵⁴, G.C. Grossi⁷⁹, Z.J. Grout¹⁴⁹, L. Guan^{33b}, J. Guenther¹²⁸, F. Guescini⁴⁹, D. Guest¹⁷⁶, O. Gueta¹⁵³, E. Guido^{50a,50b}, T. Guillemin¹¹⁷, S. Guindon², U. Gul⁵³, C. Gumpert⁴⁴, J. Guo^{33e}, S. Gupta¹²⁰, P. Gutierrez¹¹³, N.G. Gutierrez Ortiz⁵³, C. Gutsche⁴⁴, C. Guyot¹³⁶, C. Gwenlan¹²⁰, C.B. Gwilliam⁷⁴, A. Haas¹¹⁰, C. Haber¹⁵, H.K. Hadavand⁸, N. Haddad^{135e}, P. Haefner²¹, S. Hageböck²¹, Z. Hajduk³⁹, H. Hakobyan¹⁷⁷, M. Haleem⁴², J. Haley¹¹⁴, D. Hall¹²⁰, G. Halladjian⁹⁰, G.D. Hallowell⁸⁵, K. Hamacher¹⁷⁵, P. Hamal¹¹⁵, K. Hamano¹⁶⁹, M. Hamer⁵⁴, A. Hamilton^{145a}, G.N. Hamity^{145c}, P.G. Hamnett⁴², L. Han^{33b}, K. Hanagaki¹¹⁸, K. Hanawa¹⁵⁵, M. Hance¹⁵, P. Hanke^{58a}, R. Hanna¹³⁶, J.B. Hansen³⁶, J.D. Hansen³⁶, M.C. Hansen²¹, P.H. Hansen³⁶, K. Hara¹⁶⁰, A.S. Hard¹⁷³, T. Harenberg¹⁷⁵, F. Hariri¹¹⁷, S. Harkusha⁹², R.D. Harrington⁴⁶, P.F. Harrison¹⁷⁰, F. Hartjes¹⁰⁷, M. Hasegawa⁶⁷, S. Hasegawa¹⁰³, Y. Hasegawa¹⁴⁰, A. Hasib¹¹³, S. Hassani¹³⁶, S. Haug¹⁷, R. Hauser⁹⁰, L. Hauswald⁴⁴, M. Havranek¹²⁷, C.M. Hawkes¹⁸, R.J. Hawkins³⁰, A.D. Hawkins⁸¹, T. Hayashi¹⁶⁰, D. Hayden⁹⁰, C.P. Hays¹²⁰, J.M. Hays⁷⁶, H.S. Hayward⁷⁴, S.J. Haywood¹³¹, S.J. Head¹⁸, T. Heck⁸³, V. Hedberg⁸¹, L. Heelan⁸, S. Heim¹²², T. Heim¹⁷⁵, B. Heinemann¹⁵, L. Heinrich¹¹⁰, J. Hejbal¹²⁷, L. Helary²², S. Hellman^{146a,146b}, D. Hellmich²¹, C. Helsen³⁰, J. Henderson¹²⁰, R.C.W. Henderson⁷², Y. Heng¹⁷³, C. Hengler⁴², A. Henrichs¹⁷⁶, A.M. Henriques Correia³⁰, S. Henrot-Versille¹¹⁷, G.H. Herbert¹⁶, Y. Hernández Jiménez¹⁶⁷, R. Herrberg-Schubert¹⁶, G. Herten⁴⁸, R. Hertenberger¹⁰⁰, L. Hervas³⁰, G.G. Hesketh⁷⁸, N.P. Hessey¹⁰⁷, J.W. Hetherly⁴⁰, R. Hickling⁷⁶, E. Higón-Rodríguez¹⁶⁷, E. Hill¹⁶⁹, J.C. Hill²⁸, K.H. Hiller⁴², S.J. Hillier¹⁸, I. Hinchliffe¹⁵, E. Hines¹²², R.R. Hinman¹⁵, M. Hirose¹⁵⁷, D. Hirschbuehl¹⁷⁵, J. Hobbs¹⁴⁸, N. Hod¹⁰⁷, M.C. Hodgkinson¹³⁹, P. Hodgson¹³⁹, A. Hoecker³⁰, M.R. Hoferkamp¹⁰⁵, F. Hoenig¹⁰⁰, M. Hohlfeld⁸³, D. Hohn²¹, T.R. Holmes¹⁵, M. Homann⁴³, T.M. Hong¹²⁵, L. Hooft van Huysduyven¹¹⁰, W.H. Hopkins¹¹⁶, Y. Hori¹⁰³, A.J. Horton¹⁴², J.-Y. Hostachy⁵⁵, S. Hou¹⁵¹, A. Hoummada^{135a}, J. Howard¹²⁰, J. Howarth⁴², M. Hrabovsky¹¹⁵, I. Hristova¹⁶, J. Hrivnac¹¹⁷, T. Hryn'ova⁵, A. Hrynevich⁹³, C. Hsu^{145c}, P.J. Hsu^{151,p}, S.-C. Hsu¹³⁸, D. Hu³⁵, Q. Hu^{33b}, X. Hu⁸⁹, Y. Huang⁴², Z. Hubacek³⁰, F. Hubaut⁸⁵, F. Huegging²¹, T.B. Huffman¹²⁰, E.W. Hughes³⁵, G. Hughes⁷², M. Huhtinen³⁰, T.A. Hülsing⁸³, N. Huseynov^{65,b}, J. Huston⁹⁰, J. Huth⁵⁷, G. Iacobucci⁴⁹, G. Iakovidis²⁵, I. Ibragimov¹⁴¹, L. Iconomidou-Fayard¹¹⁷, E. Ideal¹⁷⁶, Z. Idrissi^{135e}, P. Iengo³⁰, O. Igonkina¹⁰⁷, T. Iizawa¹⁷¹, Y. Ikegami⁶⁶, K. Ikematsu¹⁴¹, M. Ikeno⁶⁶, Y. Ilchenko^{31,q}, D. Iliadis¹⁵⁴, N. Ilic¹⁴³, Y. Inamaru⁶⁷, T. Ince¹⁰¹, P. Ioannou⁹, M. Iodice^{134a}, K. Iordanidou³⁵, V. Ippolito⁵⁷, A. Irlles Quiles¹⁶⁷, C. Isaksson¹⁶⁶, M. Ishino⁶⁸, M. Ishitsuka¹⁵⁷, R. Ishmukhametov¹¹¹, C. Issever¹²⁰, S. Istin^{19a}, J.M. Iturbe Ponce⁸⁴, R. Iuppa^{133a,133b}, J. Ivarsson⁸¹, W. Iwanski³⁹, H. Iwasaki⁶⁶, J.M. Izen⁴¹, V. Izzo^{104a}, S. Jabbar³, B. Jackson¹²², M. Jackson⁷⁴, P. Jackson¹, M.R. Jaekel³⁰, V. Jain², K. Jakobs⁴⁸, S. Jakobsen³⁰, T. Jakoubek¹²⁷, J. Jakubek¹²⁸, D.O. Jamin¹⁵¹, D.K. Jana⁷⁹, E. Jansen⁷⁸, R.W. Jansky⁶², J. Janssen²¹, M. Janus¹⁷⁰, G. Jarlskog⁸¹,

N. Javadov^{65,b}, T. Javůrek⁴⁸, L. Jeanty¹⁵, J. Jejelava^{51a,r}, G.-Y. Jeng¹⁵⁰, D. Jennens⁸⁸, P. Jenni^{48,s},
 J. Jentzsch⁴³, C. Jeske¹⁷⁰, S. Jézéquel⁵, H. Ji¹⁷³, J. Jia¹⁴⁸, Y. Jiang^{33b}, S. Jiggins⁷⁸, J. Jimenez Pena¹⁶⁷,
 S. Jin^{33a}, A. Jinaru^{26a}, O. Jinnouchi¹⁵⁷, M.D. Joergensen³⁶, P. Johansson¹³⁹, K.A. Johns⁷,
 K. Jon-And^{146a,146b}, G. Jones¹⁷⁰, R.W.L. Jones⁷², T.J. Jones⁷⁴, J. Jongmanns^{58a}, P.M. Jorge^{126a,126b},
 K.D. Joshi⁸⁴, J. Jovicevic^{159a}, X. Ju¹⁷³, C.A. Jung⁴³, P. Jussel⁶², A. Juste Rozas^{12,o}, M. Kaci¹⁶⁷,
 A. Kaczmarzka³⁹, M. Kado¹¹⁷, H. Kagan¹¹¹, M. Kagan¹⁴³, S.J. Kahn⁸⁵, E. Kajomovitz⁴⁵,
 C.W. Kalderon¹²⁰, S. Kama⁴⁰, A. Kamenshchikov¹³⁰, N. Kanaya¹⁵⁵, M. Kaneda³⁰, S. Kaneti²⁸,
 V.A. Kantserov⁹⁸, J. Kanzaki⁶⁶, B. Kaplan¹¹⁰, A. Kapliy³¹, D. Kar⁵³, K. Karakostas¹⁰, A. Karamaoun³,
 N. Karastathis^{10,107}, M.J. Kareem⁵⁴, M. Karnevskiy⁸³, S.N. Karpov⁶⁵, Z.M. Karpova⁶⁵, K. Karthik¹¹⁰,
 V. Kartvelishvili⁷², A.N. Karyukhin¹³⁰, L. Kashif¹⁷³, R.D. Kass¹¹¹, A. Kastanas¹⁴, Y. Kataoka¹⁵⁵,
 A. Katre⁴⁹, J. Katzy⁴², K. Kawagoe⁷⁰, T. Kawamoto¹⁵⁵, G. Kawamura⁵⁴, S. Kazama¹⁵⁵,
 V.F. Kazanin^{109,c}, M.Y. Kazarinov⁶⁵, R. Keeler¹⁶⁹, R. Kehoe⁴⁰, J.S. Keller⁴², J.J. Kempster⁷⁷,
 H. Keoshkerian⁸⁴, O. Kepka¹²⁷, B.P. Kerševan⁷⁵, S. Kersten¹⁷⁵, R.A. Keyes⁸⁷, F. Khalil-zada¹¹,
 H. Khandanyan^{146a,146b}, A. Khanov¹¹⁴, A.G. Kharlamov^{109,c}, T.J. Khoo²⁸, V. Khovanskiy⁹⁷,
 E. Khramov⁶⁵, J. Khubua^{51b,t}, H.Y. Kim⁸, H. Kim^{146a,146b}, S.H. Kim¹⁶⁰, Y. Kim³¹, N. Kimura¹⁵⁴,
 O.M. Kind¹⁶, B.T. King⁷⁴, M. King¹⁶⁷, R.S.B. King¹²⁰, S.B. King¹⁶⁸, J. Kirk¹³¹, A.E. Kiryunin¹⁰¹,
 T. Kishimoto⁶⁷, D. Kisielewska^{38a}, F. Kiss⁴⁸, K. Kiuchi¹⁶⁰, O. Kivernyk¹³⁶, E. Kladiva^{144b},
 M.H. Klein³⁵, M. Klein⁷⁴, U. Klein⁷⁴, K. Kleinknecht⁸³, P. Klimek^{146a,146b}, A. Klimentov²⁵,
 R. Klingenberg⁴³, J.A. Klinger⁸⁴, T. Klioutchnikova³⁰, E.-E. Kluge^{58a}, P. Kluit¹⁰⁷, S. Kluth¹⁰¹,
 E. Kneringer⁶², E.B.F.G. Knoops⁸⁵, A. Knue⁵³, A. Kobayashi¹⁵⁵, D. Kobayashi¹⁵⁷, T. Kobayashi¹⁵⁵,
 M. Kobel⁴⁴, M. Kocian¹⁴³, P. Kodys¹²⁹, T. Koffas²⁹, E. Koffeman¹⁰⁷, L.A. Kogan¹²⁰, S. Kohlmann¹⁷⁵,
 Z. Kohout¹²⁸, T. Kohriki⁶⁶, T. Koi¹⁴³, H. Kolanoski¹⁶, I. Koletsou⁵, A.A. Komar^{96,*}, Y. Komori¹⁵⁵,
 T. Kondo⁶⁶, N. Kondrashova⁴², K. Köneke⁴⁸, A.C. König¹⁰⁶, S. König⁸³, T. Kono^{66,u}, R. Konoplich^{110,v},
 N. Konstantinidis⁷⁸, R. Kopeliansky¹⁵², S. Koperny^{38a}, L. Köpke⁸³, A.K. Kopp⁴⁸, K. Korcyl³⁹,
 K. Kordas¹⁵⁴, A. Korn⁷⁸, A.A. Korol^{109,c}, I. Korolkov¹², E.V. Korolkova¹³⁹, O. Kortner¹⁰¹, S. Kortner¹⁰¹,
 T. Kosek¹²⁹, V.V. Kostyukhin²¹, V.M. Kotov⁶⁵, A. Kotwal⁴⁵, A. Kourkoumeli-Charalampidi¹⁵⁴,
 C. Kourkoumelis⁹, V. Kouskoura²⁵, A. Koutsman^{159a}, R. Kowalewski¹⁶⁹, T.Z. Kowalski^{38a},
 W. Kozanecki¹³⁶, A.S. Kozhin¹³⁰, V.A. Kramarenko⁹⁹, G. Kramberger⁷⁵, D. Krasnopevtsev⁹⁸,
 M.W. Krasny⁸⁰, A. Krasznahorkay³⁰, J.K. Kraus²¹, A. Kravchenko²⁵, S. Kreiss¹¹⁰, M. Kretz^{58c},
 J. Kretzschmar⁷⁴, K. Kreutzfeldt⁵², P. Krieger¹⁵⁸, K. Krizka³¹, K. Kroeninger⁴³, H. Kroha¹⁰¹, J. Kroll¹²²,
 J. Kroseberg²¹, J. Krstic¹³, U. Kruchonak⁶⁵, H. Krüger²¹, N. Krumnack⁶⁴, Z.V. Krumshteyn⁶⁵,
 A. Kruse¹⁷³, M.C. Kruse⁴⁵, M. Kruskal²², T. Kubota⁸⁸, H. Kucuk⁷⁸, S. Kuday^{4c}, S. Kuehn⁴⁸,
 A. Kugel^{58c}, F. Kuger¹⁷⁴, A. Kuhl¹³⁷, T. Kuhl⁴², V. Kukhtin⁶⁵, Y. Kulchitsky⁹², S. Kuleshov^{32b},
 M. Kuna^{132a,132b}, T. Kunigo⁶⁸, A. Kupco¹²⁷, H. Kurashige⁶⁷, Y.A. Kurochkin⁹², R. Kurumida⁶⁷,
 V. Kus¹²⁷, E.S. Kuwertz¹⁶⁹, M. Kuze¹⁵⁷, J. Kvita¹¹⁵, T. Kwan¹⁶⁹, D. Kyriazopoulos¹³⁹, A. La Rosa⁴⁹,
 J.L. La Rosa Navarro^{24d}, L. La Rotonda^{37a,37b}, C. Lacasta¹⁶⁷, F. Lacava^{132a,132b}, J. Lacey²⁹, H. Lacker¹⁶,
 D. Lacour⁸⁰, V.R. Lacuesta¹⁶⁷, E. Ladygin⁶⁵, R. Lafaye⁵, B. Laforge⁸⁰, T. Lagouri¹⁷⁶, S. Lai⁴⁸,
 L. Lambourne⁷⁸, S. Lammers⁶¹, C.L. Lampen⁷, W. Lampl⁷, E. Lançon¹³⁶, U. Landgraf⁴⁸,
 M.P.J. Landon⁷⁶, V.S. Lang^{58a}, J.C. Lange¹², A.J. Lankford¹⁶³, F. Lanni²⁵, K. Lantzsch³⁰, S. Laplace⁸⁰,
 C. Lapoire³⁰, J.F. Laporte¹³⁶, T. Lari^{91a}, F. Lasagni Manghi^{20a,20b}, M. Lassnig³⁰, P. Laurelli⁴⁷,
 W. Lavrijsen¹⁵, A.T. Law¹³⁷, P. Laycock⁷⁴, O. Le Dortz⁸⁰, E. Le Guirriec⁸⁵, E. Le Menedeu¹²,
 M. LeBlanc¹⁶⁹, T. LeCompte⁶, F. Ledroit-Guillon⁵⁵, C.A. Lee^{145b}, S.C. Lee¹⁵¹, L. Lee¹, G. Lefebvre⁸⁰,
 M. Lefebvre¹⁶⁹, F. Legger¹⁰⁰, C. Leggett¹⁵, A. Lehan⁷⁴, G. Lehmann Miotto³⁰, X. Lei⁷, W.A. Leight²⁹,
 A. Leisos¹⁵⁴, A.G. Leister¹⁷⁶, M.A.L. Leite^{24d}, R. Leitner¹²⁹, D. Lellouch¹⁷², B. Lemmer⁵⁴,
 K.J.C. Leney⁷⁸, T. Lenz²¹, B. Lenzi³⁰, R. Leone⁷, S. Leone^{124a,124b}, C. Leonidopoulos⁴⁶, S. Leontsinis¹⁰,
 C. Leroy⁹⁵, C.G. Lester²⁸, M. Levchenko¹²³, J. Levêque⁵, D. Levin⁸⁹, L.J. Levinson¹⁷², M. Levy¹⁸,
 A. Lewis¹²⁰, A.M. Leyko²¹, M. Leyton⁴¹, B. Li^{33b,w}, H. Li¹⁴⁸, H.L. Li³¹, L. Li⁴⁵, L. Li^{33e}, S. Li⁴⁵,

Y. Li^{33c,x}, Z. Liang¹³⁷, H. Liao³⁴, B. Liberti^{133a}, A. Liblong¹⁵⁸, P. Lichard³⁰, K. Lie¹⁶⁵, J. Liebal²¹,
 W. Liebig¹⁴, C. Limbach²¹, A. Limosani¹⁵⁰, S.C. Lin^{151,y}, T.H. Lin⁸³, F. Linde¹⁰⁷, B.E. Lindquist¹⁴⁸,
 J.T. Linnemann⁹⁰, E. Lipeles¹²², A. Lipniacka¹⁴, M. Lisovyi^{58b}, T.M. Liss¹⁶⁵, D. Lissauer²⁵,
 A. Lister¹⁶⁸, A.M. Litke¹³⁷, B. Liu^{151,z}, D. Liu¹⁵¹, J. Liu⁸⁵, J.B. Liu^{33b}, K. Liu⁸⁵, L. Liu¹⁶⁵, M. Liu⁴⁵,
 M. Liu^{33b}, Y. Liu^{33b}, M. Livan^{121a,121b}, A. Lleres⁵⁵, J. Llorente Merino⁸², S.L. Lloyd⁷⁶, F. Lo Sterzo¹⁵¹,
 E. Lobodzinska⁴², P. Loch⁷, W.S. Lockman¹³⁷, F.K. Loebinger⁸⁴, A.E. Loevschall-Jensen³⁶,
 A. Loginov¹⁷⁶, T. Lohse¹⁶, K. Lohwasser⁴², M. Lokajicek¹²⁷, B.A. Long²², J.D. Long⁸⁹, R.E. Long⁷²,
 K.A. Looper¹¹¹, L. Lopes^{126a}, D. Lopez Mateos⁵⁷, B. Lopez Paredes¹³⁹, I. Lopez Paz¹², J. Lorenz¹⁰⁰,
 N. Lorenzo Martinez⁶¹, M. Losada¹⁶², P. Loscutoff¹⁵, P.J. Lösel¹⁰⁰, X. Lou^{33a}, A. Lounis¹¹⁷, J. Love⁶,
 P.A. Love⁷², N. Lu⁸⁹, H.J. Lubatti¹³⁸, C. Luci^{132a,132b}, A. Lucotte⁵⁵, F. Luehring⁶¹, W. Lukas⁶²,
 L. Luminari^{132a}, O. Lundberg^{146a,146b}, B. Lund-Jensen¹⁴⁷, D. Lynn²⁵, R. Lysak¹²⁷, E. Lytken⁸¹, H. Ma²⁵,
 L.L. Ma^{33d}, G. Maccarrone⁴⁷, A. Macchiolo¹⁰¹, C.M. Macdonald¹³⁹, J. Machado Miguens^{122,126b},
 D. Macina³⁰, D. Madaffari⁸⁵, R. Madar³⁴, H.J. Maddocks⁷², W.F. Mader⁴⁴, A. Madsen¹⁶⁶, S. Maeland¹⁴,
 T. Maeno²⁵, A. Maevskiy⁹⁹, E. Magradze⁵⁴, K. Mahboubi⁴⁸, J. Mahlstedt¹⁰⁷, C. Maiani¹³⁶,
 C. Maidantchik^{24a}, A.A. Maier¹⁰¹, T. Maier¹⁰⁰, A. Maio^{126a,126b,126d}, S. Majewski¹¹⁶, Y. Makida⁶⁶,
 N. Makovec¹¹⁷, B. Malaescu⁸⁰, Pa. Malecki³⁹, V.P. Maleev¹²³, F. Malek⁵⁵, U. Mallik⁶³, D. Malon⁶,
 C. Malone¹⁴³, S. Maltezos¹⁰, V.M. Malyshev¹⁰⁹, S. Malyukov³⁰, J. Mamuzic⁴², G. Mancini⁴⁷,
 B. Mandelli³⁰, L. Mandelli^{91a}, I. Mandić⁷⁵, R. Mandrysch⁶³, J. Maneira^{126a,126b}, A. Manfredini¹⁰¹,
 L. Manhaes de Andrade Filho^{24b}, J. Manjarres Ramos^{159b}, A. Mann¹⁰⁰, P.M. Manning¹³⁷,
 A. Manousakis-Katsikakis⁹, B. Mansoulie¹³⁶, R. Mantifel⁸⁷, M. Mantoani⁵⁴, L. Mapelli³⁰, L. March^{145c},
 G. Marchiori⁸⁰, M. Marcisovsky¹²⁷, C.P. Marino¹⁶⁹, M. Marjanovic¹³, F. Marroquim^{24a}, S.P. Marsden⁸⁴,
 Z. Marshall¹⁵, L.F. Marti¹⁷, S. Marti-Garcia¹⁶⁷, B. Martin⁹⁰, T.A. Martin¹⁷⁰, V.J. Martin⁴⁶,
 B. Martin dit Latour¹⁴, M. Martinez^{12,o}, S. Martin-Haugh¹³¹, V.S. Martoiu^{26a}, A.C. Martyniuk⁷⁸,
 M. Marx¹³⁸, F. Marzano^{132a}, A. Marzin³⁰, L. Masetti⁸³, T. Mashimo¹⁵⁵, R. Mashinistov⁹⁶, J. Masik⁸⁴,
 A.L. Maslennikov^{109,c}, I. Massa^{20a,20b}, L. Massa^{20a,20b}, N. Massol⁵, P. Mastrandrea¹⁴⁸,
 A. Mastroberardino^{37a,37b}, T. Masubuchi¹⁵⁵, P. Mättig¹⁷⁵, J. Mattmann⁸³, J. Maurer^{26a}, S.J. Maxfield⁷⁴,
 D.A. Maximov^{109,c}, R. Mazini¹⁵¹, S.M. Mazza^{91a,91b}, L. Mazzaferro^{133a,133b}, G. Mc Goldrick¹⁵⁸,
 S.P. Mc Kee⁸⁹, A. McCann⁸⁹, R.L. McCarthy¹⁴⁸, T.G. McCarthy²⁹, N.A. McCubbin¹³¹,
 K.W. McFarlane^{56,*}, J.A. Mcfayden⁷⁸, G. Mchedlidge⁵⁴, S.J. McMahon¹³¹, R.A. McPherson^{169,k},
 M. Medinnis⁴², S. Meehan^{145a}, S. Mehlhase¹⁰⁰, A. Mehta⁷⁴, K. Meier^{58a}, C. Meineck¹⁰⁰, B. Meirose⁴¹,
 B.R. Mellado Garcia^{145c}, F. Meloni¹⁷, A. Mengarelli^{20a,20b}, S. Menke¹⁰¹, E. Meoni¹⁶¹, K.M. Mercurio⁵⁷,
 S. Mergelmeyer²¹, P. Mermod⁴⁹, L. Merola^{104a,104b}, C. Meroni^{91a}, F.S. Merritt³¹, A. Messina^{132a,132b},
 J. Metcalfe²⁵, A.S. Mete¹⁶³, C. Meyer⁸³, C. Meyer¹²², J-P. Meyer¹³⁶, J. Meyer¹⁰⁷, R.P. Middleton¹³¹,
 S. Miglioranzi^{164a,164c}, L. Mijović²¹, G. Mikenberg¹⁷², M. Mikestikova¹²⁷, M. Mikuž⁷⁵, M. Milesi⁸⁸,
 A. Milic³⁰, D.W. Miller³¹, C. Mills⁴⁶, A. Milov¹⁷², D.A. Milstead^{146a,146b}, A.A. Minaenko¹³⁰,
 Y. Minami¹⁵⁵, I.A. Minashvili⁶⁵, A.I. Mincer¹¹⁰, B. Mindur^{38a}, M. Mineev⁶⁵, Y. Ming¹⁷³, L.M. Mir¹²,
 T. Mitani¹⁷¹, J. Mitrevski¹⁰⁰, V.A. Mitsou¹⁶⁷, A. Miucci⁴⁹, P.S. Miyagawa¹³⁹, J.U. Mjörnmark⁸¹,
 T. Moa^{146a,146b}, K. Mochizuki⁸⁵, S. Mohapatra³⁵, W. Mohr⁴⁸, S. Molander^{146a,146b}, R. Moles-Valls¹⁶⁷,
 K. Mönig⁴², C. Monini⁵⁵, J. Monk³⁶, E. Monnier⁸⁵, J. Montejo Berlingen¹², F. Monticelli⁷¹,
 S. Monzani^{132a,132b}, R.W. Moore³, N. Morange¹¹⁷, D. Moreno¹⁶², M. Moreno Llácer⁵⁴, P. Morettini^{50a},
 M. Morgenstern⁴⁴, M. Morii⁵⁷, M. Morinaga¹⁵⁵, V. Morisbak¹¹⁹, S. Moritz⁸³, A.K. Morley¹⁴⁷,
 G. Mornacchi³⁰, J.D. Morris⁷⁶, S.S. Mortensen³⁶, A. Morton⁵³, L. Morvaj¹⁰³, M. Mosidze^{51b},
 J. Moss¹¹¹, K. Motohashi¹⁵⁷, R. Mount¹⁴³, E. Mountricha²⁵, S.V. Mouraviev^{96,*}, E.J.W. Moyse⁸⁶,
 S. Muanza⁸⁵, R.D. Mudd¹⁸, F. Mueller¹⁰¹, J. Mueller¹²⁵, K. Mueller²¹, R.S.P. Mueller¹⁰⁰, T. Mueller²⁸,
 D. Muenstermann⁴⁹, P. Mullen⁵³, Y. Munwes¹⁵³, J.A. Murillo Quijada¹⁸, W.J. Murray^{170,131},
 H. Musheghyan⁵⁴, E. Musto¹⁵², A.G. Myagkov^{130,aa}, M. Myska¹²⁸, O. Nackenhorst⁵⁴, J. Nadal⁵⁴,
 K. Nagai¹²⁰, R. Nagai¹⁵⁷, Y. Nagai⁸⁵, K. Nagano⁶⁶, A. Nagarkar¹¹¹, Y. Nagasaka⁵⁹, K. Nagata¹⁶⁰,

M. Nagel¹⁰¹, E. Nagy⁸⁵, A.M. Nairz³⁰, Y. Nakahama³⁰, K. Nakamura⁶⁶, T. Nakamura¹⁵⁵, I. Nakano¹¹², H. Namasivayam⁴¹, R.F. Naranjo Garcia⁴², R. Narayan³¹, T. Naumann⁴², G. Navarro¹⁶², R. Nayyar⁷, H.A. Neal⁸⁹, P.Yu. Nechaeva⁹⁶, T.J. Neep⁸⁴, P.D. Nef¹⁴³, A. Negri^{121a,121b}, M. Negrini^{20a}, S. Nektarijevic¹⁰⁶, C. Nellist¹¹⁷, A. Nelson¹⁶³, S. Nemecek¹²⁷, P. Nemethy¹¹⁰, A.A. Nepomuceno^{24a}, M. Nessi^{30,ab}, M.S. Neubauer¹⁶⁵, M. Neumann¹⁷⁵, R.M. Neves¹¹⁰, P. Nevski²⁵, P.R. Newman¹⁸, D.H. Nguyen⁶, R.B. Nickerson¹²⁰, R. Nicolaidou¹³⁶, B. Nicquevert³⁰, J. Nielsen¹³⁷, N. Nikiforou³⁵, A. Nikiforov¹⁶, V. Nikolaenko^{130,aa}, I. Nikolic-Audit⁸⁰, K. Nikolopoulos¹⁸, J.K. Nilsen¹¹⁹, P. Nilsson²⁵, Y. Ninomiya¹⁵⁵, A. Nisati^{132a}, R. Nisius¹⁰¹, T. Nobe¹⁵⁷, M. Nomachi¹¹⁸, I. Nomidis²⁹, T. Nooney⁷⁶, S. Norberg¹¹³, M. Nordberg³⁰, O. Novgorodova⁴⁴, S. Nowak¹⁰¹, M. Nozaki⁶⁶, L. Nozka¹¹⁵, K. Ntekas¹⁰, G. Nunes Hanninger⁸⁸, T. Nunnemann¹⁰⁰, E. Nurse⁷⁸, F. Nuti⁸⁸, B.J. O'Brien⁴⁶, F. O'grady⁷, D.C. O'Neil¹⁴², V. O'Shea⁵³, F.G. Oakham^{29,d}, H. Oberlack¹⁰¹, T. Obermann²¹, J. Ocariz⁸⁰, A. Ochi⁶⁷, I. Ochoa⁷⁸, J.P. Ochoa-Ricoux^{32a}, S. Oda⁷⁰, S. Odaka⁶⁶, H. Ogren⁶¹, A. Oh⁸⁴, S.H. Oh⁴⁵, C.C. Ohm¹⁵, H. Ohman¹⁶⁶, H. Oide³⁰, W. Okamura¹¹⁸, H. Okawa¹⁶⁰, Y. Okumura³¹, T. Okuyama¹⁵⁵, A. Olariu^{26a}, S.A. Olivares Pino⁴⁶, D. Oliveira Damazio²⁵, E. Oliver Garcia¹⁶⁷, A. Olszewski³⁹, J. Olszowska³⁹, A. Onofre^{126a,126e}, P.U.E. Onyisi^{31,q}, C.J. Oram^{159a}, M.J. Oreglia³¹, Y. Oren¹⁵³, D. Orestano^{134a,134b}, N. Orlando¹⁵⁴, C. Oropeza Barrera⁵³, R.S. Orr¹⁵⁸, B. Osculati^{50a,50b}, R. Ospanov⁸⁴, G. Otero y Garzon²⁷, H. Otono⁷⁰, M. Ouchrif^{135d}, E.A. Ouellette¹⁶⁹, F. Ould-Saada¹¹⁹, A. Ouraou¹³⁶, K.P. Oussoren¹⁰⁷, Q. Ouyang^{33a}, A. Ovcharova¹⁵, M. Owen⁵³, R.E. Owen¹⁸, V.E. Ozcan^{19a}, N. Ozturk⁸, K. Pachal¹⁴², A. Pacheco Pages¹², C. Padilla Aranda¹², M. Pagáčová⁴⁸, S. Pagan Griso¹⁵, E. Paganis¹³⁹, C. Pahl¹⁰¹, F. Paige²⁵, P. Pais⁸⁶, K. Pajchel¹¹⁹, G. Palacino^{159b}, S. Palestini³⁰, M. Palka^{38b}, D. Pallin³⁴, A. Palma^{126a,126b}, Y.B. Pan¹⁷³, E. Panagiotopoulou¹⁰, C.E. Pandini⁸⁰, J.G. Panduro Vazquez⁷⁷, P. Pani^{146a,146b}, S. Panitkin²⁵, D. Pantea^{26a}, L. Paolozzi⁴⁹, Th.D. Papadopoulou¹⁰, K. Papageorgiou¹⁵⁴, A. Paramonov⁶, D. Paredes Hernandez¹⁵⁴, M.A. Parker²⁸, K.A. Parker¹³⁹, F. Parodi^{50a,50b}, J.A. Parsons³⁵, U. Parzefall⁴⁸, E. Pasqualucci^{132a}, S. Passaggio^{50a}, F. Pastore^{134a,134b,*}, Fr. Pastore⁷⁷, G. Pásztor²⁹, S. Pataraja¹⁷⁵, N.D. Patel¹⁵⁰, J.R. Pater⁸⁴, T. Pauly³⁰, J. Pearce¹⁶⁹, B. Pearson¹¹³, L.E. Pedersen³⁶, M. Pedersen¹¹⁹, S. Pedraza Lopez¹⁶⁷, R. Pedro^{126a,126b}, S.V. Peleganchuk¹⁰⁹, D. Pelikan¹⁶⁶, H. Peng^{33b}, B. Penning³¹, J. Penwell⁶¹, D.V. Perepelitsa²⁵, E. Perez Codina^{159a}, M.T. Pérez García-Estañ¹⁶⁷, L. Perini^{91a,91b}, H. Pernegger³⁰, S. Perrella^{104a,104b}, R. Peschke⁴², V.D. Peshekhonov⁶⁵, K. Peters³⁰, R.F.Y. Peters⁸⁴, B.A. Petersen³⁰, T.C. Petersen³⁶, E. Petit⁴², A. Petridis^{146a,146b}, C. Petridou¹⁵⁴, E. Petrolo^{132a}, F. Petrucci^{134a,134b}, N.E. Pettersson¹⁵⁷, R. Pezoa^{32b}, P.W. Phillips¹³¹, G. Piacquadio¹⁴³, E. Pianori¹⁷⁰, A. Picazio⁴⁹, E. Piccaro⁷⁶, M. Piccinini^{20a,20b}, M.A. Pickering¹²⁰, R. Piegaia²⁷, D.T. Pignotti¹¹¹, J.E. Pilcher³¹, A.D. Pilkington⁸⁴, J. Pina^{126a,126b,126d}, M. Pinamonti^{164a,164c,ac}, J.L. Pinfold³, A. Pingel³⁶, B. Pinto^{126a}, S. Pires⁸⁰, M. Pitt¹⁷², C. Pizio^{91a,91b}, L. Plazak^{144a}, M.-A. Pleier²⁵, V. Pleskot¹²⁹, E. Plotnikova⁶⁵, P. Plucinski^{146a,146b}, D. Pluth⁶⁴, R. Poettgen⁸³, L. Poggioli¹¹⁷, D. Pohl²¹, G. Polesello^{121a}, A. Policicchio^{37a,37b}, R. Polifka¹⁵⁸, A. Polini^{20a}, C.S. Pollard⁵³, V. Polychronakos²⁵, K. Pommès³⁰, L. Pontecorvo^{132a}, B.G. Pope⁹⁰, G.A. Popeneciu^{26b}, D.S. Popovic¹³, A. Poppleton³⁰, S. Pospisil¹²⁸, K. Potamianos¹⁵, I.N. Potrap⁶⁵, C.J. Potter¹⁴⁹, C.T. Potter¹¹⁶, G. Poulard³⁰, J. Poveda³⁰, V. Pozdnyakov⁶⁵, P. Pralavorio⁸⁵, A. Pranko¹⁵, S. Prasad³⁰, S. Prell⁶⁴, D. Price⁸⁴, L.E. Price⁶, M. Primavera^{73a}, S. Prince⁸⁷, M. Proissl⁴⁶, K. Prokofiev^{60c}, F. Prokoshin^{32b}, E. Protopapadaki¹³⁶, S. Protopopescu²⁵, J. Proudfoot⁶, M. Przybycien^{38a}, E. Ptacek¹¹⁶, D. Puddu^{134a,134b}, E. Pueschel⁸⁶, D. Poldon¹⁴⁸, M. Purohit^{25,ad}, P. Puzo¹¹⁷, J. Qian⁸⁹, G. Qin⁵³, Y. Qin⁸⁴, A. Quadt⁵⁴, D.R. Quarrie¹⁵, W.B. Quayle^{164a,164b}, M. Queitsch-Maitland⁸⁴, D. Quilty⁵³, S. Raddum¹¹⁹, V. Radeka²⁵, V. Radescu⁴², S.K. Radhakrishnan¹⁴⁸, P. Radloff¹¹⁶, P. Rados⁸⁸, F. Ragusa^{91a,91b}, G. Rahal¹⁷⁸, S. Rajagopalan²⁵, M. Rammensee³⁰, C. Rangel-Smith¹⁶⁶, F. Rauscher¹⁰⁰, S. Rave⁸³, T. Ravenscroft⁵³, M. Raymond³⁰, A.L. Read¹¹⁹, N.P. Readioff⁷⁴, D.M. Rebuffi^{121a,121b}, A. Redelbach¹⁷⁴, G. Redlinger²⁵, R. Reece¹³⁷, K. Reeves⁴¹, L. Rehnisch¹⁶, H. Reisin²⁷, M. Relich¹⁶³, C. Rembser³⁰, H. Ren^{33a}, A. Renaud¹¹⁷, M. Rescigno^{132a},

S. Resconi^{91a}, O.L. Rezanova^{109,c}, P. Reznicek¹²⁹, R. Rezvani⁹⁵, R. Richter¹⁰¹, S. Richter⁷⁸,
 E. Richter-Was^{38b}, O. Ricken²¹, M. Ridel⁸⁰, P. Rieck¹⁶, C.J. Riegel¹⁷⁵, J. Rieger⁵⁴, M. Rijssenbeek¹⁴⁸,
 A. Rimoldi^{121a,121b}, L. Rinaldi^{20a}, B. Ristic⁴⁹, E. Ritsch⁶², I. Riu¹², F. Rizatdinova¹¹⁴, E. Rizvi⁷⁶,
 S.H. Robertson^{87,k}, A. Robichaud-Veronneau⁸⁷, D. Robinson²⁸, J.E.M. Robinson⁸⁴, A. Robson⁵³,
 C. Roda^{124a,124b}, S. Roe³⁰, O. Røhne¹¹⁹, S. Rolli¹⁶¹, A. Romaniouk⁹⁸, M. Romano^{20a,20b},
 S.M. Romano Saez³⁴, E. Romero Adam¹⁶⁷, N. Rompotis¹³⁸, M. Ronzani⁴⁸, L. Roos⁸⁰, E. Ros¹⁶⁷,
 S. Rosati^{132a}, K. Rosbach⁴⁸, P. Rose¹³⁷, P.L. Rosendahl¹⁴, O. Rosenthal¹⁴¹, V. Rossetti^{146a,146b},
 E. Rossi^{104a,104b}, L.P. Rossi^{50a}, R. Rosten¹³⁸, M. Rotaru^{26a}, I. Roth¹⁷², J. Rothberg¹³⁸, D. Rousseau¹¹⁷,
 C.R. Royon¹³⁶, A. Rozanov⁸⁵, Y. Rozen¹⁵², X. Ruan^{145c}, F. Rubbo¹⁴³, I. Rubinskiy⁴², V.I. Rud⁹⁹,
 C. Rudolph⁴⁴, M.S. Rudolph¹⁵⁸, F. Rühr⁴⁸, A. Ruiz-Martinez³⁰, Z. Rurikova⁴⁸, N.A. Rusakovich⁶⁵,
 A. Ruschke¹⁰⁰, H.L. Russell¹³⁸, J.P. Rutherford⁷, N. Ruthmann⁴⁸, Y.F. Ryabov¹²³, M. Rybar¹²⁹,
 G. Rybkin¹¹⁷, N.C. Ryder¹²⁰, A.F. Saavedra¹⁵⁰, G. Sabato¹⁰⁷, S. Sacerdoti²⁷, A. Saddique³,
 H.F.W. Sadrozinski¹³⁷, R. Sadykov⁶⁵, F. Safai Tehrani^{132a}, M. Saimpert¹³⁶, H. Sakamoto¹⁵⁵,
 Y. Sakurai¹⁷¹, G. Salamanna^{134a,134b}, A. Salamon^{133a}, M. Saleem¹¹³, D. Salek¹⁰⁷,
 P.H. Sales De Bruin¹³⁸, D. Salihagic¹⁰¹, A. Salnikov¹⁴³, J. Salt¹⁶⁷, D. Salvatore^{37a,37b}, F. Salvatore¹⁴⁹,
 A. Salvucci¹⁰⁶, A. Salzburger³⁰, D. Sampsonidis¹⁵⁴, A. Sanchez^{104a,104b}, J. Sánchez¹⁶⁷,
 V. Sanchez Martinez¹⁶⁷, H. Sandaker¹⁴, R.L. Sandbach⁷⁶, H.G. Sander⁸³, M.P. Sanders¹⁰⁰,
 M. Sandhoff¹⁷⁵, C. Sandoval¹⁶², R. Sandstroem¹⁰¹, D.P.C. Sankey¹³¹, M. Sannino^{50a,50b}, A. Sansoni⁴⁷,
 C. Santoni³⁴, R. Santonico^{133a,133b}, H. Santos^{126a}, I. Santoyo Castillo¹⁴⁹, K. Sapp¹²⁵, A. Saponov⁶⁵,
 J.G. Saraiva^{126a,126d}, B. Sarrazin²¹, O. Sasaki⁶⁶, Y. Sasaki¹⁵⁵, K. Sato¹⁶⁰, G. Sauvage^{5,*}, E. Sauvan⁵,
 G. Savage⁷⁷, P. Savard^{158,d}, C. Sawyer¹²⁰, L. Sawyer^{79,n}, J. Saxon³¹, C. Sbarra^{20a}, A. Sbrizzi^{20a,20b},
 T. Scanlon⁷⁸, D.A. Scannicchio¹⁶³, M. Scarcella¹⁵⁰, V. Scarfone^{37a,37b}, J. Schaarschmidt¹⁷²,
 P. Schacht¹⁰¹, D. Schaefer³⁰, R. Schaefer⁴², J. Schaeffer⁸³, S. Schaepe²¹, S. Schaezel^{58b}, U. Schäfer⁸³,
 A.C. Schaffer¹¹⁷, D. Schaile¹⁰⁰, R.D. Schamberger¹⁴⁸, V. Scharf^{58a}, V.A. Schegelsky¹²³, D. Scheirich¹²⁹,
 M. Schernau¹⁶³, C. Schiavi^{50a,50b}, C. Schillo⁴⁸, M. Schioppa^{37a,37b}, S. Schlenker³⁰, E. Schmidt⁴⁸,
 K. Schmieden³⁰, C. Schmitt⁸³, S. Schmitt^{58b}, S. Schmitt⁴², B. Schneider^{159a}, Y.J. Schnellbach⁷⁴,
 U. Schnoor⁴⁴, L. Schoeffel¹³⁶, A. Schoening^{58b}, B.D. Schoenrock⁹⁰, E. Schopf²¹,
 A.L.S. Schorlemmer⁵⁴, M. Schott⁸³, D. Schouten^{159a}, J. Schovancova⁸, S. Schramm¹⁵⁸, M. Schreyer¹⁷⁴,
 C. Schroeder⁸³, N. Schuh⁸³, M.J. Schultens²¹, H.-C. Schultz-Coulon^{58a}, H. Schulz¹⁶, M. Schumacher⁴⁸,
 B.A. Schumm¹³⁷, Ph. Schune¹³⁶, C. Schwanenberger⁸⁴, A. Schwartzman¹⁴³, T.A. Schwarz⁸⁹,
 Ph. Schwegler¹⁰¹, Ph. Schwemling¹³⁶, R. Schwiendhorst⁹⁰, J. Schwindling¹³⁶, T. Schwindt²¹,
 M. Schwoerer⁵, F.G. Sciacca¹⁷, E. Scifo¹¹⁷, G. Sciolla²³, F. Scuri^{124a,124b}, F. Scutti²¹, J. Searcy⁸⁹,
 G. Sedov⁴², E. Sedykh¹²³, P. Seema²¹, S.C. Seidel¹⁰⁵, A. Seiden¹³⁷, F. Seifert¹²⁸, J.M. Seixas^{24a},
 G. Sekhniaidze^{104a}, K. Sekhon⁸⁹, S.J. Sekula⁴⁰, K.E. Selbach⁴⁶, D.M. Seliverstov^{123,*},
 N. Semprini-Cesari^{20a,20b}, C. Serfon³⁰, L. Serin¹¹⁷, L. Serkin^{164a,164b}, T. Serre⁸⁵, M. Sessa^{134a,134b},
 R. Seuster^{159a}, H. Severini¹¹³, T. Sfiligoi⁷⁵, F. Sforza¹⁰¹, A. Sfyrla³⁰, E. Shabalina⁵⁴, M. Shamim¹¹⁶,
 L.Y. Shan^{33a}, R. Shang¹⁶⁵, J.T. Shank²², M. Shapiro¹⁵, P.B. Shatalov⁹⁷, K. Shaw^{164a,164b}, S.M. Shaw⁸⁴,
 A. Shcherbakova^{146a,146b}, C.Y. Shehu¹⁴⁹, P. Sherwood⁷⁸, L. Shi^{151,ae}, S. Shimizu⁶⁷, C.O. Shimmin¹⁶³,
 M. Shimojima¹⁰², M. Shiyakova⁶⁵, A. Shmeleva⁹⁶, D. Shoaleh Saadi⁹⁵, M.J. Shochet³¹, S. Shojai^{91a,91b},
 S. Shrestha¹¹¹, E. Shulga⁹⁸, M.A. Shupe⁷, S. Shushkevich⁴², P. Sicho¹²⁷, O. Sidiropoulou¹⁷⁴,
 D. Sidorov¹¹⁴, A. Sidoti^{20a,20b}, F. Siegert⁴⁴, Dj. Sijacki¹³, J. Silva^{126a,126d}, Y. Silver¹⁵³,
 S.B. Silverstein^{146a}, V. Simak¹²⁸, O. Simard⁵, Lj. Simic¹³, S. Simion¹¹⁷, E. Simioni⁸³, B. Simmons⁷⁸,
 D. Simon³⁴, R. Simoniello^{91a,91b}, P. Sinervo¹⁵⁸, N.B. Sinev¹¹⁶, G. Siragusa¹⁷⁴, A.N. Sisakyan^{65,*},
 S.Yu. Sivoklov⁹⁹, J. Sjölin^{146a,146b}, T.B. Sjursen¹⁴, M.B. Skinner⁷², H.P. Skottowe⁵⁷, P. Skubic¹¹³,
 M. Slater¹⁸, T. Slavicek¹²⁸, M. Slawinska¹⁰⁷, K. Sliwa¹⁶¹, V. Smakhtin¹⁷², B.H. Smart⁴⁶, L. Smestad¹⁴,
 S.Yu. Smirnov⁹⁸, Y. Smirnov⁹⁸, L.N. Smirnova^{99,af}, O. Smirnova⁸¹, M.N.K. Smith³⁵, R.W. Smith³⁵,
 M. Smizanska⁷², K. Smolek¹²⁸, A.A. Snesev⁹⁶, G. Snidero⁷⁶, S. Snyder²⁵, R. Sobie^{169,k}, F. Socher⁴⁴,

A. Soffer¹⁵³, D.A. Soh^{151,ae}, C.A. Solans³⁰, M. Solar¹²⁸, J. Solc¹²⁸, E.Yu. Soldatov⁹⁸, U. Soldevila¹⁶⁷,
 A.A. Solodkov¹³⁰, A. Soloshenko⁶⁵, O.V. Solovyanov¹³⁰, V. Solovyev¹²³, P. Sommer⁴⁸, H.Y. Song^{33b},
 N. Soni¹, A. Sood¹⁵, A. Sopczak¹²⁸, B. Sopko¹²⁸, V. Sopko¹²⁸, V. Sorin¹², D. Sosa^{58b}, M. Sosebee⁸,
 C.L. Sotiropoulou^{124a,124b}, R. Soualah^{164a,164c}, P. Soueid⁹⁵, A.M. Soukharev^{109,c}, D. South⁴²,
 B.C. Sowden⁷⁷, S. Spagnolo^{73a,73b}, M. Spalla^{124a,124b}, F. Spanò⁷⁷, W.R. Spearman⁵⁷, F. Spettel¹⁰¹,
 R. Spighi^{20a}, G. Spigo³⁰, L.A. Spiller⁸⁸, M. Spousta¹²⁹, T. Spreitzer¹⁵⁸, R.D. St. Denis^{53,*}, S. Staerz⁴⁴,
 J. Stahlman¹²², R. Stamen^{58a}, S. Stamm¹⁶, E. Stanecka³⁹, C. Stanescu^{134a}, M. Stanescu-Bellu⁴²,
 M.M. Stanitzki⁴², S. Stapnes¹¹⁹, E.A. Starchenko¹³⁰, J. Stark⁵⁵, P. Staroba¹²⁷, P. Starovoitov⁴²,
 R. Staszewski³⁹, P. Stavina^{144a,*}, P. Steinberg²⁵, B. Stelzer¹⁴², H.J. Stelzer³⁰, O. Stelzer-Chilton^{159a},
 H. Stenzel⁵², S. Stern¹⁰¹, G.A. Stewart⁵³, J.A. Stillings²¹, M.C. Stockton⁸⁷, M. Stoebe⁸⁷, G. Stoicea^{26a},
 P. Stolte⁵⁴, S. Stonjek¹⁰¹, A.R. Stradling⁸, A. Straessner⁴⁴, M.E. Stramaglia¹⁷, J. Strandberg¹⁴⁷,
 S. Strandberg^{146a,146b}, A. Strandlie¹¹⁹, E. Strauss¹⁴³, M. Strauss¹¹³, P. Strizenec^{144b}, R. Ströhmer¹⁷⁴,
 D.M. Strom¹¹⁶, R. Stroynowski⁴⁰, A. Strubig¹⁰⁶, S.A. Stucci¹⁷, B. Stugu¹⁴, N.A. Styles⁴², D. Su¹⁴³,
 J. Su¹²⁵, R. Subramaniam⁷⁹, A. Succurro¹², Y. Sugaya¹¹⁸, C. Suhr¹⁰⁸, M. Suk¹²⁸, V.V. Sulin⁹⁶,
 S. Sultansoy^{4d}, T. Sumida⁶⁸, S. Sun⁵⁷, X. Sun^{33a}, J.E. Sundermann⁴⁸, K. Suruliz¹⁴⁹, G. Susinno^{37a,37b},
 M.R. Sutton¹⁴⁹, S. Suzuki⁶⁶, Y. Suzuki⁶⁶, M. Svatos¹²⁷, S. Swedish¹⁶⁸, M. Swiatlowski¹⁴³, I. Sykora^{144a},
 T. Sykora¹²⁹, D. Ta⁹⁰, C. Taccini^{134a,134b}, K. Tackmann⁴², J. Taenzer¹⁵⁸, A. Taffard¹⁶³, R. Tafirout^{159a},
 N. Taiblum¹⁵³, H. Takai²⁵, R. Takashima⁶⁹, H. Takeda⁶⁷, T. Takeshita¹⁴⁰, Y. Takubo⁶⁶, M. Talby⁸⁵,
 A.A. Talyshev^{109,c}, J.Y.C. Tam¹⁷⁴, K.G. Tan⁸⁸, J. Tanaka¹⁵⁵, R. Tanaka¹¹⁷, S. Tanaka⁶⁶,
 B.B. Tannenwald¹¹¹, N. Tannoury²¹, S. Tapprogge⁸³, S. Tarem¹⁵², F. Tarrade²⁹, G.F. Tartarelli^{91a},
 P. Tas¹²⁹, M. Tasevsky¹²⁷, T. Tashiro⁶⁸, E. Tassi^{37a,37b}, A. Tavares Delgado^{126a,126b}, Y. Tayalati^{135d},
 F.E. Taylor⁹⁴, G.N. Taylor⁸⁸, W. Taylor^{159b}, F.A. Teischinger³⁰, M. Teixeira Dias Castanheira⁷⁶,
 P. Teixeira-Dias⁷⁷, K.K. Temming⁴⁸, H. Ten Kate³⁰, P.K. Teng¹⁵¹, J.J. Teoh¹¹⁸, F. Tepel¹⁷⁵, S. Terada⁶⁶,
 K. Terashi¹⁵⁵, J. Terron⁸², S. Terzo¹⁰¹, M. Testa⁴⁷, R.J. Teuscher^{158,k}, J. Therhaag²¹,
 T. Thevenaux-Pelzer³⁴, J.P. Thomas¹⁸, J. Thomas-Wilsker⁷⁷, E.N. Thompson³⁵, P.D. Thompson¹⁸,
 R.J. Thompson⁸⁴, A.S. Thompson⁵³, L.A. Thomsen³⁶, E. Thomson¹²², M. Thomson²⁸, R.P. Thun^{89,*},
 M.J. Tibbetts¹⁵, R.E. Ticse Torres⁸⁵, V.O. Tikhomirov^{96,ag}, Yu.A. Tikhonov^{109,c}, S. Timoshenko⁹⁸,
 E. Tiouchichine⁸⁵, P. Tipton¹⁷⁶, S. Tisserant⁸⁵, T. Todorov^{5,*}, S. Todorova-Nova¹²⁹, J. Tojo⁷⁰,
 S. Tokár^{144a}, K. Tokushuku⁶⁶, K. Tollefson⁹⁰, E. Tolley⁵⁷, L. Tomlinson⁸⁴, M. Tomoto¹⁰³,
 L. Tompkins^{143,ah}, K. Toms¹⁰⁵, E. Torrence¹¹⁶, H. Torres¹⁴², E. Torró Pastor¹⁶⁷, J. Toth^{85,ai},
 F. Touchard⁸⁵, D.R. Tovey¹³⁹, T. Trefzger¹⁷⁴, L. Tremblet³⁰, A. Tricoli³⁰, I.M. Trigger^{159a},
 S. Trincaz-Duvoid⁸⁰, M.F. Tripiana¹², W. Trischuk¹⁵⁸, B. Trocme⁵⁵, C. Troncon^{91a},
 M. Trottier-McDonald¹⁵, M. Trovatelli^{134a,134b}, P. True⁹⁰, L. Truong^{164a,164c}, M. Trzebinski³⁹,
 A. Trzupek³⁹, C. Tsarouchas³⁰, J.C.-L. Tseng¹²⁰, P.V. Tsiarehka⁹², D. Tsionou¹⁵⁴, G. Tsipolitis¹⁰,
 N. Tsirintanis⁹, S. Tsiskaridze¹², V. Tsiskaridze⁴⁸, E.G. Tskhadadze^{51a}, I.I. Tsukerman⁹⁷, V. Tsulaia¹⁵,
 S. Tsuno⁶⁶, D. Tsybychev¹⁴⁸, A. Tudorache^{26a}, V. Tudorache^{26a}, A.N. Tuna¹²², S.A. Tuppiti^{20a,20b},
 S. Turchikhin^{99,af}, D. Turecek¹²⁸, R. Turra^{91a,91b}, A.J. Turvey⁴⁰, P.M. Tuts³⁵, A. Tykhonov⁴⁹,
 M. Tylmad^{146a,146b}, M. Tyndel¹³¹, I. Ueda¹⁵⁵, R. Ueno²⁹, M. Ughetto^{146a,146b}, M. Uglan¹⁴,
 M. Uhlenbrock²¹, F. Ukegawa¹⁶⁰, G. Unal³⁰, A. Undrus²⁵, G. Unel¹⁶³, F.C. Ungaro⁴⁸, Y. Unno⁶⁶,
 C. Unverdorben¹⁰⁰, J. Urban^{144b}, P. Urquijo⁸⁸, P. Urrejola⁸³, G. Usai⁸, A. Usanova⁶², L. Vacavant⁸⁵,
 V. Vacek¹²⁸, B. Vachon⁸⁷, C. Valderanis⁸³, N. Valencic¹⁰⁷, S. Valentinetti^{20a,20b}, A. Valero¹⁶⁷,
 L. Valery¹², S. Valkar¹²⁹, E. Valladolid Gallego¹⁶⁷, S. Vallecorsa⁴⁹, J.A. Valls Ferrer¹⁶⁷,
 W. Van Den Wollenberg¹⁰⁷, P.C. Van Der Deijl¹⁰⁷, R. van der Geer¹⁰⁷, H. van der Graaf¹⁰⁷,
 R. Van Der Leeuw¹⁰⁷, N. van Eldik¹⁵², P. van Gemmeren⁶, J. Van Nieuwkoop¹⁴², I. van Vulpen¹⁰⁷,
 M.C. van Woerden³⁰, M. Vanadia^{132a,132b}, W. Vandelli³⁰, R. Vanguri¹²², A. Vaniachine⁶, F. Vannucci⁸⁰,
 G. Vardanyan¹⁷⁷, R. Vari^{132a}, E.W. Varnes⁷, T. Varol⁴⁰, D. Varouchas⁸⁰, A. Vartapetian⁸, K.E. Varvell¹⁵⁰,
 F. Vazeille³⁴, T. Vazquez Schroeder⁸⁷, J. Veatch⁷, L.M. Veloce¹⁵⁸, F. Veloso^{126a,126c}, T. Velz²¹,

S. Veneziano^{132a}, A. Ventura^{73a,73b}, D. Ventura⁸⁶, M. Venturi¹⁶⁹, N. Venturi¹⁵⁸, A. Venturini²³, V. Vercesi^{121a}, M. Verducci^{132a,132b}, W. Verkerke¹⁰⁷, J.C. Vermeulen¹⁰⁷, A. Vest⁴⁴, M.C. Vetterli^{142,d}, O. Viazlo⁸¹, I. Vichou¹⁶⁵, T. Vickey¹³⁹, O.E. Vickey Boeriu¹³⁹, G.H.A. Viehhauser¹²⁰, S. Viel¹⁵, R. Vigne³⁰, M. Villa^{20a,20b}, M. Villaplana Perez^{91a,91b}, E. Vilucchi⁴⁷, M.G. Vincter²⁹, V.B. Vinogradov⁶⁵, I. Vivarelli¹⁴⁹, F. Vives Vaque³, S. Vlachos¹⁰, D. Vladioiu¹⁰⁰, M. Vlasak¹²⁸, M. Vogel^{32a}, P. Vokac¹²⁸, G. Volpi^{124a,124b}, M. Volpi⁸⁸, H. von der Schmitt¹⁰¹, H. von Radziewski⁴⁸, E. von Toerne²¹, V. Vorobel¹²⁹, K. Vorobev⁹⁸, M. Vos¹⁶⁷, R. Voss³⁰, J.H. Vossebeld⁷⁴, N. Vranjes¹³, M. Vranjes Milosavljevic¹³, V. Vrba¹²⁷, M. Vreeswijk¹⁰⁷, R. Vuillermet³⁰, I. Vukotic³¹, Z. Vykydal¹²⁸, P. Wagner²¹, W. Wagner¹⁷⁵, H. Wahlberg⁷¹, S. Wahrmund⁴⁴, J. Wakabayashi¹⁰³, J. Walder⁷², R. Walker¹⁰⁰, W. Walkowiak¹⁴¹, C. Wang^{33c}, F. Wang¹⁷³, H. Wang¹⁵, H. Wang⁴⁰, J. Wang⁴², J. Wang^{33a}, K. Wang⁸⁷, R. Wang⁶, S.M. Wang¹⁵¹, T. Wang²¹, X. Wang¹⁷⁶, C. Wanotayaroj¹¹⁶, A. Warburton⁸⁷, C.P. Ward²⁸, D.R. Wardrope⁷⁸, M. Warsinsky⁴⁸, A. Washbrook⁴⁶, C. Wasicki⁴², P.M. Watkins¹⁸, A.T. Watson¹⁸, I.J. Watson¹⁵⁰, M.F. Watson¹⁸, G. Watts¹³⁸, S. Watts⁸⁴, B.M. Waugh⁷⁸, S. Webb⁸⁴, M.S. Weber¹⁷, S.W. Weber¹⁷⁴, J.S. Webster³¹, A.R. Weidberg¹²⁰, B. Weinert⁶¹, J. Weingarten⁵⁴, C. Weiser⁴⁸, H. Weits¹⁰⁷, P.S. Wells³⁰, T. Wenaus²⁵, T. Wengler³⁰, S. Wenig³⁰, N. Vermes²¹, M. Werner⁴⁸, P. Werner³⁰, M. Wessels^{58a}, J. Wetter¹⁶¹, K. Whalen²⁹, A.M. Wharton⁷², A. White⁸, M.J. White¹, R. White^{32b}, S. White^{124a,124b}, D. Whiteson¹⁶³, F.J. Wickens¹³¹, W. Wiedenmann¹⁷³, M. Wielers¹³¹, P. Wienemann²¹, C. Wiglesworth³⁶, L.A.M. Wiik-Fuchs²¹, A. Wildauer¹⁰¹, H.G. Wilkens³⁰, H.H. Williams¹²², S. Williams¹⁰⁷, C. Willis⁹⁰, S. Willocq⁸⁶, A. Wilson⁸⁹, J.A. Wilson¹⁸, I. Wingerter-Seez⁵, F. Winklmeier¹¹⁶, B.T. Winter²¹, M. Wittgen¹⁴³, J. Wittkowski¹⁰⁰, S.J. Wollstadt⁸³, M.W. Wolter³⁹, H. Wolters^{126a,126c}, B.K. Wosiek³⁹, J. Wotschack³⁰, M.J. Woudstra⁸⁴, K.W. Wozniak³⁹, M. Wu⁵⁵, M. Wu³¹, S.L. Wu¹⁷³, X. Wu⁴⁹, Y. Wu⁸⁹, T.R. Wyatt⁸⁴, B.M. Wynne⁴⁶, S. Xella³⁶, D. Xu^{33a}, L. Xu^{33b,aj}, B. Yabsley¹⁵⁰, S. Yacoob^{145b,ak}, R. Yakabe⁶⁷, M. Yamada⁶⁶, Y. Yamaguchi¹¹⁸, A. Yamamoto⁶⁶, S. Yamamoto¹⁵⁵, T. Yamanaka¹⁵⁵, K. Yamauchi¹⁰³, Y. Yamazaki⁶⁷, Z. Yan²², H. Yang^{33e}, H. Yang¹⁷³, Y. Yang¹⁵¹, L. Yao^{33a}, W-M. Yao¹⁵, Y. Yasu⁶⁶, E. Yatsenko⁵, K.H. Yau Wong²¹, J. Ye⁴⁰, S. Ye²⁵, I. Yeletsikh⁶⁵, A.L. Yen⁵⁷, E. Yildirim⁴², K. Yorita¹⁷¹, R. Yoshida⁶, K. Yoshihara¹²², C. Young¹⁴³, C.J.S. Young³⁰, S. Youssef²², D.R. Yu¹⁵, J. Yu⁸, J.M. Yu⁸⁹, J. Yu¹¹⁴, L. Yuan⁶⁷, A. Yurkewicz¹⁰⁸, I. Yusuff^{28,al}, B. Zabinski³⁹, R. Zaidan⁶³, A.M. Zaitsev^{130,aa}, J. Zalieckas¹⁴, A. Zaman¹⁴⁸, S. Zambito⁵⁷, L. Zanello^{132a,132b}, D. Zanzi⁸⁸, C. Zeitnitz¹⁷⁵, M. Zeman¹²⁸, A. Zemla^{38a}, K. Zengel²³, O. Zenin¹³⁰, T. Ženiš^{144a}, D. Zerwas¹¹⁷, D. Zhang⁸⁹, F. Zhang¹⁷³, J. Zhang⁶, L. Zhang⁴⁸, R. Zhang^{33b}, X. Zhang^{33d}, Z. Zhang¹¹⁷, X. Zhao⁴⁰, Y. Zhao^{33d,117}, Z. Zhao^{33b}, A. Zhemchugov⁶⁵, J. Zhong¹²⁰, B. Zhou⁸⁹, C. Zhou⁴⁵, L. Zhou³⁵, L. Zhou⁴⁰, N. Zhou¹⁶³, C.G. Zhu^{33d}, H. Zhu^{33a}, J. Zhu⁸⁹, Y. Zhu^{33b}, X. Zhuang^{33a}, K. Zhukov⁹⁶, A. Zibell¹⁷⁴, D. Ziemska⁶¹, N.I. Zimine⁶⁵, C. Zimmermann⁸³, S. Zimmermann⁴⁸, Z. Zinonos⁵⁴, M. Zinser⁸³, M. Ziolkowski¹⁴¹, L. Živković¹³, G. Zobernig¹⁷³, A. Zoccoli^{20a,20b}, M. zur Nedden¹⁶, G. Zurzolo^{104a,104b}, L. Zwalinski³⁰.

¹ Department of Physics, University of Adelaide, Adelaide, Australia

² Physics Department, SUNY Albany, Albany NY, United States of America

³ Department of Physics, University of Alberta, Edmonton AB, Canada

⁴ (a) Department of Physics, Ankara University, Ankara; (c) Istanbul Aydin University, Istanbul; (d)

Division of Physics, TOBB University of Economics and Technology, Ankara, Turkey

⁵ LAPP, CNRS/IN2P3 and Université Savoie Mont Blanc, Annecy-le-Vieux, France

⁶ High Energy Physics Division, Argonne National Laboratory, Argonne IL, United States of America

⁷ Department of Physics, University of Arizona, Tucson AZ, United States of America

⁸ Department of Physics, The University of Texas at Arlington, Arlington TX, United States of America

⁹ Physics Department, University of Athens, Athens, Greece

¹⁰ Physics Department, National Technical University of Athens, Zografou, Greece

- ¹¹ Institute of Physics, Azerbaijan Academy of Sciences, Baku, Azerbaijan
- ¹² Institut de Física d'Altes Energies and Departament de Física de la Universitat Autònoma de Barcelona, Barcelona, Spain
- ¹³ Institute of Physics, University of Belgrade, Belgrade, Serbia
- ¹⁴ Department for Physics and Technology, University of Bergen, Bergen, Norway
- ¹⁵ Physics Division, Lawrence Berkeley National Laboratory and University of California, Berkeley CA, United States of America
- ¹⁶ Department of Physics, Humboldt University, Berlin, Germany
- ¹⁷ Albert Einstein Center for Fundamental Physics and Laboratory for High Energy Physics, University of Bern, Bern, Switzerland
- ¹⁸ School of Physics and Astronomy, University of Birmingham, Birmingham, United Kingdom
- ¹⁹ ^(a) Department of Physics, Bogazici University, Istanbul; ^(b) Department of Physics, Dogus University, Istanbul; ^(c) Department of Physics Engineering, Gaziantep University, Gaziantep, Turkey
- ²⁰ ^(a) INFN Sezione di Bologna; ^(b) Dipartimento di Fisica e Astronomia, Università di Bologna, Bologna, Italy
- ²¹ Physikalisches Institut, University of Bonn, Bonn, Germany
- ²² Department of Physics, Boston University, Boston MA, United States of America
- ²³ Department of Physics, Brandeis University, Waltham MA, United States of America
- ²⁴ ^(a) Universidade Federal do Rio De Janeiro COPPE/EE/IF, Rio de Janeiro; ^(b) Electrical Circuits Department, Federal University of Juiz de Fora (UFJF), Juiz de Fora; ^(c) Federal University of Sao Joao del Rei (UFSJ), Sao Joao del Rei; ^(d) Instituto de Fisica, Universidade de Sao Paulo, Sao Paulo, Brazil
- ²⁵ Physics Department, Brookhaven National Laboratory, Upton NY, United States of America
- ²⁶ ^(a) National Institute of Physics and Nuclear Engineering, Bucharest; ^(b) National Institute for Research and Development of Isotopic and Molecular Technologies, Physics Department, Cluj Napoca; ^(c) University Politehnica Bucharest, Bucharest; ^(d) West University in Timisoara, Timisoara, Romania
- ²⁷ Departamento de Física, Universidad de Buenos Aires, Buenos Aires, Argentina
- ²⁸ Cavendish Laboratory, University of Cambridge, Cambridge, United Kingdom
- ²⁹ Department of Physics, Carleton University, Ottawa ON, Canada
- ³⁰ CERN, Geneva, Switzerland
- ³¹ Enrico Fermi Institute, University of Chicago, Chicago IL, United States of America
- ³² ^(a) Departamento de Física, Pontificia Universidad Católica de Chile, Santiago; ^(b) Departamento de Física, Universidad Técnica Federico Santa María, Valparaíso, Chile
- ³³ ^(a) Institute of High Energy Physics, Chinese Academy of Sciences, Beijing; ^(b) Department of Modern Physics, University of Science and Technology of China, Anhui; ^(c) Department of Physics, Nanjing University, Jiangsu; ^(d) School of Physics, Shandong University, Shandong; ^(e) Department of Physics and Astronomy, Shanghai Key Laboratory for Particle Physics and Cosmology, Shanghai Jiao Tong University, Shanghai; ^(f) Physics Department, Tsinghua University, Beijing 100084, China
- ³⁴ Laboratoire de Physique Corpusculaire, Clermont Université and Université Blaise Pascal and CNRS/IN2P3, Clermont-Ferrand, France
- ³⁵ Nevis Laboratory, Columbia University, Irvington NY, United States of America
- ³⁶ Niels Bohr Institute, University of Copenhagen, Kobenhavn, Denmark
- ³⁷ ^(a) INFN Gruppo Collegato di Cosenza, Laboratori Nazionali di Frascati; ^(b) Dipartimento di Fisica, Università della Calabria, Rende, Italy
- ³⁸ ^(a) AGH University of Science and Technology, Faculty of Physics and Applied Computer Science, Krakow; ^(b) Marian Smoluchowski Institute of Physics, Jagiellonian University, Krakow, Poland
- ³⁹ Institute of Nuclear Physics Polish Academy of Sciences, Krakow, Poland
- ⁴⁰ Physics Department, Southern Methodist University, Dallas TX, United States of America

- 41 Physics Department, University of Texas at Dallas, Richardson TX, United States of America
- 42 DESY, Hamburg and Zeuthen, Germany
- 43 Institut für Experimentelle Physik IV, Technische Universität Dortmund, Dortmund, Germany
- 44 Institut für Kern- und Teilchenphysik, Technische Universität Dresden, Dresden, Germany
- 45 Department of Physics, Duke University, Durham NC, United States of America
- 46 SUPA - School of Physics and Astronomy, University of Edinburgh, Edinburgh, United Kingdom
- 47 INFN Laboratori Nazionali di Frascati, Frascati, Italy
- 48 Fakultät für Mathematik und Physik, Albert-Ludwigs-Universität, Freiburg, Germany
- 49 Section de Physique, Université de Genève, Geneva, Switzerland
- 50 ^(a) INFN Sezione di Genova; ^(b) Dipartimento di Fisica, Università di Genova, Genova, Italy
- 51 ^(a) E. Andronikashvili Institute of Physics, Iv. Javakhishvili Tbilisi State University, Tbilisi; ^(b) High Energy Physics Institute, Tbilisi State University, Tbilisi, Georgia
- 52 II Physikalisches Institut, Justus-Liebig-Universität Giessen, Giessen, Germany
- 53 SUPA - School of Physics and Astronomy, University of Glasgow, Glasgow, United Kingdom
- 54 II Physikalisches Institut, Georg-August-Universität, Göttingen, Germany
- 55 Laboratoire de Physique Subatomique et de Cosmologie, Université Grenoble-Alpes, CNRS/IN2P3, Grenoble, France
- 56 Department of Physics, Hampton University, Hampton VA, United States of America
- 57 Laboratory for Particle Physics and Cosmology, Harvard University, Cambridge MA, United States of America
- 58 ^(a) Kirchhoff-Institut für Physik, Ruprecht-Karls-Universität Heidelberg, Heidelberg; ^(b) Physikalisches Institut, Ruprecht-Karls-Universität Heidelberg, Heidelberg; ^(c) ZITI Institut für technische Informatik, Ruprecht-Karls-Universität Heidelberg, Mannheim, Germany
- 59 Faculty of Applied Information Science, Hiroshima Institute of Technology, Hiroshima, Japan
- 60 ^(a) Department of Physics, The Chinese University of Hong Kong, Shatin, N.T., Hong Kong; ^(b) Department of Physics, The University of Hong Kong, Hong Kong; ^(c) Department of Physics, The Hong Kong University of Science and Technology, Clear Water Bay, Kowloon, Hong Kong, China
- 61 Department of Physics, Indiana University, Bloomington IN, United States of America
- 62 Institut für Astro- und Teilchenphysik, Leopold-Franzens-Universität, Innsbruck, Austria
- 63 University of Iowa, Iowa City IA, United States of America
- 64 Department of Physics and Astronomy, Iowa State University, Ames IA, United States of America
- 65 Joint Institute for Nuclear Research, JINR Dubna, Dubna, Russia
- 66 KEK, High Energy Accelerator Research Organization, Tsukuba, Japan
- 67 Graduate School of Science, Kobe University, Kobe, Japan
- 68 Faculty of Science, Kyoto University, Kyoto, Japan
- 69 Kyoto University of Education, Kyoto, Japan
- 70 Department of Physics, Kyushu University, Fukuoka, Japan
- 71 Instituto de Física La Plata, Universidad Nacional de La Plata and CONICET, La Plata, Argentina
- 72 Physics Department, Lancaster University, Lancaster, United Kingdom
- 73 ^(a) INFN Sezione di Lecce; ^(b) Dipartimento di Matematica e Fisica, Università del Salento, Lecce, Italy
- 74 Oliver Lodge Laboratory, University of Liverpool, Liverpool, United Kingdom
- 75 Department of Physics, Jožef Stefan Institute and University of Ljubljana, Ljubljana, Slovenia
- 76 School of Physics and Astronomy, Queen Mary University of London, London, United Kingdom
- 77 Department of Physics, Royal Holloway University of London, Surrey, United Kingdom
- 78 Department of Physics and Astronomy, University College London, London, United Kingdom
- 79 Louisiana Tech University, Ruston LA, United States of America

- ⁸⁰ Laboratoire de Physique Nucléaire et de Hautes Energies, UPMC and Université Paris-Diderot and CNRS/IN2P3, Paris, France
- ⁸¹ Fysiska institutionen, Lunds universitet, Lund, Sweden
- ⁸² Departamento de Física Teórica C-15, Universidad Autónoma de Madrid, Madrid, Spain
- ⁸³ Institut für Physik, Universität Mainz, Mainz, Germany
- ⁸⁴ School of Physics and Astronomy, University of Manchester, Manchester, United Kingdom
- ⁸⁵ CPPM, Aix-Marseille Université and CNRS/IN2P3, Marseille, France
- ⁸⁶ Department of Physics, University of Massachusetts, Amherst MA, United States of America
- ⁸⁷ Department of Physics, McGill University, Montreal QC, Canada
- ⁸⁸ School of Physics, University of Melbourne, Victoria, Australia
- ⁸⁹ Department of Physics, The University of Michigan, Ann Arbor MI, United States of America
- ⁹⁰ Department of Physics and Astronomy, Michigan State University, East Lansing MI, United States of America
- ⁹¹ ^(a) INFN Sezione di Milano; ^(b) Dipartimento di Fisica, Università di Milano, Milano, Italy
- ⁹² B.I. Stepanov Institute of Physics, National Academy of Sciences of Belarus, Minsk, Republic of Belarus
- ⁹³ National Scientific and Educational Centre for Particle and High Energy Physics, Minsk, Republic of Belarus
- ⁹⁴ Department of Physics, Massachusetts Institute of Technology, Cambridge MA, United States of America
- ⁹⁵ Group of Particle Physics, University of Montreal, Montreal QC, Canada
- ⁹⁶ P.N. Lebedev Institute of Physics, Academy of Sciences, Moscow, Russia
- ⁹⁷ Institute for Theoretical and Experimental Physics (ITEP), Moscow, Russia
- ⁹⁸ National Research Nuclear University MEPhI, Moscow, Russia
- ⁹⁹ D.V. Skobeltsyn Institute of Nuclear Physics, M.V. Lomonosov Moscow State University, Moscow, Russia
- ¹⁰⁰ Fakultät für Physik, Ludwig-Maximilians-Universität München, München, Germany
- ¹⁰¹ Max-Planck-Institut für Physik (Werner-Heisenberg-Institut), München, Germany
- ¹⁰² Nagasaki Institute of Applied Science, Nagasaki, Japan
- ¹⁰³ Graduate School of Science and Kobayashi-Maskawa Institute, Nagoya University, Nagoya, Japan
- ¹⁰⁴ ^(a) INFN Sezione di Napoli; ^(b) Dipartimento di Fisica, Università di Napoli, Napoli, Italy
- ¹⁰⁵ Department of Physics and Astronomy, University of New Mexico, Albuquerque NM, United States of America
- ¹⁰⁶ Institute for Mathematics, Astrophysics and Particle Physics, Radboud University Nijmegen/Nikhef, Nijmegen, Netherlands
- ¹⁰⁷ Nikhef National Institute for Subatomic Physics and University of Amsterdam, Amsterdam, Netherlands
- ¹⁰⁸ Department of Physics, Northern Illinois University, DeKalb IL, United States of America
- ¹⁰⁹ Budker Institute of Nuclear Physics, SB RAS, Novosibirsk, Russia
- ¹¹⁰ Department of Physics, New York University, New York NY, United States of America
- ¹¹¹ Ohio State University, Columbus OH, United States of America
- ¹¹² Faculty of Science, Okayama University, Okayama, Japan
- ¹¹³ Homer L. Dodge Department of Physics and Astronomy, University of Oklahoma, Norman OK, United States of America
- ¹¹⁴ Department of Physics, Oklahoma State University, Stillwater OK, United States of America
- ¹¹⁵ Palacký University, RCPTM, Olomouc, Czech Republic
- ¹¹⁶ Center for High Energy Physics, University of Oregon, Eugene OR, United States of America

- ¹¹⁷ LAL, Université Paris-Sud and CNRS/IN2P3, Orsay, France
- ¹¹⁸ Graduate School of Science, Osaka University, Osaka, Japan
- ¹¹⁹ Department of Physics, University of Oslo, Oslo, Norway
- ¹²⁰ Department of Physics, Oxford University, Oxford, United Kingdom
- ¹²¹ ^(a) INFN Sezione di Pavia; ^(b) Dipartimento di Fisica, Università di Pavia, Pavia, Italy
- ¹²² Department of Physics, University of Pennsylvania, Philadelphia PA, United States of America
- ¹²³ National Research Centre "Kurchatov Institute" B.P.Konstantinov Petersburg Nuclear Physics Institute, St. Petersburg, Russia
- ¹²⁴ ^(a) INFN Sezione di Pisa; ^(b) Dipartimento di Fisica E. Fermi, Università di Pisa, Pisa, Italy
- ¹²⁵ Department of Physics and Astronomy, University of Pittsburgh, Pittsburgh PA, United States of America
- ¹²⁶ ^(a) Laboratório de Instrumentação e Física Experimental de Partículas - LIP, Lisboa; ^(b) Faculdade de Ciências, Universidade de Lisboa, Lisboa; ^(c) Department of Physics, University of Coimbra, Coimbra; ^(d) Centro de Física Nuclear da Universidade de Lisboa, Lisboa; ^(e) Departamento de Física, Universidade do Minho, Braga; ^(f) Departamento de Física Teórica y del Cosmos and CAFPE, Universidad de Granada, Granada (Spain); ^(g) Dep Física and CEFITEC of Faculdade de Ciências e Tecnologia, Universidade Nova de Lisboa, Caparica, Portugal
- ¹²⁷ Institute of Physics, Academy of Sciences of the Czech Republic, Praha, Czech Republic
- ¹²⁸ Czech Technical University in Prague, Praha, Czech Republic
- ¹²⁹ Faculty of Mathematics and Physics, Charles University in Prague, Praha, Czech Republic
- ¹³⁰ State Research Center Institute for High Energy Physics, Protvino, Russia
- ¹³¹ Particle Physics Department, Rutherford Appleton Laboratory, Didcot, United Kingdom
- ¹³² ^(a) INFN Sezione di Roma; ^(b) Dipartimento di Fisica, Sapienza Università di Roma, Roma, Italy
- ¹³³ ^(a) INFN Sezione di Roma Tor Vergata; ^(b) Dipartimento di Fisica, Università di Roma Tor Vergata, Roma, Italy
- ¹³⁴ ^(a) INFN Sezione di Roma Tre; ^(b) Dipartimento di Matematica e Fisica, Università Roma Tre, Roma, Italy
- ¹³⁵ ^(a) Faculté des Sciences Ain Chock, Réseau Universitaire de Physique des Hautes Energies - Université Hassan II, Casablanca; ^(b) Centre National de l'Énergie des Sciences Techniques Nucleaires, Rabat; ^(c) Faculté des Sciences Semlalia, Université Cadi Ayyad, LPHEA-Marrakech; ^(d) Faculté des Sciences, Université Mohamed Premier and LPTPM, Oujda; ^(e) Faculté des sciences, Université Mohammed V-Agdal, Rabat, Morocco
- ¹³⁶ DSM/IRFU (Institut de Recherches sur les Lois Fondamentales de l'Univers), CEA Saclay (Commissariat à l'Énergie Atomique et aux Énergies Alternatives), Gif-sur-Yvette, France
- ¹³⁷ Santa Cruz Institute for Particle Physics, University of California Santa Cruz, Santa Cruz CA, United States of America
- ¹³⁸ Department of Physics, University of Washington, Seattle WA, United States of America
- ¹³⁹ Department of Physics and Astronomy, University of Sheffield, Sheffield, United Kingdom
- ¹⁴⁰ Department of Physics, Shinshu University, Nagano, Japan
- ¹⁴¹ Fachbereich Physik, Universität Siegen, Siegen, Germany
- ¹⁴² Department of Physics, Simon Fraser University, Burnaby BC, Canada
- ¹⁴³ SLAC National Accelerator Laboratory, Stanford CA, United States of America
- ¹⁴⁴ ^(a) Faculty of Mathematics, Physics & Informatics, Comenius University, Bratislava; ^(b) Department of Subnuclear Physics, Institute of Experimental Physics of the Slovak Academy of Sciences, Kosice, Slovak Republic
- ¹⁴⁵ ^(a) Department of Physics, University of Cape Town, Cape Town; ^(b) Department of Physics, University of Johannesburg, Johannesburg; ^(c) School of Physics, University of the Witwatersrand,

Johannesburg, South Africa

¹⁴⁶ ^(a) Department of Physics, Stockholm University; ^(b) The Oskar Klein Centre, Stockholm, Sweden

¹⁴⁷ Physics Department, Royal Institute of Technology, Stockholm, Sweden

¹⁴⁸ Departments of Physics & Astronomy and Chemistry, Stony Brook University, Stony Brook NY, United States of America

¹⁴⁹ Department of Physics and Astronomy, University of Sussex, Brighton, United Kingdom

¹⁵⁰ School of Physics, University of Sydney, Sydney, Australia

¹⁵¹ Institute of Physics, Academia Sinica, Taipei, Taiwan

¹⁵² Department of Physics, Technion: Israel Institute of Technology, Haifa, Israel

¹⁵³ Raymond and Beverly Sackler School of Physics and Astronomy, Tel Aviv University, Tel Aviv, Israel

¹⁵⁴ Department of Physics, Aristotle University of Thessaloniki, Thessaloniki, Greece

¹⁵⁵ International Center for Elementary Particle Physics and Department of Physics, The University of Tokyo, Tokyo, Japan

¹⁵⁶ Graduate School of Science and Technology, Tokyo Metropolitan University, Tokyo, Japan

¹⁵⁷ Department of Physics, Tokyo Institute of Technology, Tokyo, Japan

¹⁵⁸ Department of Physics, University of Toronto, Toronto ON, Canada

¹⁵⁹ ^(a) TRIUMF, Vancouver BC; ^(b) Department of Physics and Astronomy, York University, Toronto ON, Canada

¹⁶⁰ Faculty of Pure and Applied Sciences, University of Tsukuba, Tsukuba, Japan

¹⁶¹ Department of Physics and Astronomy, Tufts University, Medford MA, United States of America

¹⁶² Centro de Investigaciones, Universidad Antonio Narino, Bogota, Colombia

¹⁶³ Department of Physics and Astronomy, University of California Irvine, Irvine CA, United States of America

¹⁶⁴ ^(a) INFN Gruppo Collegato di Udine, Sezione di Trieste, Udine; ^(b) ICTP, Trieste; ^(c) Dipartimento di Chimica, Fisica e Ambiente, Università di Udine, Udine, Italy

¹⁶⁵ Department of Physics, University of Illinois, Urbana IL, United States of America

¹⁶⁶ Department of Physics and Astronomy, University of Uppsala, Uppsala, Sweden

¹⁶⁷ Instituto de Física Corpuscular (IFIC) and Departamento de Física Atómica, Molecular y Nuclear and Departamento de Ingeniería Electrónica and Instituto de Microelectrónica de Barcelona (IMB-CNM), University of Valencia and CSIC, Valencia, Spain

¹⁶⁸ Department of Physics, University of British Columbia, Vancouver BC, Canada

¹⁶⁹ Department of Physics and Astronomy, University of Victoria, Victoria BC, Canada

¹⁷⁰ Department of Physics, University of Warwick, Coventry, United Kingdom

¹⁷¹ Waseda University, Tokyo, Japan

¹⁷² Department of Particle Physics, The Weizmann Institute of Science, Rehovot, Israel

¹⁷³ Department of Physics, University of Wisconsin, Madison WI, United States of America

¹⁷⁴ Fakultät für Physik und Astronomie, Julius-Maximilians-Universität, Würzburg, Germany

¹⁷⁵ Fachbereich C Physik, Bergische Universität Wuppertal, Wuppertal, Germany

¹⁷⁶ Department of Physics, Yale University, New Haven CT, United States of America

¹⁷⁷ Yerevan Physics Institute, Yerevan, Armenia

¹⁷⁸ Centre de Calcul de l'Institut National de Physique Nucléaire et de Physique des Particules (IN2P3), Villeurbanne, France

^a Also at Department of Physics, King's College London, London, United Kingdom

^b Also at Institute of Physics, Azerbaijan Academy of Sciences, Baku, Azerbaijan

^c Also at Novosibirsk State University, Novosibirsk, Russia

^d Also at TRIUMF, Vancouver BC, Canada

- ^e Also at Department of Physics, California State University, Fresno CA, United States of America
- ^f Also at Department of Physics, University of Fribourg, Fribourg, Switzerland
- ^g Also at Departamento de Física e Astronomia, Faculdade de Ciências, Universidade do Porto, Portugal
- ^h Also at Tomsk State University, Tomsk, Russia
- ⁱ Also at CPPM, Aix-Marseille Université and CNRS/IN2P3, Marseille, France
- ^j Also at Università di Napoli Parthenope, Napoli, Italy
- ^k Also at Institute of Particle Physics (IPP), Canada
- ^l Also at Particle Physics Department, Rutherford Appleton Laboratory, Didcot, United Kingdom
- ^m Also at Department of Physics, St. Petersburg State Polytechnical University, St. Petersburg, Russia
- ⁿ Also at Louisiana Tech University, Ruston LA, United States of America
- ^o Also at Institucio Catalana de Recerca i Estudis Avancats, ICREA, Barcelona, Spain
- ^p Also at Department of Physics, National Tsing Hua University, Taiwan
- ^q Also at Department of Physics, The University of Texas at Austin, Austin TX, United States of America
- ^r Also at Institute of Theoretical Physics, Ilia State University, Tbilisi, Georgia
- ^s Also at CERN, Geneva, Switzerland
- ^t Also at Georgian Technical University (GTU), Tbilisi, Georgia
- ^u Also at O Chadai Academic Production, Ochanomizu University, Tokyo, Japan
- ^v Also at Manhattan College, New York NY, United States of America
- ^w Also at Institute of Physics, Academia Sinica, Taipei, Taiwan
- ^x Also at LAL, Université Paris-Sud and CNRS/IN2P3, Orsay, France
- ^y Also at Academia Sinica Grid Computing, Institute of Physics, Academia Sinica, Taipei, Taiwan
- ^z Also at School of Physics, Shandong University, Shandong, China
- ^{aa} Also at Moscow Institute of Physics and Technology State University, Dolgoprudny, Russia
- ^{ab} Also at Section de Physique, Université de Genève, Geneva, Switzerland
- ^{ac} Also at International School for Advanced Studies (SISSA), Trieste, Italy
- ^{ad} Also at Department of Physics and Astronomy, University of South Carolina, Columbia SC, United States of America
- ^{ae} Also at School of Physics and Engineering, Sun Yat-sen University, Guangzhou, China
- ^{af} Also at Faculty of Physics, M.V.Lomonosov Moscow State University, Moscow, Russia
- ^{ag} Also at National Research Nuclear University MEPhI, Moscow, Russia
- ^{ah} Also at Department of Physics, Stanford University, Stanford CA, United States of America
- ^{ai} Also at Institute for Particle and Nuclear Physics, Wigner Research Centre for Physics, Budapest, Hungary
- ^{aj} Also at Department of Physics, The University of Michigan, Ann Arbor MI, United States of America
- ^{ak} Also at Discipline of Physics, University of KwaZulu-Natal, Durban, South Africa
- ^{al} Also at University of Malaya, Department of Physics, Kuala Lumpur, Malaysia
- * Deceased